CHARACTERIZING THE PERMEABILITY OF CONCRETE MIXES USED IN TRANSPORTATION APPLICATIONS: A NEURONET APPROACH

by

HAKAN I. YASARER

B.S., Mustafa Kemal University, Turkey, 2004

A THESIS

Submitted in partial fulfillment of the requirements for the degree

MASTER OF SCIENCE

Department of Civil Engineering
College of Engineering

KANSAS STATE UNIVERSITY
Manhattan, Kansas

2010

Approved by:

Major Professor
Dr. Yacoub M. Najjar

Abstract

Reliable and economical design of Portland Cement Concrete (PCC) pavement structural systems relies on various factors, among which is the proper characterization of the expected permeability response of the concrete mixes. Permeability is a highly important factor which strongly relates the durability of concrete structures and pavement systems to changing environmental conditions. One of the most common environmental attacks which cause the deterioration of concrete structures is the corrosion of reinforcing steel due to chloride penetration. On an annual basis, corrosion-related structural repairs typically cost millions of dollars. This durability problem has gotten widespread interest in recent years due to its incidence rate and the associated high repair costs. For this reason, material characterization is one of the best methods to reduce repair costs. To properly characterize the permeability response of PCC pavement structure, the Kansas Department of Transportation (KDOT) generally runs the Rapid Chloride Permeability test to determine the resistance of concrete to penetration of chloride ions as well as the Boil test to determine the percent voids in hardened concrete. Rapid Chloride test typically measures the number of coulombs passing through a concrete sample over a period of six hours at a concrete age of 7, 28, and 56 days. Boil Test measures the volume of permeable pore space of the concrete sample over a period of five hours at a concrete age of 7, 28, and 56 days. In this research, backpropagation Artificial Neural Network (ANN)-based and Regression-based permeability response prediction models for Rapid Chloride and Boil tests are developed by using the databases provided by KDOT in order to reduce or eliminate the duration of the testing period. Moreover, another set of ANN- and Regression-based permeability prediction models, based on mix-design parameters, are

developed using datasets obtained from the literature. The backpropagation ANN learning technique proved to be an efficient methodology to produce a relatively accurate permeability response prediction models. Comparison of the prediction accuracy of the developed ANN models and regression models proved that ANN models have outperformed their counterpart regression-based models. Overall, it can be inferred that the developed ANN-Based permeability prediction models are effective and applicable in characterizing the permeability response of concrete mixes used in transportation applications.

Table of Contents

List of Figures

List of Tables

Acknowledgements

I would like to express my deepest and sincere appreciation to Professor Yacoub Najjar for his support and encouragement throughout the course of this work which would not have been possible without his generous help and guidance. I am indebted to Dr. Najjar for his patience in reviewing this manuscript. I'm also very grateful to my committee members, Professor Kyle Riding and Asad Esmaeily for their advice and assistance during the course of this work. Also, many thanks to Professor Hayder A. Rasheed for attending my final examination and making valuable comments.

Financial support received from Kansas State University Transportation Center under grant KSUTC-08-9 to conduct this research study is gratefully acknowledged. In addition, I owe great appreciation to the entire Department of Civil Engineering, which includes faculty, staff, and graduate students. Also, I must acknowledge my Turkish friends, Ahmet Kosembay, Gazi Dogan, Emin Akarcay, and Tulu Toros for their priceless support.

My deepest gratitude goes to my family for their unflagging love and support throughout my life. This thesis would be impossible without them. I am indebted to my parents: To my father, who has worked industriously to support the family and provide the best possible environment for me to have a wonderful future and to my Mother, the unbelievably loving and caring.

Last but not least, my gratitude is to God for everything…

Dedication

I dedicate this thesis to my father,

İsmet Yaşarer and my mother, **Hulkiye Yaşarer.**

CHAPTER 1 - INTRODUCTION

1.1 Overview

Material modeling is a fundamental phenomenon in engineering research and practice. A model is typically developed to describe the material constitutive/mechanical behavior under certain boundary conditions. Material model serves as the basis for numerical calculations and guidance for analyzing, designing, constructing and rehabilitating the structures including the material. Many concrete structures are built today with specifications emphasizing for low-permeability concrete because the durability problem of the concrete structures has become widespread in recent years. Due to its incidence and related high repair costs, many research projects have been conducted by government agencies to better understand the testing methods used and to evaluate the concrete behavior when subjected to various environmental and/or loading conditions. The long-term durability of concrete is dependent on its permeable pores. In other words, the permeability of concrete is used as the main assessment criterion which has been established based on empirical, conventional and correlation techniques. In this study, concrete which is one of the most important and widely used construction materials is evaluated in order to develop a material permeability response model. The permeability of concrete mixes mainly depends on the internal pore structure. The pore structure in turn depends on some factors such as the mix design, curing condition, degree of hydration, use of supplementary cementitious materials, and construction practices. Concrete behavior has to be evaluated in terms of movement of water, sulphate ions, alkali ions, and other causes of chemical attack within the interconnected pores. This evaluation is typically conducted to avoid a potential risk of chloride-ingress which may lead to corrosion of the reinforcing steel and a subsequent reduction in strength, serviceability, and structural aesthetic. For appropriate design and quality control of reinforced concrete structures, the ability of chloride ions to penetrate the concrete must be known. However, the penetration of chlorides in concrete is a slow process which can not be directly determined in a time frame that would be useful as a quality control measure (Mackechnie and Alexander, 2004). In other words, concrete permeability to water and chloride ion is a design feature which can not be measured quickly for upcoming projects. For this reason, the Federal Highway Administration developed a rapid test method for determining the apparent chloride permeability of various concrete mixes. It is commonly called the AASHTO T277 test method and also known as the "Rapid Chloride Permeability Test". The Rapid Chloride Permeability test is the most widely used and suitable test method for evaluation of materials and material properties for design purposes, research and development. This method measures the electrical conductance of concrete to provide a rapid indication of its resistance to the penetration of chloride ions. Another alternative method for Rapid Chloride test that has been published by American Society for Testing Materials (ASTM) is the Boil test which is conducted to measure the percent (%) volume of permeable pore space by determining the concrete sample's weight before and after the test.

A new period of engineering material modeling emerged with the utilization of the Artificial Neural Networks (ANNs) approach to properly characterize the behavior of geo-materials during the 1990s by Ghaboussi et al. (1991), Basheer and Najjar (1994), Najjar and Basheer (1996a) and Najjar et al (1996b). ANN is a mathematical or computational model that attempts to emulate the structure and/or functional aspects of biological neural networks. ANNs-based material modeling approach has been receiving increasing interest in the engineering area during the past 20 years. ANNs approach is considered the best function approximation technique that is well suited for proper material behavior characterization. In a typical modeling process, ANNs-based model is trained to attain a specific knowledge through training or retraining via mathematically-based process. As a result, the resulting model stores the extracted knowledge, features embodied in the database, within its connection weights. ANNs possess the following unique advantages in information processing tasks:

1. ANNs are capable of directly learning complex nonlinear relationships from a large body of datasets without the need for any simplifying assumptions;
2. Model prediction accuracy can be improved by adding new training datasets which can internally adjust the model's connection weights in order to capture new features hidden within the new datasets;
3. ANNs have the ability to extract information from incomplete or partially incorrect datasets;
4. ANNs can be used to develop general purpose models to characterize various responses of material behavior.

ANNs-based material modeling approach has been successfully used to properly characterize the material behavior for various geo-materials such as concrete, sand, clay, and asphalt. The research conducted in this thesis aims at exploring the potential use of ANNs to efficiently model the permeability response of concrete mixes used in transportation applications such as PCC pavements and bridges. To properly characterize the permeability responses, various ANN- and Regression-based prediction models were developed and their prediction accuracy measures were numerically and graphically assessed. Rapid Chloride and Boil Test based prediction models were developed from previously conducted experimental tests performed by Kansas Department of Transportation (KDOT). Furthermore, another set of ANN and regression Rapid Chloride prediction models involving mix-design input variables were developed by using datasets obtained from the literature. In the following chapters, test procedure protocols, databases used, ANN model developments phases and their corresponding prediction accuracy measures obtained will be discussed in details.

1.2 Organization of the Thesis

Chapter 1- Introduction: This chapter presents a brief discussion on ANNs-based modeling approach and advantages of using ANN method in material modeling. Also, brief summaries about the contents of each chapter are presented.

Chapter 2- Literature Review: This chapter contains a brief literature review related to the research conducted in this study. Several relevant publications on ANN material modeling that contributed significantly to this research study are highlighted.

Chapter 3- Artificial Neural Network: This chapter discusses the aspects of ANN computational algorithms. Basic definition, elements, and Backpropagation learning algorithm used in ANN approach are discussed in details. Statistical prediction accuracy measures used to identify the best performing ANN models are also defined in this chapter.

Chapter 4- Rapid Chloride Testing: Development of KDOT-Based Rapid Chloride Prediction Model: This chapter describes the experimental procedure of the “Rapid Chloride Test” and the data collection process. ANN and Regression, permeability prediction models, as well as their development stages are discussed in details. Corresponding graphical results and their statistical accuracy measures are presented at the end of the chapter.

Chapter 5- Rapid Chloride Testing: Development of Mix-Design Based Prediction Model: This chapter gives information about the mix-design parameters used in relation to the Rapid Chloride Test discussed in Chapter 4. Data collection process, ANN and Regression model development phases for the mix-design based permeability prediction models are discussed in details. Prediction accuracy comparisons in graphical and statistical terms for the developed ANN and regression models are also presented in this chapter.

Chapter 6-Boil Testing: Development of KDOT-Based Prediction Model: This chapter describes the experimental procedure of the KDOT used “Boil Test” and the data collection process used to build the needed database. ANN and Regression, % void prediction models, and their development phases are discussed in details. Graphical prediction comparisons and associated statistical accuracy measures for all developed models are presented at the end of this chapter.

Chapter 7- Summary, Conclusions and Recommendations: Summary of the research work performed in this study and major conclusions obtained are presented in this chapter. Recommendations for future research studies are also presented.

CHAPTER 2 - BACKGROUND

One of the most important properties of concrete affecting the durability of a structure is chloride diffusivity. The diffusivity of porous materials is determined formally by diffusion cells or by immersion in a solution. However, these methods are time-consuming and typically require months or years to obtain the needed results. Engineers and researchers need a rapid method to evaluate existing structures, new materials, and treatments. For this reason, the conventional methods can not meet engineering requirements. An existing rapid method, Whiting's coulomb test (1981), has been adopted as an ASSHTO standard method. However, there have been a number of criticisms of this technique (Stanish et al., 2000).

One of the criticisms is that the coulomb test does not only measure the chloride ion, but rather measures all ions in the pore solution. As an alternative method to avoid this drawback, Luping and Nilsson (1992) established a mathematical model of ion diffusion under the action of a constant electrical field and found the exact analytical solution for the differential equation describing the modeled behavior by utilizing the semi-infinite diffusion concept. A simple method characterizing chloride penetration into concrete was proposed by Luping and Nilsson (1992) which enables rapid assessment of chloride penetration profiles and their associated depths. Furthermore, Shi (2004) has reported that Rapid Chloride Test is not a valid test for the evaluation of permeability of concrete mixes made from different materials and/or different proportions. He accordingly recommended the use of the reliable and fast test method developed by Luping and Nilsson (1992).

The other criticism is concerning the fact that the conditions under which all measurements are made may cause notable changes to the tested concrete specimens. A study was conducted by Feldman et al. (1994) to observe how changes in the testing procedure can affect the obtained results. Factors such as temperature, alternating current (AC) impedance, initial direct current (DC), amount of charge passed, and chloride ion profiles were monitored during polarization of four different concrete mixes. It was found that simple measurement of initial current or resistivity yielded the same ranking as those obtained via conventional testing for the four concrete mixes. As a result, Feldman et al. (1994) believed that the proposed simple initial measurements can be used to produce reliable results similar to those obtained from conventional chloride testing method but at much faster time. Therefore, yielding a considerable time saving benefits.

A simplified method of measuring concrete resistivity was established by Riding et al. (2008). Cylinders measuring 100 mm x 200 mm were cured in 100% relative humidity and tested using the same equipment as specified in ASTM C1202. The method has been developed to eliminate the problem of the temperature rise in the sample during the test. In this method, concrete resistivity can be calculated by taking only one current reading 5 minutes after the test had started. Therefore, potential temperature rise in the concrete sample is avoided especially when testing low quality concrete. The good correlation reported between the new method and the standard testing method proves the validity and potential promise of the proposed method.

A computer model has been developed by Claisse et al. (2010) to simulate the Rapid Chloride Permeability test described in ASTM C1202. The key process of diffusion and electromigration using standard equations is represented in the model. The model also maintains charge neutrality by modeling changes to in voltage distribution. This method empowers the model to predict current-time transient similar to those recorded in experiments. It can also be utilized to obtain basic parameters such as diffusion coefficients for tested samples from the observed data.

A faster and simpler alternative testing method to AASHTO T277/ASTM C1202 based on the AC impedance techniques is proposed by Liu and Beaudoin (2000). This method provides at least an equivalent indication of the concrete permeability with respect to AASHTO T277/ASTM C1202. Moreover, it overcomes many of the shortcomings of current methods. The result can be obtained within minutes and without the potential for heat build up. Therefore, causing no microstructural changes. A similar alternative method has already been proposed by Zhao (1998). However, it appears to be too simplistic when compared with the method proposed by Liu and Beaudoin (2000).

Another accelerated testing method has been developed by Srinivasan et al. (2007). This method requires a simple experimental set-up. The method involves polarization of a coated concrete cylindrical specimen containing rebar under a constant voltage in sodium chloride solution with respect to an external cathode. In this research, it was reported that the current time-dependent response was found to be similar to that of a typical service life model indicating depassivation and corrosion propagation. This test method can be used for performance evaluation of coatings and high performance concrete containing different mineral admixtures.

Based on a set of multi-scale computer models, an equation has been developed by Bentz (2000) for predicting the chloride ion diffusivity of high performance concretes containing silica fume as a function of mixture proportions and expected degree of hydration. It is indicated that the model-predicted relative improvements appear to be in good agreement with the experimental data generated in two recent studies (Hooton et al., 1997; Alexander and Magee, 1999). By using the technical background and employing the numerical assumptions, Bentz (2007) has presented a prototype virtual test method that includes prediction of the conductivity of the cementitious binder pore solution and total charge passed during an ASTM C1202/AASHTO T277 Rapid Chloride Permeability test. In addition, the computer implementation of the virtual test is presented as a set of HTML/Java-Script web documents. Validation against existing datasets is presented with a reasonable agreement noted between the experimental and virtual test results.

Boil Test (ASTM C642) has been used as another alternative method for Rapid Chloride Permeability test (AASHTO T277/ASTM C1202). In ASTM C642, the volume of the sample is determined by the displacement method, in which the difference between weighing in air and weighing in water is attributed to the buoyant effect of the water. This in turn is related to the density of the water and the displaced volume. In informal testing, the volume of the specimen is frequently calculated from the physical dimensions of the sample. As a result, this approach can be useful only when the shape of the specimen is highly regular and the dimensions can be accurately measured (Lamond and Pielert, 2006). Due to the fact that there is no reference standard available for comparison, bias for this test method can not be determined. However several research studies (i.e., Gonzalez-Fonteboa and Martinez-Abella, 2008; Padmini et al., 2002; Lomboy and Wang, 2009; Tosun et al., 2008; Sahmaran and Li, 2009) have considered the Boil Test method to be a viable method for determining the percent volume of voids in their research studies.

CHAPTER 3 - ARTIFICIAL NEURAL NETWORK

3.1 Definition and Elements

3.1.1 Definition

An artificial neural network (ANN) is a method based on the operation of biological neural networks. In other words, is a simulation of biological neural system. ANN is a mathematical model or computational model that attempts to emulate the structure and/or functional aspects of biological neural networks. The interest in neural networks re-emerged only after some important theoretical results were attained in the early eighties, notably after the discovery of the error back-propagation scheme. Nowadays, artificial neural networks can be most adequately characterized as 'computational models' with particular properties such as the ability to adapt, learn, generalize, cluster or organize data in an operation based on parallel processing. However, many of the mentioned properties can be attributed to existing models for which the neural network approach can be suited better in certain applications. Parallel processing is often described with biological systems. However, there is still so little known about biological systems. Models developed by artificial neural network approach can be identified as oversimplification of the biological systems (Krose and Smagt, 1996). Artificial neural networks are highly interconnected structures consisting of many simple processors (neurons) that perform massively parallel computation for data processing and knowledge representation. ANNs approach is represented by mathematical algorithms designed to imitate methods of information processing and knowledge acquisition of the human brain (Pham 1994). ANNs systems typically consist of the same following basic components (Agrawal and Daiutolo, 1992):

i. a neuron or node,
ii. an activation function associated to each node,
iii. a real-valued weight associated with each link between two nodes,
iv. a real-valued bias associated with each node,
v. a transfer function,
vi. a propagation rule, and
vii. a learning rule.

The ANNs have generalization capability which is highly dependent on the size of training samples, range of data domain, and density of solution space. Generalization process by an ANNs approach is very much similar to the human nervous system by increasing the acquainted knowledge through long-term experimentations.

3.1.2 Elements

The most important element in every ANN architecture is the neuron which is similar to the biological neurons. It is considered as a cell with a built-in activation function connected to other neurons by a set of connections. Main elements of an Artificial Neural Network are the input layer, hidden layer(s), output layer, and connection weights. An example of an ANN structure is depicted in Figure 3.1. Prediction accuracy of the network depends on its interconnected weights. A network usually performs the following three sequential tasks (Najjar et., 1996a):

a. Input variables fed to the input layer,
b. Processing of information within the hidden layer,
c. Production of outputs at the output layer.

The input layer contains the input nodes and does not perform any mathematical operation. The number of the input nodes is based on input variables which are assumed to influence the output. The number of the input variables affects the performance of the network. Information is received, processed and forwarded to the hidden nodes by the input layer. The hidden layer may contain one or more layers consisting of a set of nodes which processes information within the network body. The hidden layer which is a transition layer between input layer and output layer is the most important element in the network. The hidden layer processes the information passed on from the input layer and feeds it forward towards the output layer. In other words, it facilitates the flow of information between the input nodes and the output node via the connecting links. The accuracy of the developed models is considerably affected by the number of the hidden layers as well as the number of neurons involved within each layer. Connection weights are the interconnecting links between the neurons in sequential layers. Each neuron is connected to every other neuron in the next layer via links which have individual and adjustable connection weights. There are no side connections used in this modeling approach.

3.2 Backpropagation Learning Algorithm

Backpropagation neural networks consist of a number of layers including a specified number of neurons. The input layer includes the input neurons corresponding to parameters which are assumed to affect the outcome of the phenomenon. The output layer consists of the output neuron(s) which represent(s) the solution of the problem. The hidden layer located between the input layer and the output layer is not designed to have any direct contact with the outside environment. It has been shown (Hornik et al., 1989; Funahashi, 1989; Cybenko, 1989; Hartman et al., 1990) that only one layer of hidden units can approximate any function with finitely many discontinuities to arbitrary precision, provided that the activation functions of the hidden units are non-linear (the universal approximation theorem). In most applications, a feed-forward network with a single layer of hidden units is used.

A sigmoidal function which is the most widely used function is where the input passes through to calculate the output of a neuron at the output layer. The calculated outputs are then compared to actual outputs to determine the error which is consequently used for error function determination. Then, the error function is used to adjust the error starting from the connection weights linked with the output, and backward to the input layers. In other words, the generated error by the network is used to adjust the connection weights. The connection weights are initially not known and typically assigned random or specified values. The output value obtained using the initial connection weights may not be close to the target value. The error correction is done based on the calculated error and the initial connection weights are adjusted by propagating the error backwards. With the new adjusted connection weights between input layer nodes and hidden layer nodes as well as hidden layer nodes and output layer node, the inputs are forwarded once again to determine the new output value accordingly, then the new error is determined and is used to adjust the connection weights. The forward activation of signals and the backpropagation of error are continuously repeated on all training datasets until the error is reduced to a predetermined minimum or an allowed tolerance (Najjar *et al.*, 1997; Najjar and

Zhang, 2000). The final connection weights which produce an error within the allowed tolerance range are then stored to represent the network. The final network can be used to predict the desired output(s) of a new dataset that have no actual output values. Note that, backpropagation ANN is a feedforward network and the backpropagation term does not mean the same with feedbackward propagation since the backpropagation is used for the error distribution in contrast to direction of signals' flow. In other words, the training algorithm starts with a feedforward of the input variables, followed by backpropagation of the associated error and connection weights' adjustment.

3.3 Learning Algorithm

The learning process of a standard Backpropagation Neural Network is demonstrated in this section.

Nodal Input Values

The nodes in a certain layer are connected to all other nodes in the following layer. Each node receives signals from all other neurons in previous layer and integrates those signals as a weighted average. For instance, input value for neuron "A" is the sum of the integrated signals multiplied by their corresponding connection weights. The input value for a neuron "A" can be expressed with the following equation:

$$(Input)_A = \sum (node\,value) \times connection\ weight \tag{3.1}$$

As depicted in Figure 3.2, the input of one node (i.e., Neuron A) is the all incoming signals and collective effect signal calculated as the weighted sum of all incoming signals is calculated according to the following equation:

$$Net_j^L = \sum_{i=1}^{m} w_{ji}^L \, Out_i^{(L-1)} \tag{3.2}$$

Where Net_j^L refers to the excitation of neuron j in the L^{th} layer, w_{ji}^L represents the numerical value of the interconnection weight between neuron i in the $(L-1)^{th}$ layer and neuron j in the

L^{th} layer. $Out_i^{(L-1)}$ is the output from the i^{th} neuron in the $(L-1)^{th}$ layer. Finally, Net_j^L is nonlinearly transferred via an appropriate activation function.

Activation Function: Sigmoidal Function

To calculate the output of a neuron, the input (i.e., excitation) must be processed through a transfer function because the input might either be very large or negative. In order to avoid large or negative values and to introduce nonlinearity in the model, the neuron's input experiences an additional nonlinear transformation to produce an output based on the following equation:

$$(Out)_A = f(input)_A \qquad 3.3$$

Where "f" is a transfer function and "$(input)_A$" is the input value for node A previously calculated using equation 3.1.

In this study, the Sigmoidal function, among the most common activation functions, was used as the activation function. The Sigmoidal function is the most widely used activation function in Backpropagation networks. The final output signal is positive, continuous and has a specified interval between 0 and 1. Sigmoidal function is expressed as

$$f(Input) = \frac{1}{1+e^{-(Input)}} \qquad 3.4$$

Since a neuron receives a total excitation (i.e., input) which is equivalent to "Net", then the output from the neuron can be expressed as

$$a = f(Net) = \frac{1}{1+e^{-(Net)}} \qquad 3.5$$

As "Net" reaches a high (approx. 4.0) or low (approx. -4.0) values, activation stabilizes at values between 0 and 1, respectively.

Weight Adjustment

At the last stage of the backpropagation algorithm, the latest adjusted weights are updated by adding the weight adjustment values to the previous weight values. While the inputs are processed forward through every single layer of the network to produce outputs, the error between predicted and target values is used to adjust the connection weights. The incremental change for the current weight can be calculated as follows:

$$\Delta w_{ji}^{L} = w_{ji}^{L(new)} - w_{ji}^{L(previous)} \qquad 3.6$$

where “new” and “previous” stand for the current and previous iterations. According to Backpropagation neural network algorithm (Zupan and Gasteiger, 1993), incremental change, Δw_{ji}^{L} can be computed using the Delta-rule:

$$\Delta w_{ji}^{L} = \eta \, \delta_{j}^{L} \, Out_{i}^{L-1} \qquad 3.7$$

where η is the learning rate which controls the size of the updating process. The error factor, δ, reflects the weighted error on the connection ji. The Out_{i}^{L-1} term represents the output from the i^{th} neuron in the $(L-1)^{th}$ layer.

Learning Process

The learning process of a neural network is given as follows

1) Input vectors are marked as $X_1, X_2, \ldots\ldots, X_n, 1$ where n refers to total number of input variables and last input stands for the threshold or the bias.
2) Propagate the input vectors, $X_1, X_2, \ldots\ldots, X_n$, via the connection weights to compute the output vectors, Out^{1} using the Equation 3.3 until consequently reaching Out^{last}.
3) Itemize initial weights, w_{ji}^{L} and update connection weights on output layer using the equation:

$$\Delta w_{ji}^{last} = \eta \delta_{j}^{last} \, Out_{i}^{last-1} + \mu \Delta w_{ji}^{last(previous)} \qquad 3.8$$

Where δ is the correction factor (i.e., the weighted error) and is computed as

$$\delta_j^{last} = \left(y_j - Out_j^{last}\right) Out_j^{last} \left(1 - Out_j^{last}\right) \tag{3.9}$$

in which y_j is target value of component, j in the output vector, Y. The function shown in Equation 3.8 is called generalized Delta-rule with a momentum rate (μ) where, $(0 < \mu < 1)$ (Rumelhart *et al.*, 1986). The current connection weight is updated by adding the adjustment to the previous connection weight. Biases are similarly updated on the last layer based on the following equation:

$$\Delta b_{ji}^{last} = \eta \delta_j^{last} + \mu \Delta b_{ji}^{last(previous)} \tag{3.10}$$

4) All weights on any hidden layer are updated by using the following equation:

$$\Delta w_{ji}^{L} = \eta \delta_j^{L} Out_i^{L-1} + \mu \Delta w_{ji}^{L(previous)} \tag{3.11}$$

Where δ is the correction factor and is computed as

$$\delta_j^{L} = \left(\sum_{k=1}^{r} \delta_k^{L+1} w_{kj}^{L+1} \right) Out_j^{L} \left(1 - Out_j^{L}\right) \tag{3.12}$$

The biases are corrected within the hidden layer(s) using

$$\Delta b_{ji}^{L} = \eta \delta_j^{L} + \mu \Delta b_{ji}^{L(previous)} \tag{3.13}$$

5) Steps (1) through (4) are repeated for each training dataset.
6) Steps (1) through (5) are repeated until the predicted output meets the corresponding target output within a predetermined tolerance or the training iterations reaches the maximum limit.

3.4 Initial Number of Hidden Nodes

The number of initial hidden nodes and the maximum allowed hidden nodes in ANN model development are specified by the user. ANN process starts with a user-specified initial hidden node and goes up to the maximum allowed number of hidden nodes. At the end of this process, ANN structures which have the least number of hidden nodes and the best statistical accuracy errors are chosen to be reevaluated in terms of statistical accuracy measures as well as graphical accuracy measures. The maximum number of hidden nodes (HN) can be calculated by the following equation:

$$HN \leq \frac{(number\ of\ training\ datasets) - (number\ of\ ouput\ \mathrm{var}iables)}{(number\ of\ input\ \ \mathrm{var}iables) + (number\ of\ output\ \ \mathrm{var}iables) + 1} \qquad 3.14$$

Note that, choosing too many hidden nodes could lead to overtraining situation. On the other hand, very few hidden nodes may not be enough to obtain a model for a complex phenomenon. Concerning the number of hidden layers, networks with one hidden layer are more adequate and efficient. In this research, only one hidden layer was used for ANN architecture.

3.4 Model Selection Criteria

In order to compare the performance of generated networks and to select the best performing network, statistical accuracy measures such as the Coefficient of Determination (also known as R^2), the Mean Absolute Relative Error (MARE), and the Averaged of Squared Error (ASE) are evaluated. Training, testing, validation and overall performance parameters should be considered during the evaluation process. The level of agreement between the predicted and actual output values is interpreted based on statistical measures of the network producing the minimum values of ASE and MARE; and the highest R^2. The ASE value can be expressed by the following equation:

$$ASE = \frac{\sum^{No}\sum^{P}(y'-y)^2}{(\#of\ datasets)_P(\#of\ outputs)_{No}} \tag{3.16}$$

Where y' is the output (i.e., predicted permeability value in this study) produced by the network and y is the real value (i.e., actual permeability value in this study). The MARE value is computed by the following equation:

$$MARE(\%) = \frac{\dfrac{\sum^{No}\sum^{P}(y'-y)}{y}\times 100}{(\#of\ outputs)_{No}(\#of\ datasets)_P} \tag{3.17}$$

Further information about ANN can be found from the following references: Rumelhart and McClelland (1986); Hopfield (1982); Haykin (1999); Rumelhart et al. (1986); Fausett (1994); Basheer (1998); Ali (2000); Herz et al. (1991); Wu and Ghaboussi (1995); Ghaboussi et al. (1991). ANN method is used to develop permeability prediction models in the following chapters. Model development process for each chapter is described in details and the statistical accuracy measures and graphical comparisons for the best performing networks are shown at the end of their corresponding chapter.

3.4 Figures

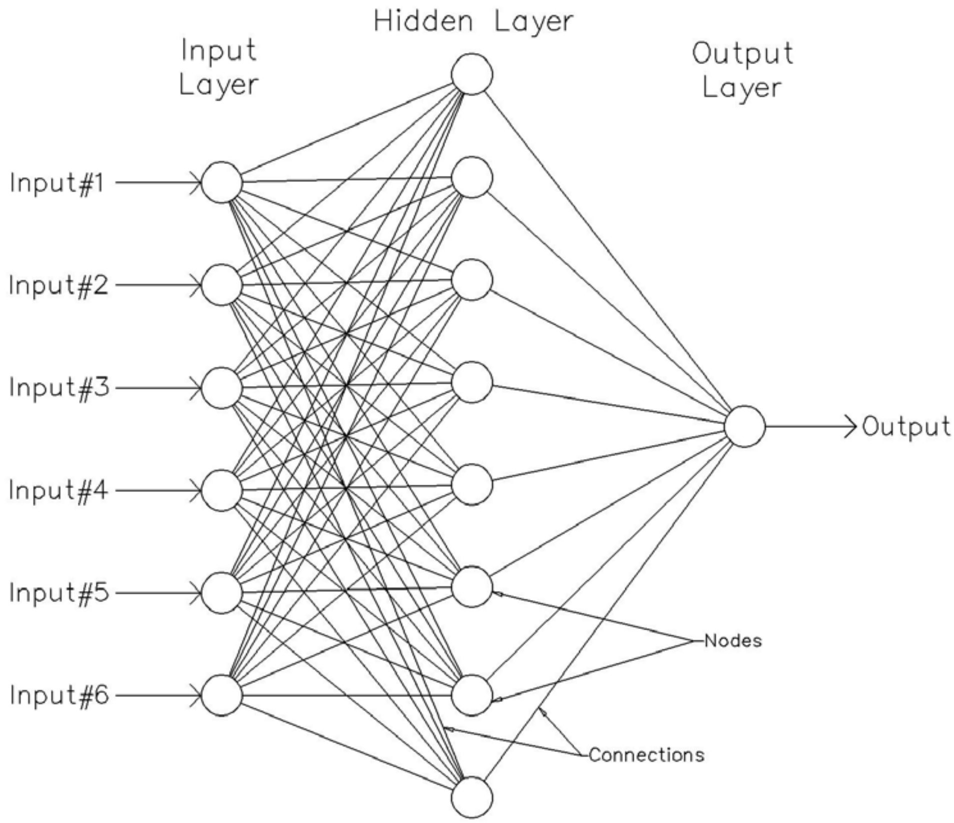

Figure 3.1 Structure of an ANN

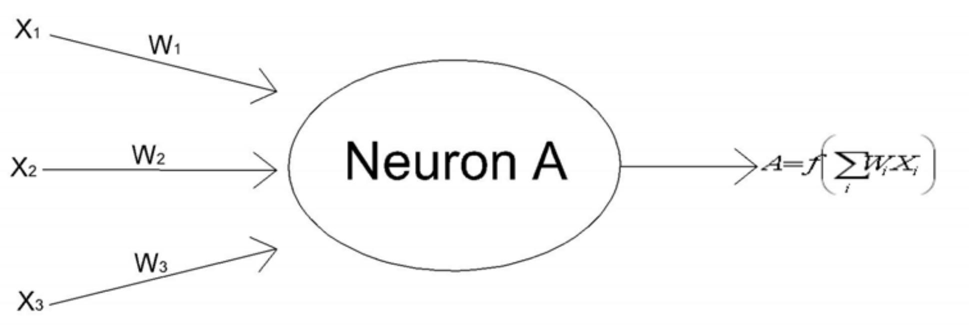

Figure 3.2 Activation Process of a Neuron

CHAPTER 4 – RAPID CHLORIDE TESTING: DEVELOPMENT OF KDOT-BASED RAPID CHLORIDE PREDICTION MODEL

4.1 Introduction

Permeability of the concrete in PCC pavement is an important factor for long-term durability. Wherever there is a potential risk of chloride-induced corrosion, the concrete should be evaluated for chloride permeability (Joshi and Chan, 2002). Rapid Chloride Test is the most widely used and suitable test method for evaluation of materials and material proportions for design purposes, research and development. This method measures the electrical conductance of concrete to provide a rapid indication of its resistance to the penetration of chloride ions. In other words, this test method basically monitors the amount of electrical current passing through 50-mm (2-in) during a six-hour period. It is well known that diffusion controls the transport of chloride ions in concrete. The AASHTO T-259 90-day ponding test requires considerable time to enable measurement of the diffusion of chloride ions in hardened concrete (Shi et al., 1998). Based on a preliminary study, a potential difference of 60 V dc is applied across the ends of the specimen, one of which is immersed in 3 percent (by mass) chloride solution (NaCl), the other is in 0.3M sodium hydroxide solution (NaOH). The total charge, in coulombs, passed through the specimen can be related to the resistance of the specimen to chloride penetration. It is marked in AASHTO T277-05 that the correlations between this test procedure and long-term chloride ponding procedures have to be established in order for this method to be applicable. The laboratory evaluation of the electrical conductance of concrete samples provides a rapid indication of their resistance to chloride ion penetration. In applications such as quality control and acceptance testing, the experimental results (total charge passed, in coulombs) must be evaluated by using Table 4.1 unless otherwise noted by the specifying agency.

When this test is used on surface-treated concrete, for instance, treated with penetrating sealers, interpreting results should be done carefully because the results from this test show low resistance to chloride ions while 90-day chloride ponding tests indicate high resistance. Misleading results can be obtained if calcium nitrite is admixed into concrete. Therefore, as a result of this case, it is expected to indicate higher coulomb values than from tests on identical concrete mixtures without calcium nitrite. AASHTO T277-05 recommends long-term ponding tests if an admixture, which might similarly affect results of this test, is suspected.

Depending on the type of concrete and curing procedure, sample age may have significant effects on the test results. Most concrete becomes significantly less permeable with time, if it is cured properly. The relation between chloride ion permeability (coulomb) and time of moist curing (day) for different water/cement ratios is depicted by Plante and Bilodeau (1989) in Figure 4.1.

In this chapter, ANN approach is used to characterize the Rapid Chloride permeability response of concrete. Regression approach was also used to ensure the developed ANN model has comparable accuracy measures. In the following sections, the procedure of the test method and model development procedure are described in details.

4.2 Problem Statement

In recent years, the durability problem of the concrete structures has been widespread. Due to its incidents and repair costs, there have been many research investigations (Examples: Feldman *et al.*, 1994; Bassuoni *et al.*, 2005) conducted to better understand the test methods. Rapid Chloride Test is one of the test methods commonly referred to by researchers and government agencies. However, its cost, inadequate test equipment and need for qualified technicians to conduct the sample preparation and test procedure, and the six hours actual testing time needed are the main issues needing to be addressed. During the summer time, construction industry is really active and because of that numerous amounts of concrete samples, either collected in the field or mixed in the lab by the government agencies, are placed in the curing room for 7, 28, and 56 days and will be processed for testing at later dates. However, due to inadequate test equipments, concrete samples must be kept in curing room for more than 56 days. This is the reason that concrete samples in the database used have an age range from 7 to 111 days. A prediction model is purposed to overcome this issue. Thus, in this chapter, the question to be answered with this research is: Can the six hours testing time be replaced, with reasonable degree of accuracy, with a permeability response prediction model?

4.3 Data Description

The database for the development of the Rapid Chloride permeability prediction model was provided by KDOT. The samples included in the database are either prepared in the laboratory or collected in the field. In order to properly characterize the permeability of concrete, total 265 datasets are used to build the desired database; 133, 73 and 59 datasets are used, respectively, for training, testing and validation purposes. By using the database, the ANN- and Regression-Based models are developed to predict the permeability response in order to choose the best prediction model. Three ANN-based models are developed and the most accurate model has been selected based on the accuracy measure criteria such as Mean Absolute Relative Error (MARE), Averaged-Squared-Error (ASE) and Coefficient of Determination (R^2) values. The predicted permeability response is computed via Excel-based Program by entering the needed input variables such as oven dry weight (A), saturated surface dry weight (B), weight in water (C), and curing time. Further details are given in the following sections.

4.3.1 Lab Procedure

The concrete samples either prepared in the lab or collected in the field are placed in curing room for 7, 28, and 56 days. The cured specimens for 7, 28, and 56 days are taken out of the curing room and cut into three 2 inch thick pieces. The sliced concrete samples are let to dry for one hour, Dry Unit Weight (A) is measured afterwards and then the cylindrical surface is covered with epoxy. After the epoxy is tack free, the concrete slice is placed into vacuum desiccator and vacuuming is applied for three hours. While the vacuum pump still running, the desiccator is filled with de-aerated water to cover the specimen. Vacuuming is applied for another hour, then it is shut off and the concrete slice is soaked for 18 hours. The surfaces of the saturated specimens are dried out with a towel and then Saturated Surface Dry Weight (B) is measured as well as the Weight in Water (C). It is important that to obtain consistent chloride permeability values for a concrete batch, each slice must be conditioned to start the test at the same moisture content (Suprenant, 1991). After 18 hours soaking, the specimens are removed, excess water is blotted off and the specimen is stored in a sealed container. The specimens are connected to voltage cell where one side of the specimen is in contact with a sodium chloride solution and the other side is in contact with a sodium hydroxide solution. After connecting the voltage cell, a voltage of 60V dc is maintained across the ends of the sample throughout the test. Electrical current (in amperes) versus time (in seconds) are plotted. A smooth curve is drawn through the data and the area underneath the curve is integrated in order to obtain the ampere-seconds, or coulombs, of charge passed during the six hours test period. As given in AASHTO T277-05, a sample calculation by assuming the current recorded at 30 minute intervals is given by:

$$Q = 900\left(I_0 + 2I_{30} + 2I_{60} + \dots\dots\dots\dots + 2I_{300} + 2I_{330} + 2I_{360}\right) \qquad 4.1$$

where:

Q = charge passed (coulomb)

I_0 = current (amperes) immediately after voltage is applied, and

I_t = current (amperes) at t min after voltage is applied.

After determining the charge passed through the concrete sample, Table 4.1 is used to classify the test results. If the specimen diameter is different from the standard 95 mm (3.75 in.) value, then the value for the total charge passed must be adjusted by using the following equation:

$$Q_s = Q_x \times \left(\frac{3.75}{x}\right)^2 \qquad 4.2$$

where:

Q_s = charge passed (coulombs) through a 95-mm (3.75-in) diameter specimen,

Q_x = charge passed (coulombs) through x mm (in) diameter specimen, and

x = diameter mm (in) of the nonstandard specimen

The input parameters used in model development includes the measurements taken before the test, which are; surface dry weight (A), saturated surface dry weight (B), weight in water (C), and curing time. The total charge passed through sample during the six hours test is used as the output variable. Also, Specific Gravity (Gs) and Water absorbed (W %) dependent variables are calculated out of the measured values prior to the test. In terms of A, B and C, Specific Gravity and Absorbed Water are given by:

$$\text{Specific Gravity} = \frac{A}{B-C} \tag{4.3}$$

$$\text{Water absorbed} = \frac{(\text{B - A})}{(\text{A - C})} \times 100 \tag{4.4}$$

4.4 ANN Model Development

The ANN model was developed in four sequential stages. In the first stage, the ANN architecture was determined based on problem characteristics and ANN knowledge, and input and output categories were chosen accordingly. This step also includes classifying the datasets as training, testing or validation sets. In the second stage, the network was trained and tested on the experimental data to obtain the optimum number of hidden nodes and iterations for the ANN architecture determined in stage one. In the third stage, the best performing network obtained from the second stage is validated on the validation database. If accuracy measures from training, testing and validation database are very comparable, then the model may not be trained on all data. In the fourth stage, the best performing network obtained in the second stage is retrained on all experimental data to increase the prediction accuracy and evaluate how well the ANN model characterized the desired behavior. Normally, retraining the network on all experimental data is expected to provide reliable predictions and accuracy measures if the dataset classification is done in an appropriate manner. However, it has been shown through several research studies by Najjar and Coworkers [Najjar & Mryyan (2009), Najjar & Huang (2007), and Najjar & McRyenold (2003)] that the stage four is recommended to arrive at a better performing network model.

4.4.1 ANN Model Architecture

Based on the knowledge gained from experimental data analysis, ANN model architecture has been built by considering 6 inputs and 1 output, which respectively are:

1- (A) Surface dry weight (grams)

2- (B) Saturated surface dry weight (grams)
3- (C) Weight in water (grams)
4- Curing time (days)
5- (Gs) Specific gravity
6- (W %) Percent of water absorbed

and

1- Output (Q): Total charge passed through the concrete sample (coulombs)

The number of inputs could have been reduced to 4 by removing dependent variables such as Specific Gravity and Water absorbed. However, any additional inputs will most likely assist the network to find out the best correlation between the inputs and the output. In this study, 3 models giving appropriate statistical measures have been selected based on optimum hidden nodes, minimum values of Mean Absolute Relative Error (MARE) and Averaged-Squared-Error (ASE) and maximum values of Coefficient of Determination (R^2). Total 265 datasets are used to build the desired database; 133, 73 and 59 sub-databases are used, respectively, for training, testing and validation purposes. Datasets that include that the minimum and maximum values of each variable are included in the training phase in order for the network to represent the characteristics of the response. The maximum and minimum ranges of each input/output variable for ANN model development are chosen on purpose to be wider than their actual ranges for better mathematical mapping.

4.4.2 Model Training and Testing

Based on statistical measures such as Averaged-Squared-Error (ASE), Coefficient of determination (R^2) and Mean Absolute Relative Error (MARE), the optimal network structure for the Model 1 was found at 8 hidden nodes and 20,000 iterations. The corresponding accuracy measures for this network are ASE_{tr}=0.004984, R^2_{tr}=0.89, $MARE_{tr}$=15.73% (for training database) and ASE_{ts}=0.008256, R^2_{ts}=0.83, $MARE_{ts}$= 21.099% (for testing database). The optimal network for Model 2 was found at 14 hidden nodes and 20,000 iterations. The corresponding accuracy measures for this network are ASE_{tr}=0.004585, R^2_{tr}=0.90, $MARE_{tr}$=13.34% (for training database) and ASE_{ts}=0.008662, R^2_{ts}=0.828, $MARE_{ts}$= 19.609% (for testing database). The optimal network for Model 3 was found at 15 hidden nodes and 19,900 iterations. The corresponding accuracy measures for this network are ASE_{tr}=0.005034, R^2_{tr}=0.89, $MARE_{tr}$=13.949% (for training database) and ASE_{ts}=0.009042, R^2_{ts}=0.815, $MARE_{ts}$= 23.021% (for testing database). The training graphical comparison plots between predicted and actual response for Model 1, Model 2 and Model 3 are shown, respectively, in Figure 4.2, Figure 4.3 and Figure 4.4. The testing graphical comparison plots between predicted and actual response for Model 1, Model 2 and Model 3 are shown, respectively, in Figures 4.5, Figure 4.6 and Figure 4.7. Also, statistical accuracy measures for the training and testing are shown in Table 4.2 with the best performing model is identified in bold.

4.4.3 Model Validation

After training and testing procedures by using, respectively, 133 and 73 datasets, validation is conducted by using 59 datasets. After classifying the datasets as training, testing, and validation as described in Section 4.4, each network was trained and tested on experimental data to obtain the optimum number of hidden nodes and iterations for the ANN architecture determined in the stage one. The graphical comparison plots, for the validation stage, between predicted and actual responses for Model 1, Model 2 and Model 3 are shown, respectively, in Figures 4.8, 4.9 and 4.10. Also, statistical accuracy measures are shown in Table 4.2 where the best performing network is identified in bold.

4.4.4 Model Selection

Statistical accuracy measures for training and testing databases at optimal ANN structure with 8 hidden nodes and 20,000 iterations showed considerable difference. Even though Model 2 has better accuracy measures, Model 1 has less number of hidden nodes which means that Model 1 has less complicated structure which will potentially show more consistent response. For this reason, Model 1 has been chosen to be used as the best network structure. Thus, all of the 265 datasets from the Rapid Chloride test were used to retrain the network at this optimal structure to obtain the generalized response throughout the entire database. Statistical measures of Model 1 model trained with all data are: ASE_{all}=0.004841, R^2_{all} =0.894 and $MARE_{all}$=15.484%. The graphical comparison plots between predicted and actual response for Model 1, Model 2 and Model 3 are shown, respectively, in Figures 4.11, 4.12 and 4.13. Statistical accuracy measures for all 3 models are shown in Table 4.2. The good agreement between predicted results and experimentally acquired results is apparent. The network structure of the best performing model is depicted in Figure 4.14.

4.5 Regression Model

Regression analysis is another method to understand how the typical value of the dependent variable changes when the independent variables are varied. In other words, it is to understand which among the independent variables are related to the dependent variables. Regression model development has been accomplished using Excel Data Analysis Toolkit. Total 265 datasets used for ANN-Model development was processed to obtain the prediction model. The input variables and the output as used in ANN-Model development are respectively:

X_1 = (A) Surface dry weight (grams)
X_2 = (B) Saturated surface dry weight (grams)
X_3 = (C) Weight in water (grams)
X_4 = Curing time (days)
X_5 = (Gs) Specific Gravity
X_6 = (W %) Percent of water absorbed

and

X_7 =Output (Q) Total charge passed through the concrete sample (coulomb)

Using linear regression approach, the following equation was developed;

$$Q = -18579.71 - 436.87X_1 + 476.77X_2 - 78.50X_3 + 11423.43X_4 + 1483.43X_5 - 68.15X_6 \qquad 4.5$$

Statistical measures of the linear regression model obtained using Excel Data Analysis Toolkit are: MARE (%) = 36.90%, R^2_{all} = 0.61566 and Standard Deviation of Error, SDE, (%) = 63.1%. The graphical comparison plots between predicted and actual response is shown in Figure 4.15. The statistical measures' comparison of ANN Model and Regression Model are depicted in Table 4.3. It is very clear from the comparison plots in Figure 4.11 and 4.15 that the ANN model is out performing the regression-based model. It is possible to increase the accuracy measures of the regression model by non-linear regression. However, the effort spent on this task will be unbounded since many trials have to be performed. Over the past 17 years, Najjar and Coworkers [Najjar & Ali (1998a, b), Najjar & Basheer (1996a), and Najjar et al. (1996b)] have shown that the best non-linear regression model will not produce accuracy measures that are better than those obtained via an appropriately developed ANN-based model. Typically, the accuracy measures by the ANN-based model are the upper bounds to any non-linear regression model describing the same behavior. Therefore, the development of nonlinear regression model was not carried in this research study.

4.6 Excel Application

By using the connections weights, threshold values and coefficients which are described in Chapter 3, the excel-based application is developed. In this application, by entering the measured input variables for A, B, C and Curing time in the Excel interface shown in Figure 4.15, W% (Water Absorbed), and Gs (Specific Gravity) are automatically calculated. Following that, ANN- and Regression-based models utilize all 6 input values (4 user-provided and 2 calculated) to predict the corresponding permeability value (i.e., the charge passed through the sample). The computed permeability response values and categorical variables converted using table 4.1 by ANN and Regression are placed in the output cells colored with blue as depicted in Figure 4.15. The applicable ranges for the input variables are also shown in Figure 4.15. Any value of an input variable that is outside the applicable range may cause the models to produce unreliable predictions.

4.7 Concluding Remarks

In this chapter, a static artificial neural network with backpropagation learning algorithm was developed to predict the Rapid Chloride permeability response of concrete. As seen from the graphical results depicted in Figures 4.2 to 4.13 and the accuracy measures of the developed ANN models listed in Table 4.2, Model 1 has been selected to characterize the permeability response. The comparison of the predicted responses by ANN and Regression shown in Table 4.3 indicates that ANN model attains better prediction accuracy than the Regression model. It is apparent that the ANN model has efficiently characterized the Rapid Chloride test response when compared to the regression model. Moreover, the predicted permeability responses by ANN and Regression models are converted to categorical variables using Table 4.1 and evaluated in terms of success and failure classification cases. The results of classification evaluation in terms of success and failure percentages, depicted in Table 4.4, have shown a good trend between predicted-based and actual-based categorical results. Therefore, ANN-based model can reliably be used for permeability prediction tasks to reduce the duration of the 6 hours testing period as long as the input variables fall within the applicable ranges. Moreover, developed ANN model can be used to verify measured responses for planned-to-be conducted Rapid Chloride tests without the need for any additional experimental-based information. Even though, development of the ANN model requires good fundamental understanding of the Rapid Chloride Test procedure and ANN knowledge, Excel-based application, which is the utilization tool of the developed ANN model, is simple and does not require the user to have prior knowledge of model development. The ANN model overcomes the drawback of the 6 hours testing time; making it a powerful, rapid, and low cost alternative to obtain the permeability of concrete with a reliable level of accuracy. Note that, A, B and C variables are the measurements which are not essentially specified in AASHTO T277-05. However, they are the measurements conducted as part of ASTM C 642-97 Standard Test Method for Density, Absorption, and Voids in Hardened Concrete. This procedure has also been applied to AASHTO T277-05 by KDOT to understand the correlation between Boil Test and Rapid Chloride penetration test method. For this reason, the developed Rapid Chloride permeability prediction model is applicable only for KDOT applications such as experimental studies, quality control and testing acceptance.

4.8 Figures and Tables

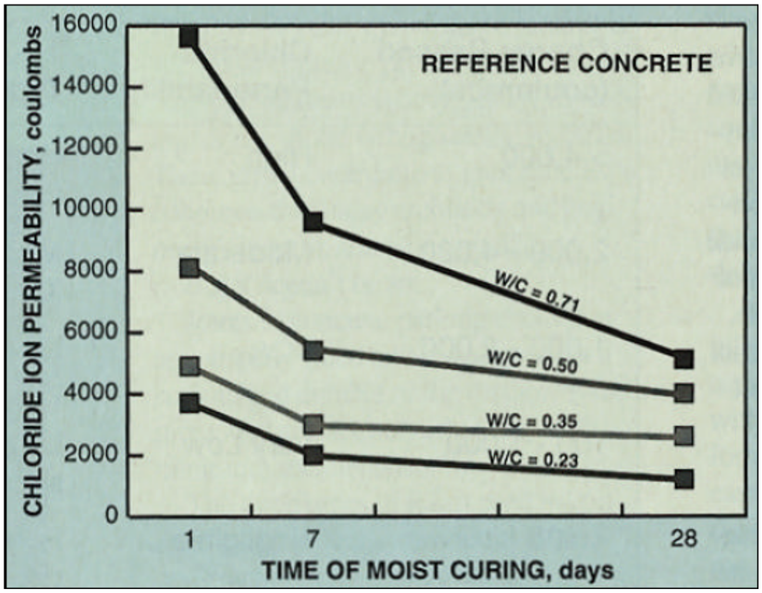

Figure 4.1 Change in permeability with time (adopted from Plante and Bilodeau, 1989)

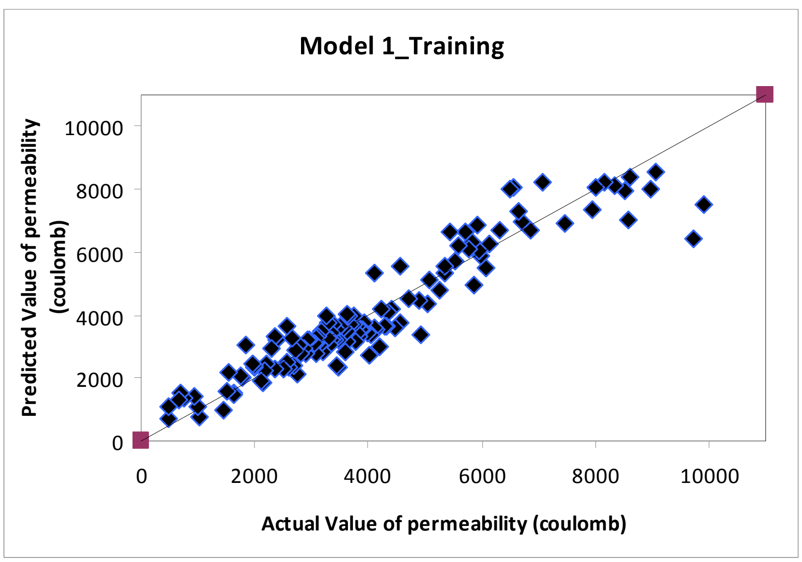

Figure 4.2 Training Graphical Prediction Accuracy for the Model 1

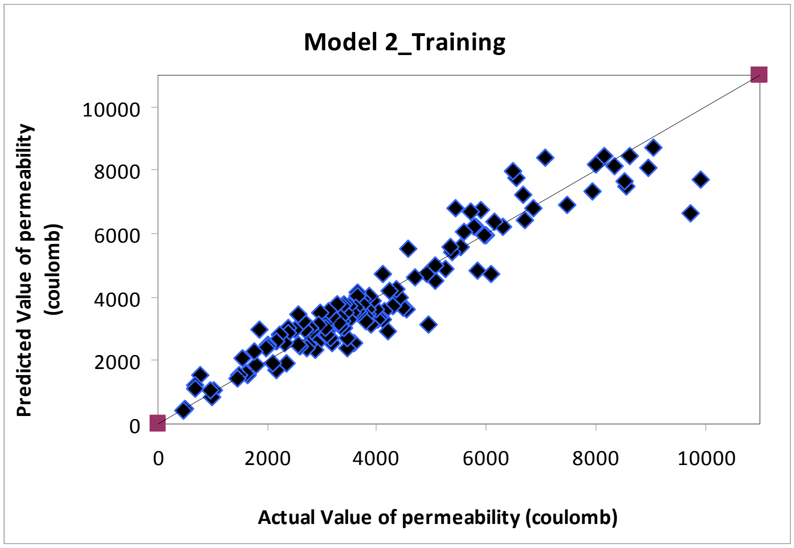

Figure 4.3 Training Graphical Prediction Accuracy for the Model 2

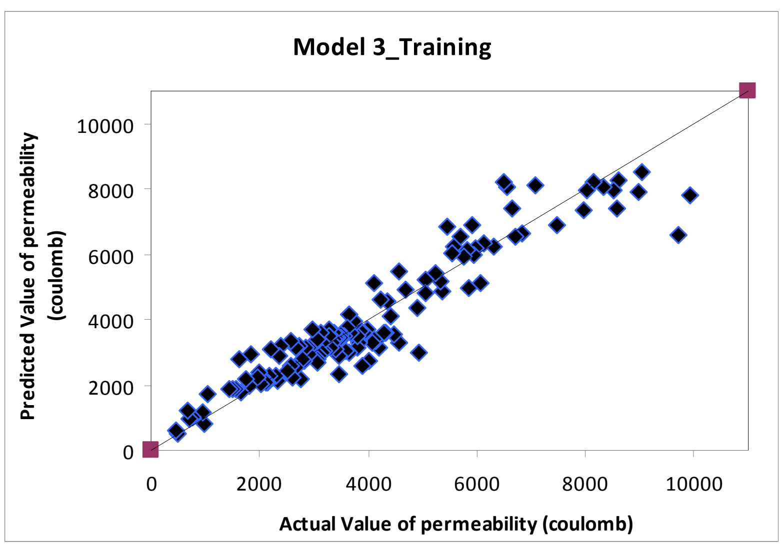

Figure 4.4 Training Graphical Prediction Accuracy for the Model 3

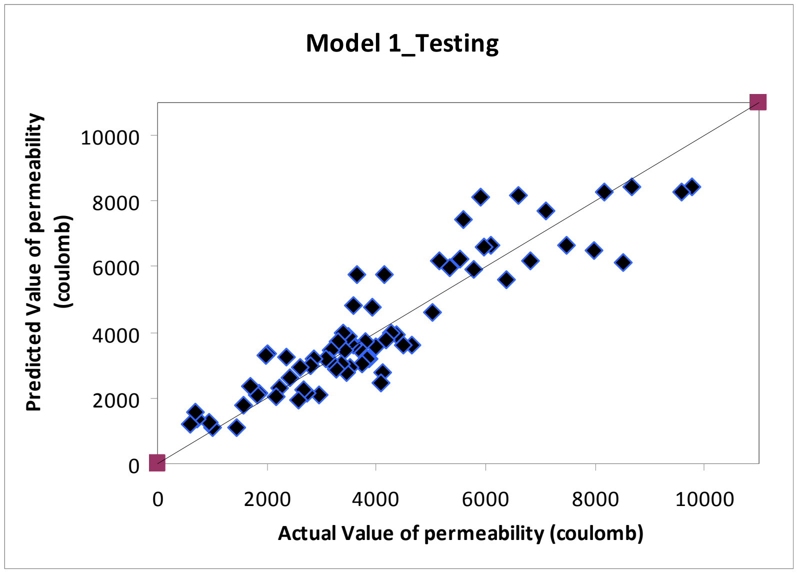

Figure 4.5 Testing Graphical Prediction Accuracy for the Model 1

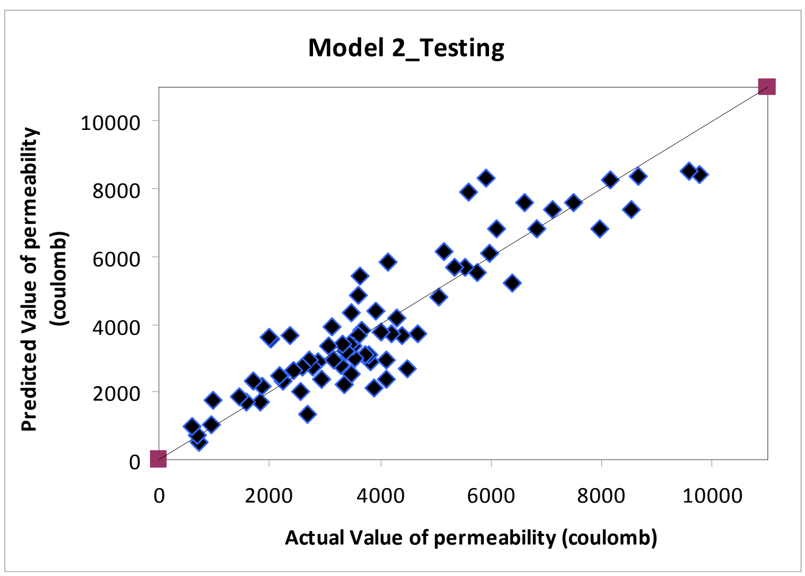

Figure 4.6 Testing Graphical Prediction Accuracy for the Model 2

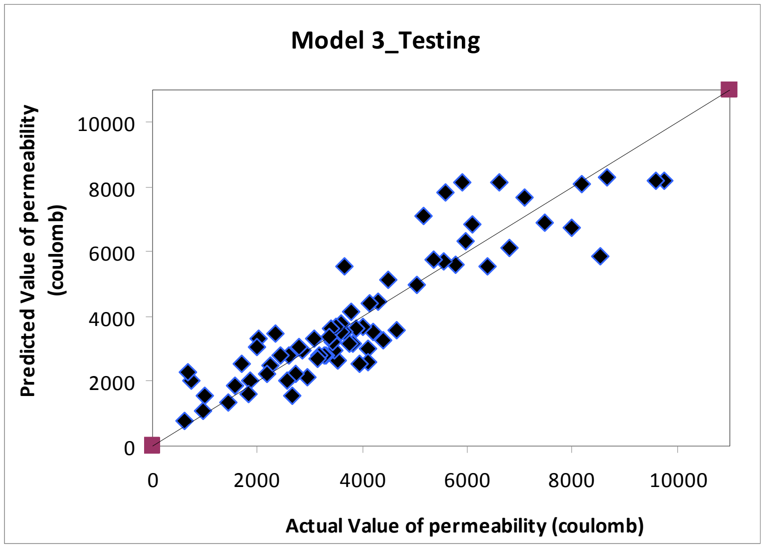

Figure 4.7 Testing Graphical Prediction Accuracy for the Model 3

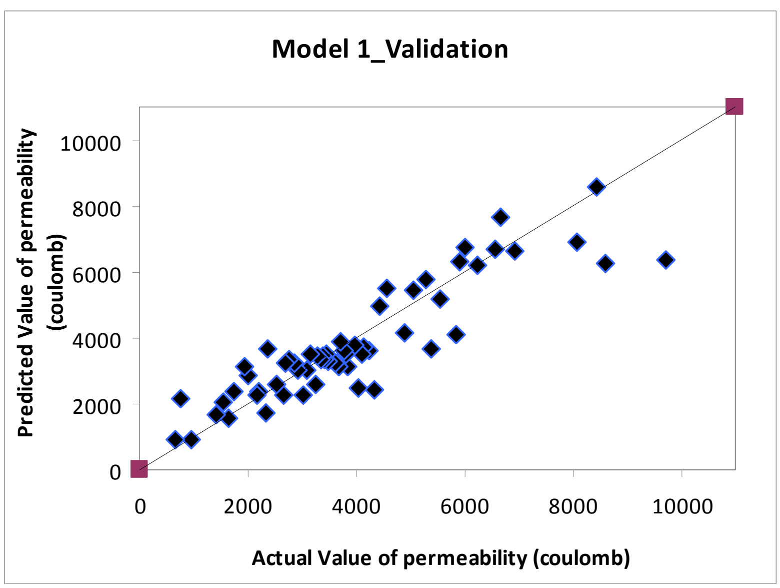

Figure 4.8 Validation Graphical Prediction Accuracy for the Model 1

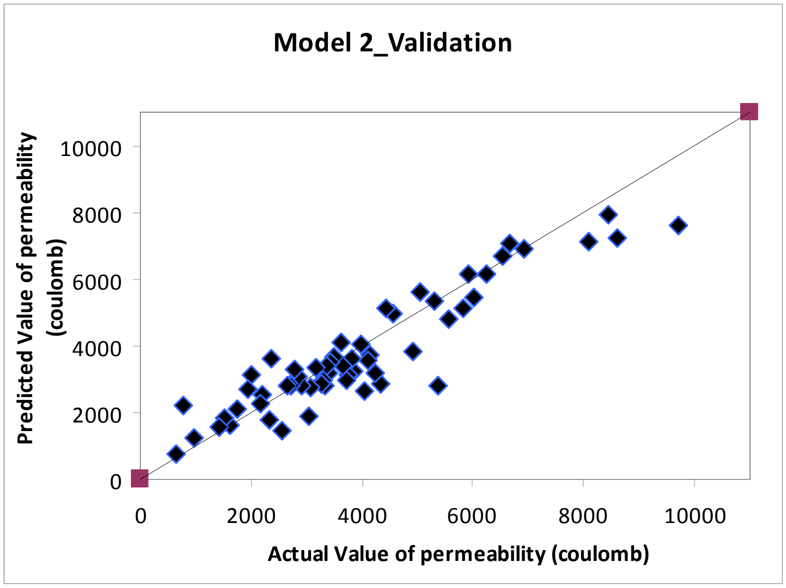

Figure 4.9 Validation Graphical Prediction Accuracy for the Model 2

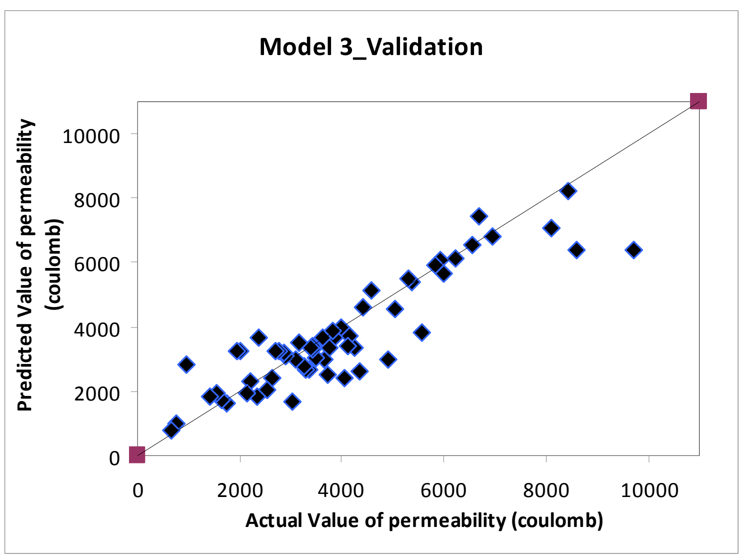

Figure 4.10 Validation Graphical Prediction Accuracy for the Model 3

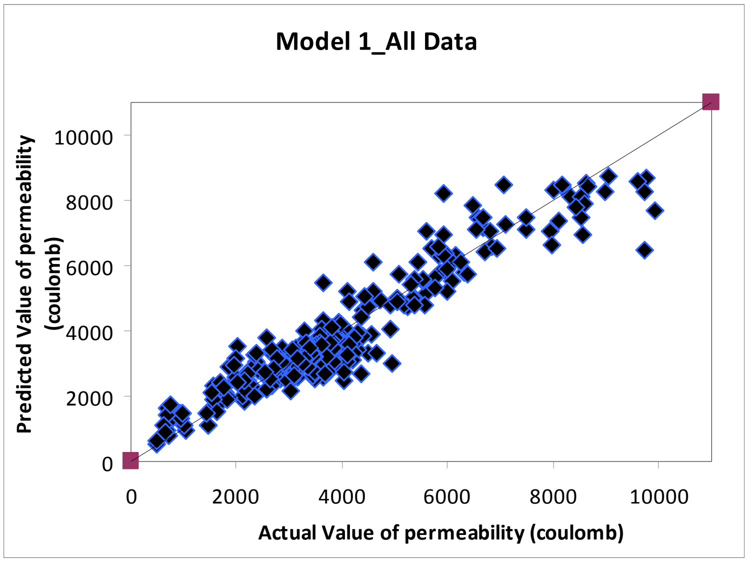

Figure 4.11 All Data Graphical Prediction Accuracy for the Model 1

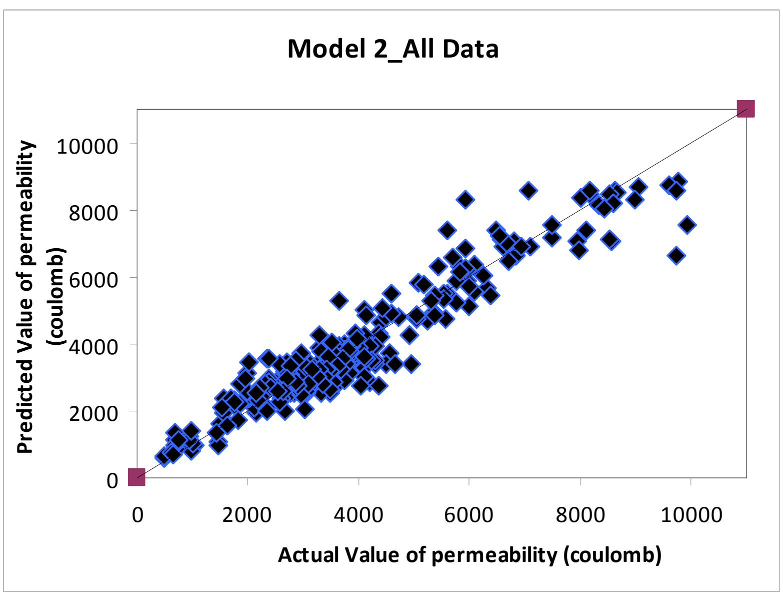

Figure 4.12 All Data Graphical Prediction Accuracy for the Model 2

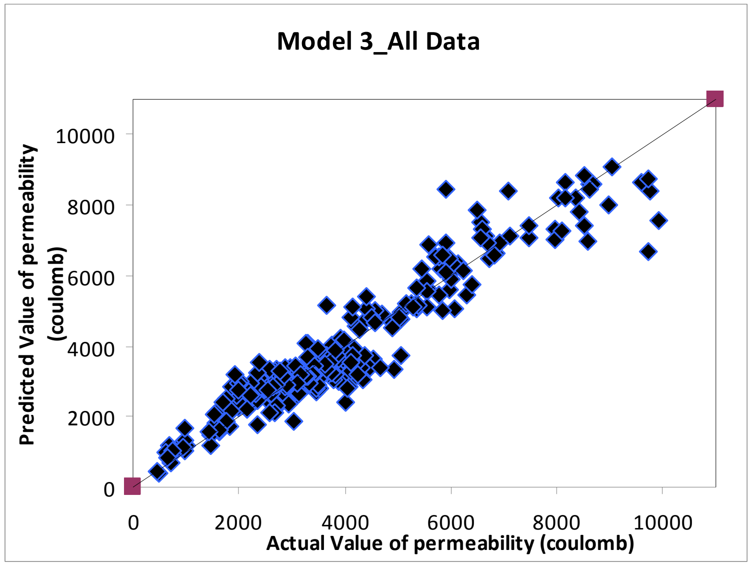

Figure 4.13 All Data Graphical Prediction Accuracy for the Model 3

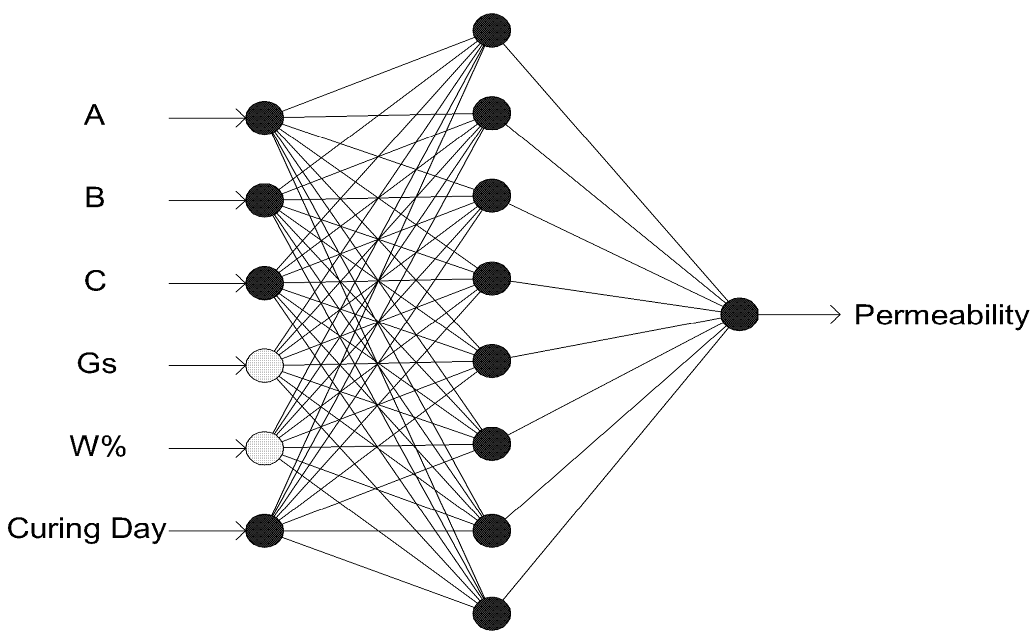

Figure 4.14 The Network Structure of the Best Performing Model (Model 1)

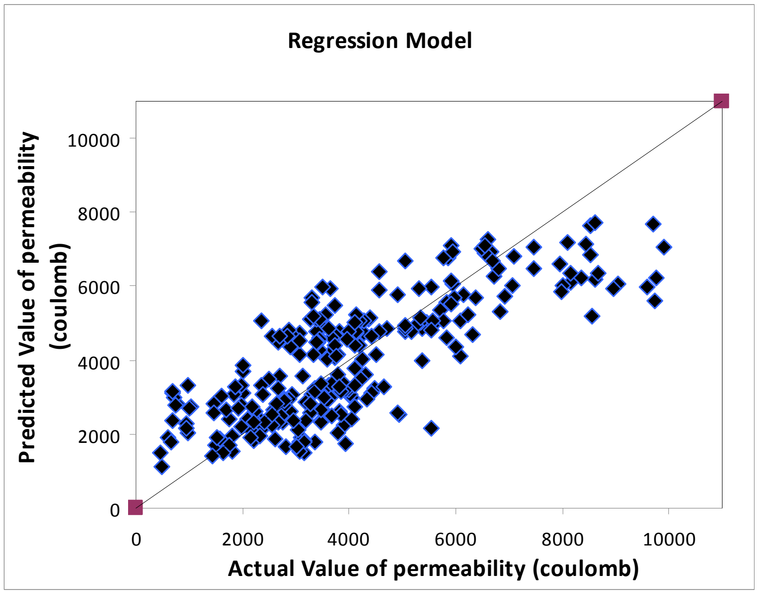

Figure 4.15 Graphical Prediction Accuracy for the Regression Model

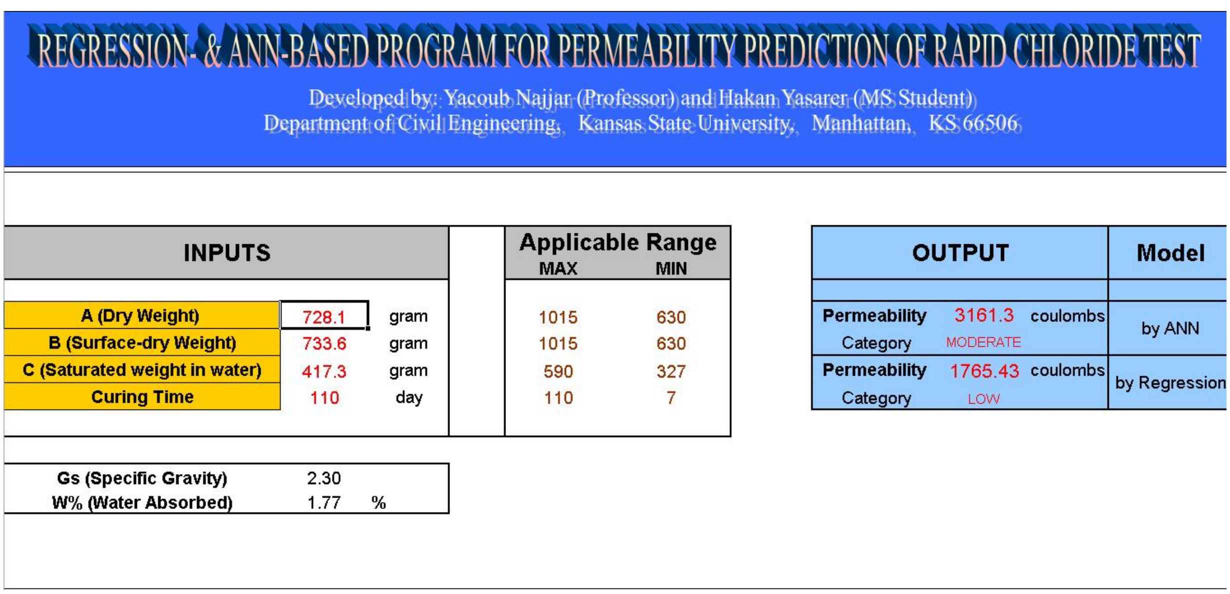

Figure 4.16 Excel Application Screen-shot

Table 4.1 Chloride Permeability Category Based on Charge Passed (ASTM C1202)

Charge Passed (coulombs)	Chloride Permeability Category	Typical of
>4,000	High	High W/C ratio (0.6) conventional PCC
2,000 - 4,000	Moderate	Moderate W/C ratio (0.4 - 0.5) conventional PCC
1,000 - 2,000	Low	Low W/C ratio (<0.4) conventional PCC
100 - 1,000	Very Low	Latex-modified concrete or internally-sealed concrete
<100	Negligible	Polymer-impregnated concrete, Polymer concrete

Table 4.2 Statistical Accuracy Measures of the ANN-Models

Model		**Model 1**	Model 2	Model 3
Architecture		**6-(5-8-17-20000)-1**	6-(2-14-17-20000)-1	6-(9-15-17-19900)-1
Training	MARE (%)	**15.73%**	13.34%	13.95%
	R2	**0.89191**	0.90096	0.89082
	ASE	**0.004984**	0.004585	0.005034
Testing	MARE (%)	**21.10%**	19.61%	23.02%
	R2	**0.83121**	0.82831	0.81521
	ASE	**0.008256**	0.008662	0.009042
Validation	MARE (%)	**18.71%**	18.30%	19.48%
	R2	**0.80618**	0.85658	0.80521
	ASE	**0.008349**	0.006554	0.008763
All Data	MARE (%)	**15.48%**	14.16%	13.86%
	R2	**0.89427**	0.90479	0.9047
	ASE	**0.004841**	0.004363	0.004354
Final Structure		**6 - 8 - 1**	6 - 14 - 1	6 - 15 - 1

Table 4.3 Comparisons of Statistical Accuracy Measures for ANN and Regression Models

Statistical Measures	ANN (6 – 8 – 1)	REGRESSION
MARE (%)	15.48%	36.90%
SDE (%)	23.61%	63.10%
R^2	0.894	0.616

Table 4.4 Classification Evaluation Results for ANN and Regression Models

Classification	ANN	REGRESSION
Success (%)	80.38%	61.89%
Failure (%)	19.62%	38.11%
Max. Degree of miss-classification	1	2

CHAPTER 5 –RAPID CHLORIDE TESTING: DEVELOPMENT OF MIX-DESIGN BASED PREDICTION MODEL

5.1 Introduction

As stated before in Chapter 4, permeability is an important factor which is directly related to concrete durability. Permeability of concrete depends on the volume of the interconnected capillary pores in the cement paste, and also on the intensity of microcracks at the aggregate-cement paste interface as well as within the paste itself. The resistance to the movement of water, sulphate ions, alkali ions, other causes of chemical attack can be improved by obtaining low permeability (Alhozaimy *et al.*, 1996). The chloride permeability of concrete is such an inherent property of the concrete needing to be assessed independently, especially in the design and construction of structures to be built in a salt-laden environment. If the chloride concentration of concrete exceeds a certain threshold value, depassivation of the steel occurs and corrosion of reinforcing bars starts to take place (Thomas, 1996; Alonso *et al.*, 2000). Blended (or pozzolanic) cements are being used worldwide to obtain dense and impermeable concrete. They enclose a blend of portland cement clinker and a variety of natural pozzolans and/or supplementary cementing materials such as blast furnace slag, fly ash, silica fume, etc. The use of these materials is also environmentally friendly because it conduces to reduce the CO_2 emission to the atmosphere (Malhotra, 1998). The positive effects of combining these materials are widely discussed in the literature (Examples: Berke, 1989; Swamy, 1991; Hussain, 1994). Permeability of concrete is considerably reduced by using pozzolanic materials. Use of wide range of blending materials of differing chemical composition introduces significant diversity into cementing system. Since pozzolanic reaction is extremely dependent on appropriate curing day, there is often concern as to the effect of curing on the permeability of pozzolanic cement concrete. Manhoman and Mehta (1981) and Nagataki and Ujike (1986) believe that a curing period of about 28-90 days is required for the pozzolanic cement concrete specimens to achieve properties better than that of the plain cement concrete. In a composite material such as concrete, the parameters of the mixture composition and the interactions between them determine the behavior of the material. Some basic properties of concrete depending on the concrete mixture parameters using different mathematical modeling techniques has been modeled by many researchers. Various experimental studies regarding the chloride permeability of the concrete have been conducted over the years. The main governing factors affecting the performance of the concrete against chloride ingress are: curing condition, testing age, water-cement ratio, and mineral admixture such as silica fume, fly ash, slag, etc. (Alhozaimy, 1996; Berke, 1989; Ozyildirim and Halstead, 1994; Guneyisi *et al.*, 2002). For this reason, in this chapter, ANN approach is used to characterize the Rapid Chloride permeability response of concrete by utilizing the mix-design parameters. A regression approach was also used to ensure the developed ANN model has comparable accuracy measures. In the following sections, model development procedure and results are discussed in details.

5.2 Problem Statement

In recent years, as discussed in Chapter 4, the durability problem of the concrete structures has been widespread. Due to its incidents and repair costs, there have been many research investigations (Examples: Feldman *et al.*, 1994; Bassuoni *et al.*, 2005) conducted to better understand the test methods. The ASTM C 1202 test is one of the widespread and easy-to-perform test methods typically preferred by researchers and government agencies. However, its cost, required test equipment and qualified technicians to conduct the sample preparation and test procedure, sample preparation time, and the six hours actual testing time needed are the main issues needing to be addressed. A prediction model based off of mix-design information is proposed to overcome these issues. Thus, in this chapter, the question to be answered with this research is: Can the six hours testing time and sample preparation procedure be replaced, with reasonable degree of accuracy, with a permeability response prediction model?

5.3 Data Description

In this Chapter, a database for ANN model development is collected from the literature (i.e., Ramzanianpour and Malhotra, 1995; Feldman et al., 1999; Oh et al., 2001; Naik et al, 1998; Mackechnie and Alexander, 2000; Ozyildirim, 1994; Feng et al, 2002; Yang and Chiang, 2005; Guneyisi, 1999; Boddy et al., 2001; Gu et al., 1999.) Guneyisi et al. (2009) has evaluated the influence of cement type, curing condition, and testing age on the chloride permeability of concretes by conducting Rapid Chloride permeability test on 90 samples. In this database, five different cement types and two water-cement ratios were deployed. After casting concrete samples, they were subjected to three different curing conditions and tested at the age of 28, 90, and 180 days to determine the chloride permeability of concrete samples through the rapid chloride permeability test. Using this experimental database, ANN model was developed to estimate the chloride permeability of concrete as a function of water-cement ratio (W/C), aggregate-cement ratio (Ag/C), superplasticizer-cement ratio (SP/C), cement type (CT), curing condition (namely, uncontrolled curing (UC), controlled curing (CC), and wet curing (WC)), and testing age (A). In order to properly characterize the permeability of concrete, a total of 128 datasets were used to build the desired database; 57, 39 and 32 datasets were used, respectively, for training, testing and validation purposes. By using the database, the ANN- and Regression-Based models were developed to predict the permeability response in order to choose the best prediction model. Three ANN-based models were developed and the most accurate model has been selected based on the accuracy measure criteria such as Mean Absolute Relative Error (MARE), Average-Squared-Error (ASE) and Coefficient of Determination (R^2) values. The predicted permeability response is computed via Excel-based Program by entering the needed input variables such as Cement Type (CT), Water-cement ratio (W/C), Aggregate-cement ratio (Ag/C), Superplasticizer-cement ratio (SP/C), Curing condition (CC), and Testing age (A). Further details are given in the following sections.

5.3.1 Experimental Program

5.3.1.1 Materials

Five different cements, specifically portland cement (CEM I), Portland composite cements (CEM II/A-M and CEM II/B-M), composite cement (CEM V/A), and blast furnace slag cement (CEM III/A) were used (Guneyisi et al., 2009). These cement types meet the requirements of Turkish Standards (TS EN 197-1), which correspond to European Standard (EN 197-1). The physical and chemical properties with the composition details of the cements are given in Table 5.1. The coarse aggregate was crushed limestone with a maximum particle size of 20 mm whereas the fine aggregate was a mixture of natural and crushed sand. Proporties of the aggregates are depicted in Table 5.2. A sulphonated naphthalene formaldehyde-based superplasticizer was used to obtain a workable and fresh concrete. The properties of the superplasticizer are shown in Table 5.3.

5.3.1.2 Mixture Proportions, Casting and Curing Methods

In the first phase of making concrete, the samples having W/C ratio of 0.65 with a cement content of 300 kg/m^3 were produced. Following that, the samples having W/C ratio of 0.45 with a cement content of 400 kg/m^3 were produced. Five different cements such as CEM I, CEM II/A-M, CEM II/B-M, CEM V/A, and CEM III/A were used in the two phase of making concrete. Gradation of the aggregate mixture was kept constant for all samples. The concrete mixtures designed to have a slump of 17± 2 cm for practical easiness. All concrete mixtures were mixed as per ASTM C192 in a power-driven revolving pan mixer. For each mixture, 18 cylinder samples of 100 mm diameter and 200 mm height were cast for the determination of chloride ion permeability. The specimens were cast in three layers and compacted using a vibrating table. After casting, the molded specimens were covered with a plastic sheet and left in the casting room for 24 hours. They were then demolded and divided into three equal groups and cured under following conditions:

Uncontrolled Curing (UC): Specimens were air cured without controlling the temperature and relative humidity until the testing age. The variable relative humidity and temperature of the room was considered as uncontrolled curing.

Controlled Curing (CC): Specimens were soaked in 20 ± 2ºC water for 7 days and then air cured in a room at 20 ± 1ºC and 50 ± 5% relative humidity until the testing age.

Wet Curing (WC): Specimens were soaked in 20 ± 2ºC water until the testing age.

5.3.1.3 Test Procedure

The rapid chloride permeability test was conducted to determine the resistance of the concrete to the penetration of chloride ions according to AASHTO T277 as discussed in Section 4.1.3.

5.4 ANN Model Development

The ANN model was developed in four sequential stages. In the first stage, the ANN architecture was determined based on problem characteristics and ANN knowledge, and input and output categories were chosen accordingly. This step also includes classifying the datasets as training, testing or validation sets. In the second stage, the network was trained and tested on the experimental data to obtain the optimum number of hidden nodes and iterations for the ANN architecture determined in stage one. In the third stage, the best performing network obtained from the second stage was validated on the validation database. If accuracy measures from training, testing and validation database are very comparable, then the model may not be trained on all data. In the fourth stage, the best performing network obtained in the second stage is retrained on all experimental data to increase the prediction accuracy and evaluate how well the ANN model characterized the desired behavior. Normally, retraining the network with all experimental data is expected to provide reliable predictions and accuracy measures if the dataset classification is done in an appropriate manner. However, it has been shown through several research studies by Najjar and Coworkers [Najjar & Mandavilli (2004), Najjar & Mryyan (2009), and Najjar et al. (2003)] that stage four is recommended to arrive at a better performing network model.

5.4.1 ANN Model Architecture

Based on the knowledge gained from experimental data analysis, ANN model architecture has been built by considering 12 inputs and 1 output, which respectively are:

1. (CT1) Cement Type (CEM I=1, CEM II/A-M=0, CEM II/B-M =0, CEM V/A=0, and CEM III/A=0)
2. (CT2) Cement Type (CEM I=0, CEM II/A-M=1, CEM II/B-M =0, CEM V/A=0, and CEM III/A=0)
3. (CT3) Cement Type (CEM I=0, CEM II/A-M=0, CEM II/B-M =1, CEM V/A=0, and CEM III/A=0)
4. (CT4) Cement Type (CEM I=0, CEM II/A-M=0, CEM II/B-M =0, CEM V/A=1, and CEM III/A=0)
5. (CT5) Cement Type (CEM I=0, CEM II/A-M=0, CEM II/B-M =0, CEM V/A=0, and CEM III/A=1)
6. (W/C) Water-cement Ratio
7. (Ag/C) Aggregate-cement Ratio
8. (SP/C) Superplasticizer-cement Ratio
9. (CC1) Curing Condition (UC=1, CC=0, and WC=0)
10. (CC2) Curing Condition (UC=0, CC=1, and WC=0)

11. (CC3) Curing Condition (UC=0, CC=0, and WC=1)
12. (A) Testing Age

and

1. Output (Q): Total charge passed through the concrete sample (coulombs)

Instead of using 6 inputs, twelve inputs were used because the cement type was categorized in 5 groups and curing condition was categorized in 3 groups. The reason for the categorizations of cement type and curing condition is that there is no mathematical relation among the sub-categories which can be expressed numerically. Since only one of the sub-categories can be used at a time, categorical variables were used to model these inputs parameters to evaluate the correlation between cement type and the permeability response as well as curing condition and the permeability response. For this reason, five different cement types were considered as individual inputs which are, respectively, CEM I (CT1), CEM II/A-M (CT2), CEM II/B-M (CT3), CEM V/A (CT4) and CEM III/A (CT5) and curing condition as UC (CC1), CC(CC2) and WC (CC3). For instance, if cement type and curing condition are specified ,respectively, CEM I and Uncontrolled curing, then CT1 is coded as "1", all other cement types, CT2, CT3, CT4, and CT5, are as "0" and CC1 is coded as "1" and other curing conditions, CC2 and CC3, are coded as "0".

In this study, 3 models giving appropriate statistical measures have been selected based on optimum hidden nodes, minimum values of Mean Absolute Relative Error (MARE) and Averaged-Squared-Error (ASE) and maximum values of Coefficient of Determination (R^2). A total of 128 datasets were used to build the desired database; 57, 39 and 32 sub-database were used, respectively, for training, testing and validation purposes. Datasets which include minimum and maximum values of each variable were included in the training phase in order for the network to represent the characteristics of the response. The maximum and minimum ranges of each input/output variable for ANN model development were chosen on purpose to be wider than their actual ranges for better mathematical mapping.

5.4.2 Model Training and Testing

Based on statistical measures such as Averaged-Squared-Error (ASE), Coefficient of determination (R^2) and Mean Absolute Relative Error (MARE), the optimal network structure for the Model 1 was found at 5 hidden nodes and 4,500 iterations. The corresponding accuracy measures for this network are ASE_{tr}=0.001242, R^2_{tr}=0.972, $MARE_{tr}$=8.46% (for training database) and ASE_{ts}=0.010815, R^2_{ts}=0.785, $MARE_{ts}$= 27.22% (for testing database). The optimal network for Model 2 was found at 4 hidden nodes and 4,900 iterations. The corresponding accuracy measures for this network are ASE_{tr}=0.001812, R^2_{tr}=0.960, $MARE_{tr}$=14.48% (for training database) and ASE_{ts}=0.007625, R^2_{ts}=0.831, $MARE_{ts}$= 27.83% (for testing database). The optimal network for Model 3 was found at 6 hidden nodes and 600 iterations. The corresponding accuracy measures for this network are ASE_{tr}=0.009302, R^2_{tr}=0.854, $MARE_{tr}$=18.52% (for training database) and ASE_{ts}=0.01043, R^2_{ts}=0.780, $MARE_{ts}$= 27.48% (for testing database). The training graphical comparison plots between predicted and actual response for Model 1, Model 2 and Model 3 are shown, respectively, in Figure 5.1, Figure 5.2 and Figure 5.3. The testing graphical comparison plots between predicted and actual response for Model 1, Model 2 and Model 3 are shown, respectively, in Figures 5.4, 5.5 and 5.6. Also, statistical accuracy measures for the training and testing are shown in Table 5.4 while the best performing model is identified in bold.

5.4.3 Model Validation

After training and testing, respectively, on 57 and 39 datasets, validation is conducted by using the remaining 32 datasets. After classifying the datasets as training, testing, and validation as described in Section 5.4, the network was trained and tested on experimental data to obtain the optimum number of hidden nodes and iterations for the ANN architecture determined in stage one. For the model validation, the third stage is performed by utilizing the best performing network, identified in stage two, to predict the output of the validation datasets. The graphical comparison plots between predicted and actual response, for validation datasets, for Model 1, Model 2 and Model 3 are shown, respectively, in Figures 5.7, 5.8 and 5.9. Also, corresponding statistical accuracy measures are shown in Table 5.4 where the best performing network is identified in bold.

5.4.4 Model Selection

Statistical accuracy measures for training and testing databases for, Model 1, at optimal ANN structure with 5 hidden nodes and 4,500 iterations showed better prediction accuracy compared with those for Model 2 and 3. Even though Model 3 has a better accuracy with validation dataset, Model 1 has overall the best performance. For this reason, Model 1 has been chosen to be used as the best network structure. Thus, all of the 128 datasets from the Rapid Chloride test were used to retrain the network at this optimal structure to obtain the generalized response throughout the entire database. Statistical measures of Model 1 trained with all data are: ASE_{all}=0.002965, R^2_{all} =0.93 and $MARE_{all}$=15.68%. The graphical comparison plots between predicted and actual response for Model 1, Model 2 and Model 3 are shown, respectively, in Figures 5.10, 5.11 and 5.12. Statistical accuracy measures for all 3 models are shown in Table 5.4. The good agreement between predicted results and experimentally acquired results is apparent. The network structure of the best performing model (Model 1) is depicted in Figure 5.13.

5.5 Regression Model

Regression model development, discussed in Chapter 4, has been accomplished using Excel Data Analysis Toolkit. For the regression model development, categorical variables are also used similar to ANN Model development, discussed in Section 5.4.1. The 128 datasets used for ANN-Model development were utilized herein to obtain the regression prediction model. The input variables and the output as used in ANN-Model development are respectively:

Inputs:

1. X_1= (CT1) Cement Type (CEM I=1, CEM II/A-M=0, CEM II/B-M =0, CEM V/A=0, and CEM III/A=0)
2. X_2= (CT2) Cement Type (CEM I=0, CEM II/A-M=1, CEM II/B-M =0, CEM V/A=0, and CEM III/A=0)
3. X_3= (CT3) Cement Type (CEM I=0, CEM II/A-M=0, CEM II/B-M =1, CEM V/A=0, and CEM III/A=0)
4. X_4= (CT4) Cement Type (CEM I=0, CEM II/A-M=0, CEM II/B-M =0, CEM V/A=1, and CEM III/A=0)

5. X_5= (CT5) Cement Type (CEM I=0, CEM II/A-M=0, CEM II/B-M =0, CEM V/A=0, and CEM III/A=1)
6. X_6= (W/C) Water-cement Ratio
7. X_7= (Ag/C) Aggregate-cement Ratio
8. X_8= (SP/C) Superplasticizer-cement Ratio
9. X_9= (CC1) Curing Condition (UC=1, CC=0, and WC=0)
10. X_{10}= (CC2) Curing Condition (UC=0, CC=1, and WC=0)
11. X_{11}= (CC3) Curing Condition (UC=0, CC=0, and WC=1)
12. X_{12}= (A) Testing Age

Output:

1. Output (Q): Total charge passed through the concrete sample (coulombs)

Using linear regression approach, the following equation was developed;

$$\begin{aligned} Q = &-1299 + 2143.42X_1 + 1409.22X_2 - 822.35X_4 - 1438.49X_5 + 25056.35X_6 - 1642.99X_7 \\ &- 2979.63X_8 - 1599.57X_{10} - 1966.57X_{11} - 9.70X_{12} \end{aligned} \qquad 5.1$$

Statistical measures of linear regression model obtained using Excel Data Analysis Toolkit are: MARE (%) = 32.68%, R^2_{all} = 0.676 and Standard Deviation of Error, SDE, (%) = 56.2%. The graphical comparison plots between predicted and actual response is shown in Figure 5.14. Comparison between accuracy measures of ANN Model and Regression Model are depicted in Table 5.5. It is very evident from the comparison plots in Figure 5.10 and 5.14 that the ANN model is out performing the regression-based model. It is possible to increase the accuracy measures of the regression model by non-linear regression. However, the effort spent on this task will be unbounded since many trials have to be performed. Over the past 17 years, Najjar and Coworkers [Najjar & Ali (1998a, b), Najjar & Basheer (1996a), and Najjar et al. (1996b)] have shown that the best non-linear regression model will not produce accuracy measures that are better than those obtained via an appropriately developed ANN-based model. Typically, the accuracy measures by the ANN-based model are the upper bounds to any non-linear regression model describing the same behavior.

5.6 Excel Application

Even though twelve input variables were used in ANN and Regression model development process, the developed excel application has only 6 input variables because the codification process of cement type and curing condition in the excel application are programmed by excel operational functions. By using the connections weights, threshold values and coefficients which are described in Chapter 3, the excel-based application is developed. In this application, by entering the appropriate input variables for Cement Type, Water-cement ratio, Aggregate-cement ratio, Superplasticizer-cement ratio and Testing age in the Excel interface shown in Figure 5.15, chloride permeability response is calculated automatically by ANN and Regression Models. Following that, ANN- and Regression-based models utilize all 6 input values to predict the corresponding permeability value (i.e., the charge passed through the sample). The computed permeability response values and categorical variables, converted using table 4.1, by ANN and Regression are placed in the output cells colored with blue as depicted in Figure 5.15. The applicable ranges for the input variables are also shown in Figure 5.15. Any value of input variable that is outside the applicable range may cause the models to produce unreliable predictions.

5.7 Concluding Remarks

In this chapter, a static artificial neural network with backpropagation learning algorithm was developed to predict the Rapid Chloride permeability response of concrete. As seen from the graphical results depicted in Figures 5.1 to 5.12 and the accuracy measures of the developed ANN models listed in Table 5.4, Model 1 has been selected to characterize the permeability response. The comparison of the predicted responses by ANN and Regression shown in Table 5.5 indicates that ANN model attains better prediction accuracy than the Regression model. It is apparent that the ANN model has efficiently characterized the Rapid Chloride test response when compared to the regression model. Moreover, the predicted permeability responses by ANN and Regression models are converted to categorical variables using Table 4.1 and evaluated in terms of success and failure classification cases. The results of classification evaluation in terms of success and failure percentages, depicted in Table 5.6, have shown a good trend between predicted-based and actual-based categorical results. Therefore, ANN-based model can reliably be used for permeability prediction tasks to reduce the duration of the 6 hours testing period and sample preparation period as long as the input variables fall within the applicable ranges. Moreover, developed ANN model can be used to verify measured responses for planned-to-be conducted Rapid Chloride tests without the need for any additional experimental-based information. Even though the development of the ANN model requires good fundamental understanding of the Rapid Chloride Test procedure and ANN knowledge, an Excel-based application, which is the utilization tool of ANN model, is simple and does not require for the user to have specific knowledge needed for model development. ANN model overcomes the drawback of the 6 hours testing time and sample preparation procedure; making it a powerful, rapid, and low cost alternative to obtain the permeability of concrete with a reliable level of accuracy. As a result, it can be inferred that the developed ANN model has high prediction accuracy for the chloride permeability of concrete samples when presented with the appropriate water-cement ratio, aggregate-cement ratio, superplasticizer-cement ratio, cement type, curing condition, and testing age. This study has proven that ANN approach is an effective function approximation method that can also be used for modelling concrete mixture properties.

5.8 Figures and Tables

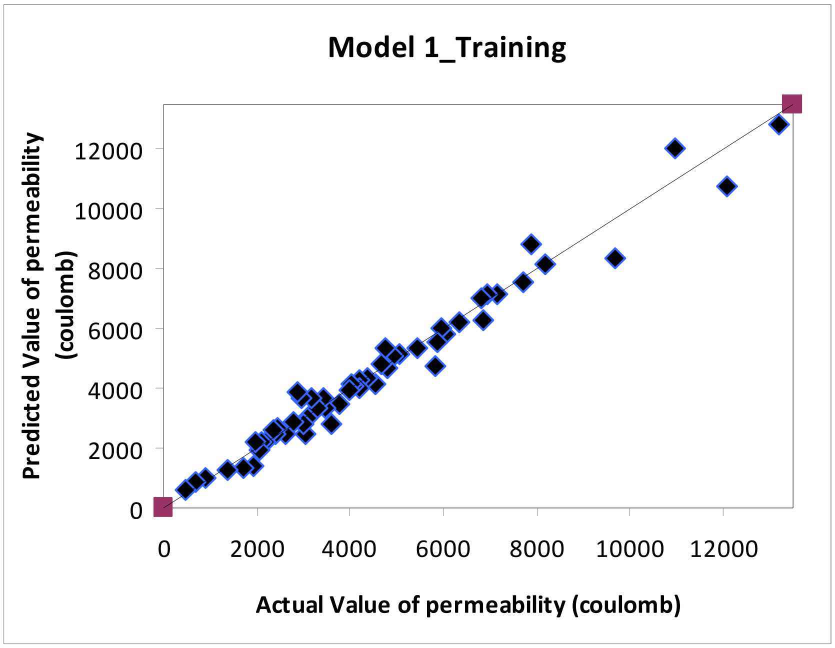

Figure 5.1 Training Graphical Prediction Accuracy for the Model 1

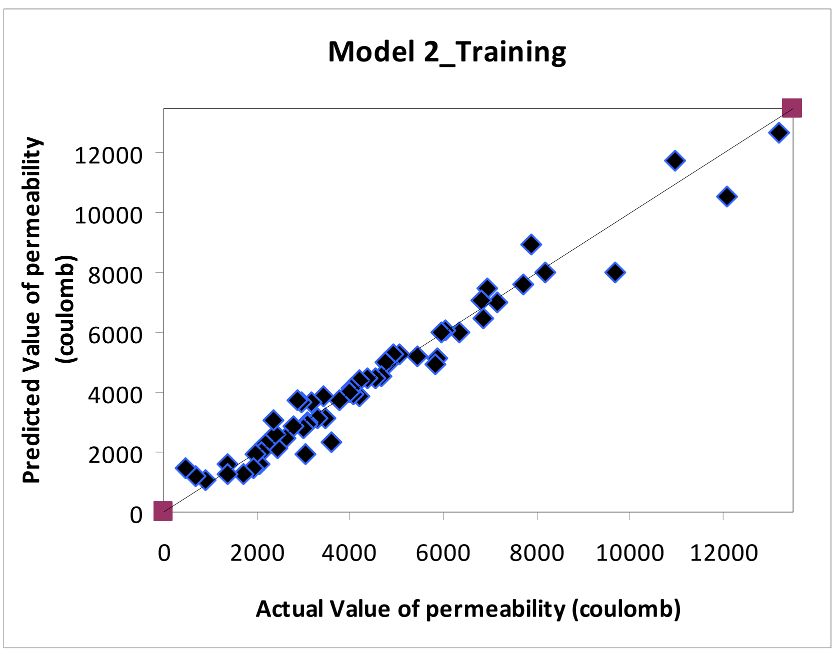

Figure 5.2 Training Graphical Prediction Accuracy for the Model 2

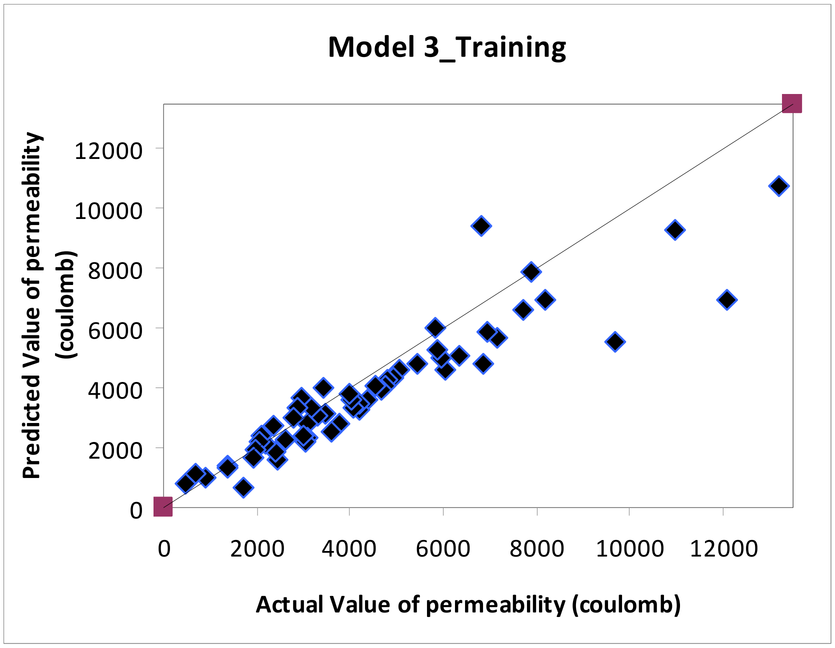

Figure 5.3 Training Graphical Prediction Accuracy for the Model 3

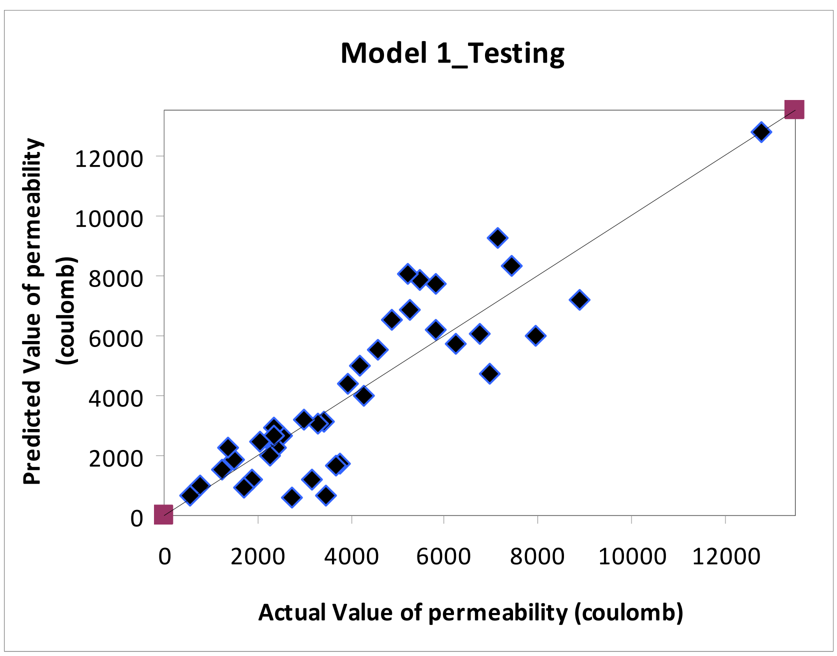

Figure 5.4 Testing Graphical Prediction Accuracy for the Model 1

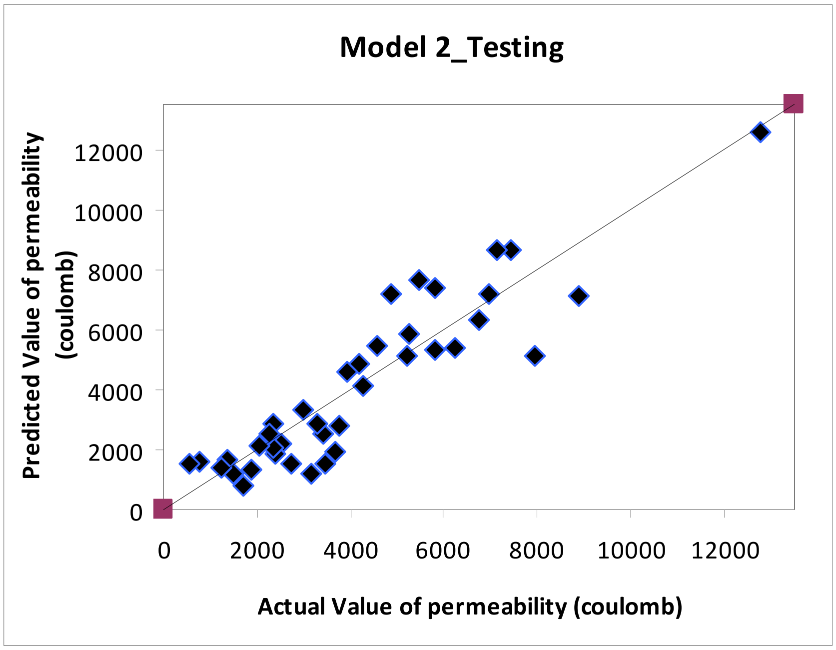

Figure 5.5 Testing Graphical Prediction Accuracy for the Model 2

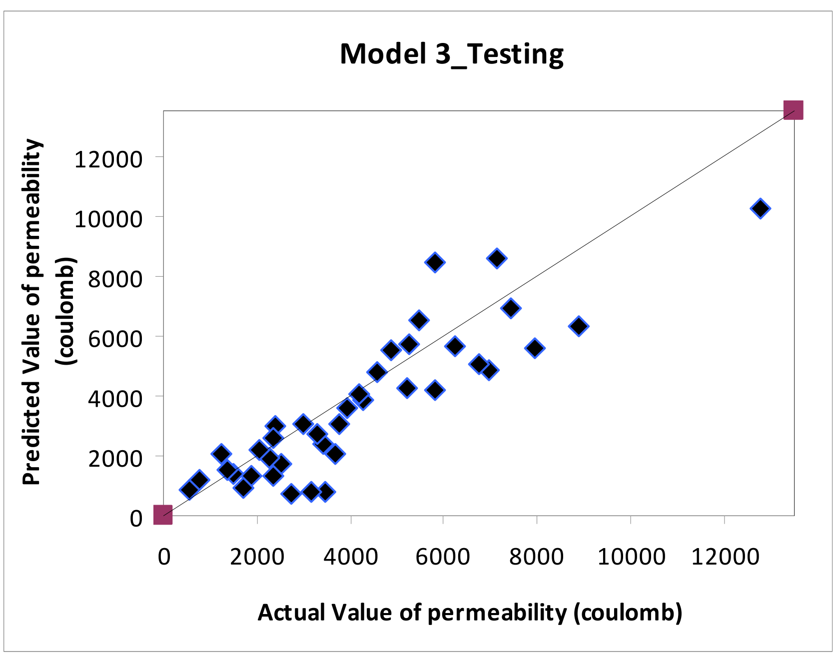

Figure 5.6 Testing Graphical Prediction Accuracy for the Model 3

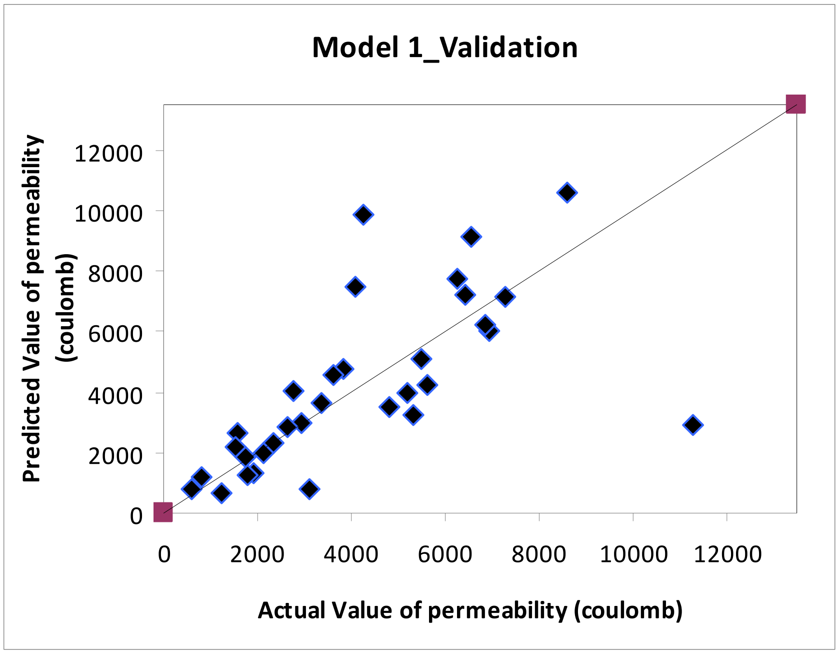

Figure 5.7 Validation Graphical Prediction Accuracy for the Model 1

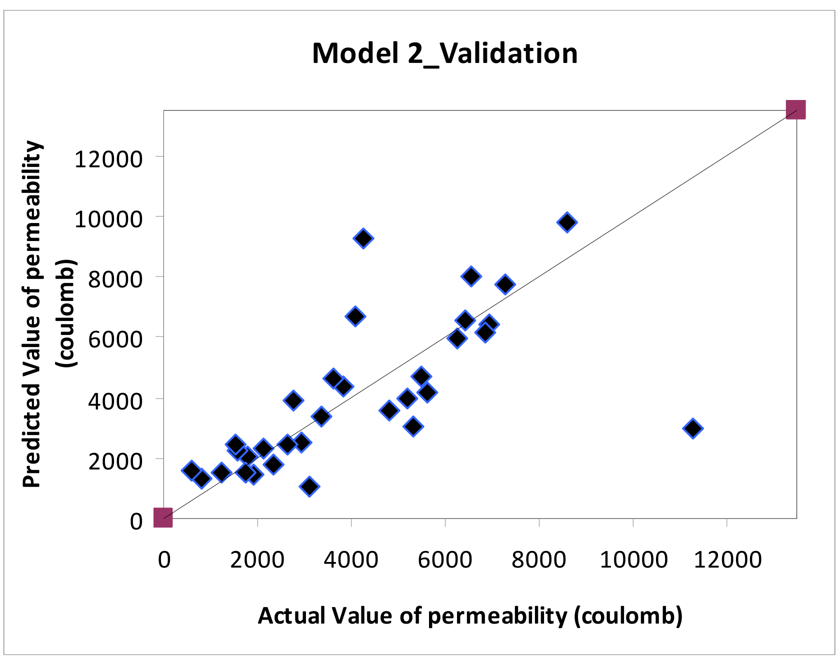

Figure 5.8 Validation Graphical Prediction Accuracy for the Model 2

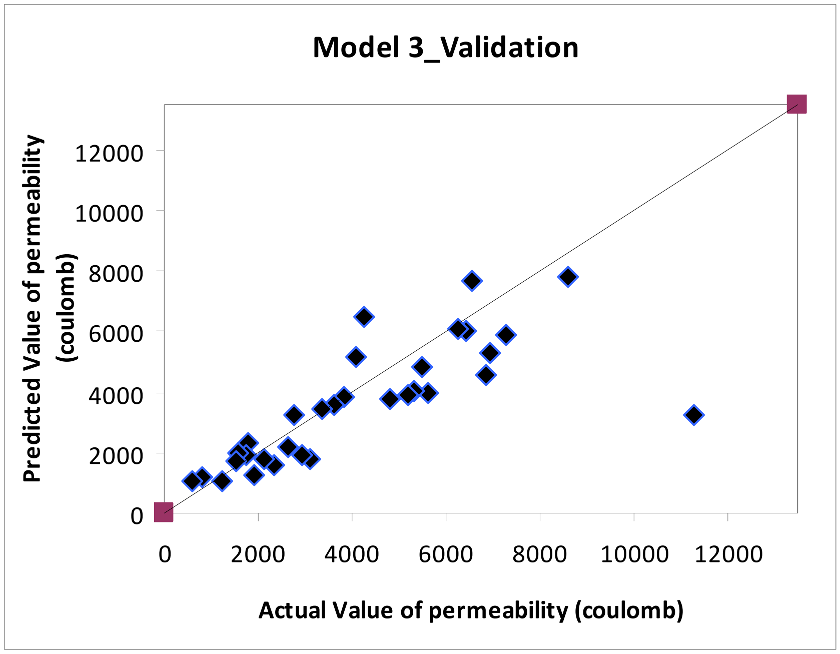

Figure 5.9 Validation Graphical Prediction Accuracy for the Model 3

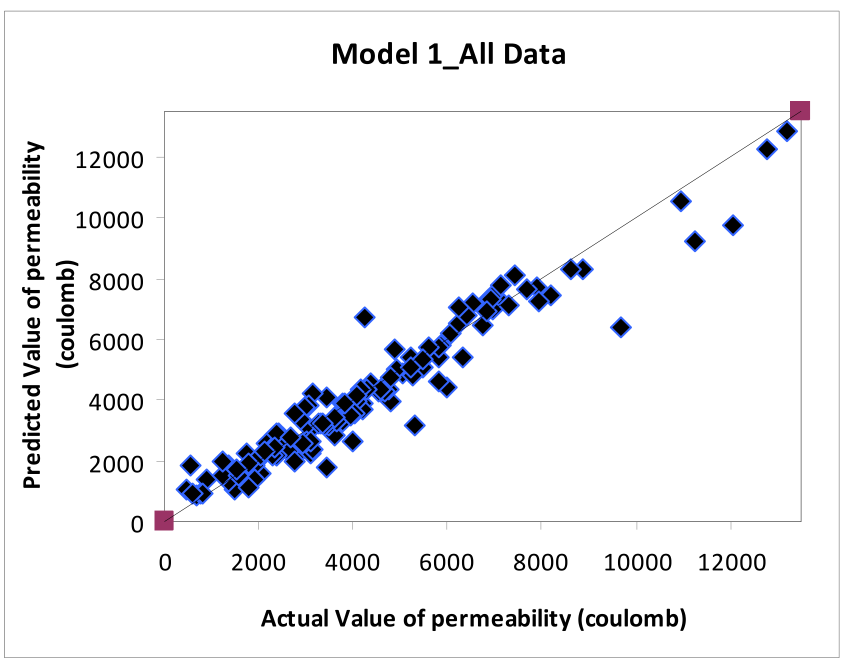

Figure 5.10 All Data Graphical Prediction Accuracy for the Model 1

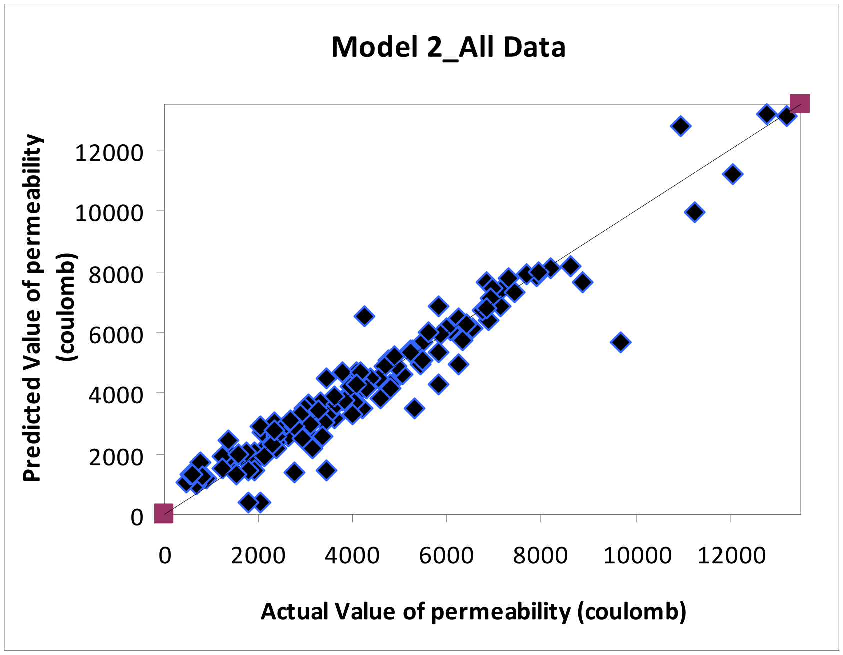

Figure 5.11 All Data Graphical Prediction Accuracy for the Model 2

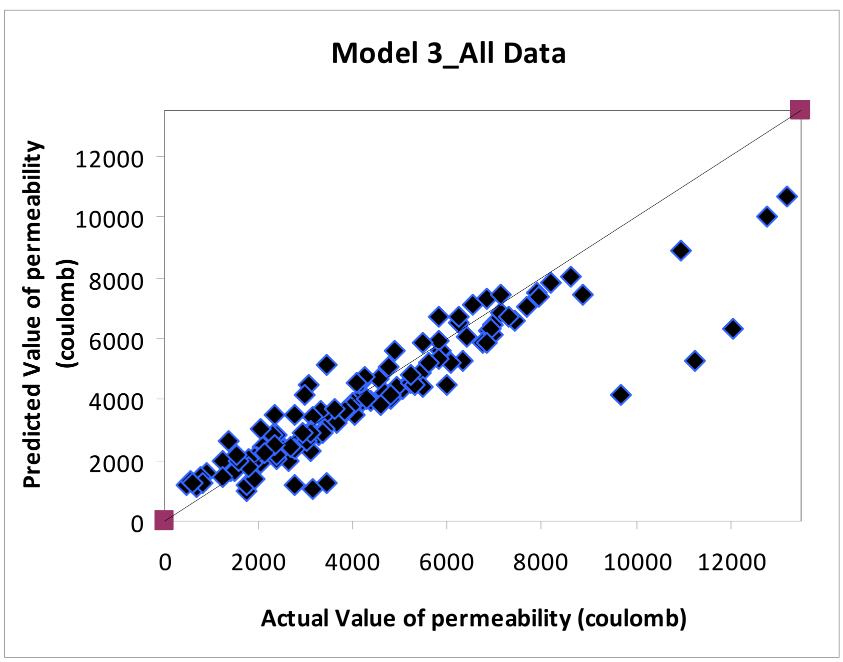

Figure 5.12 All Data Graphical Prediction Accuracy for the Model 3

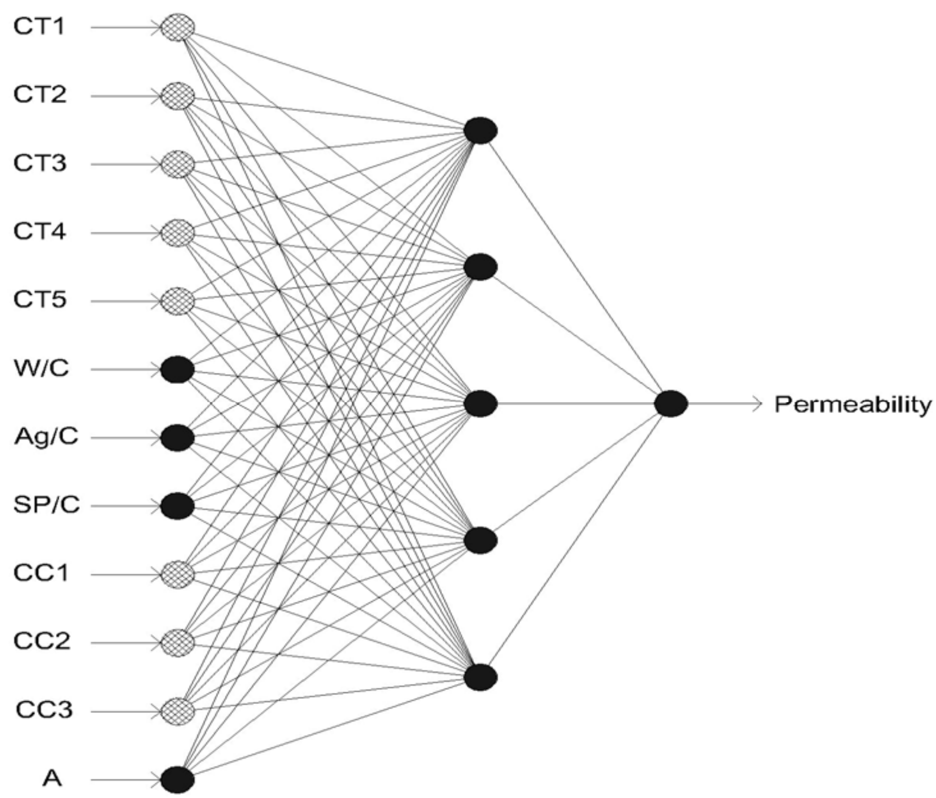

Figure 5.13 The Network Structure of the Best Performing Model (Model 1)

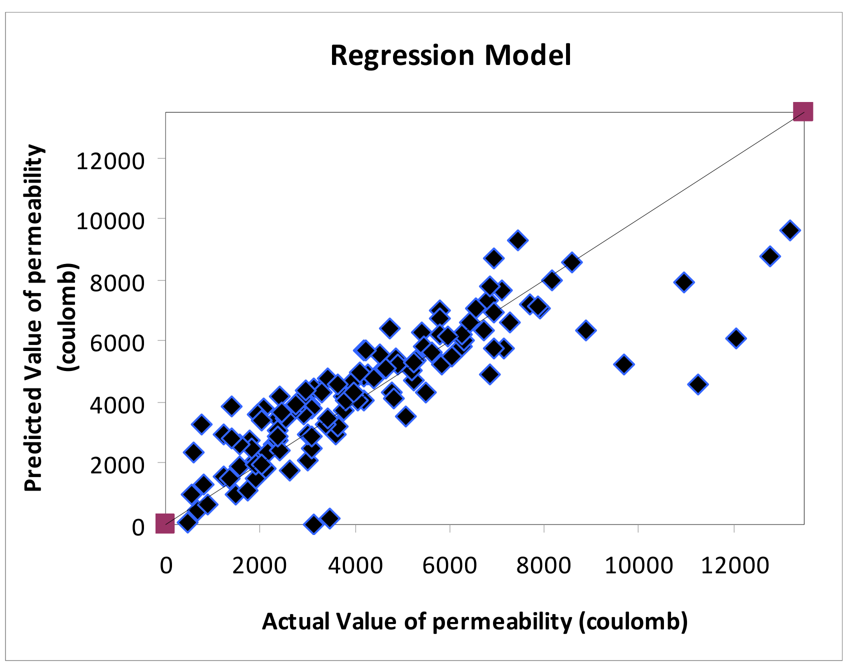

Figure 5.14 Graphical Prediction Accuracy for the Regression Model

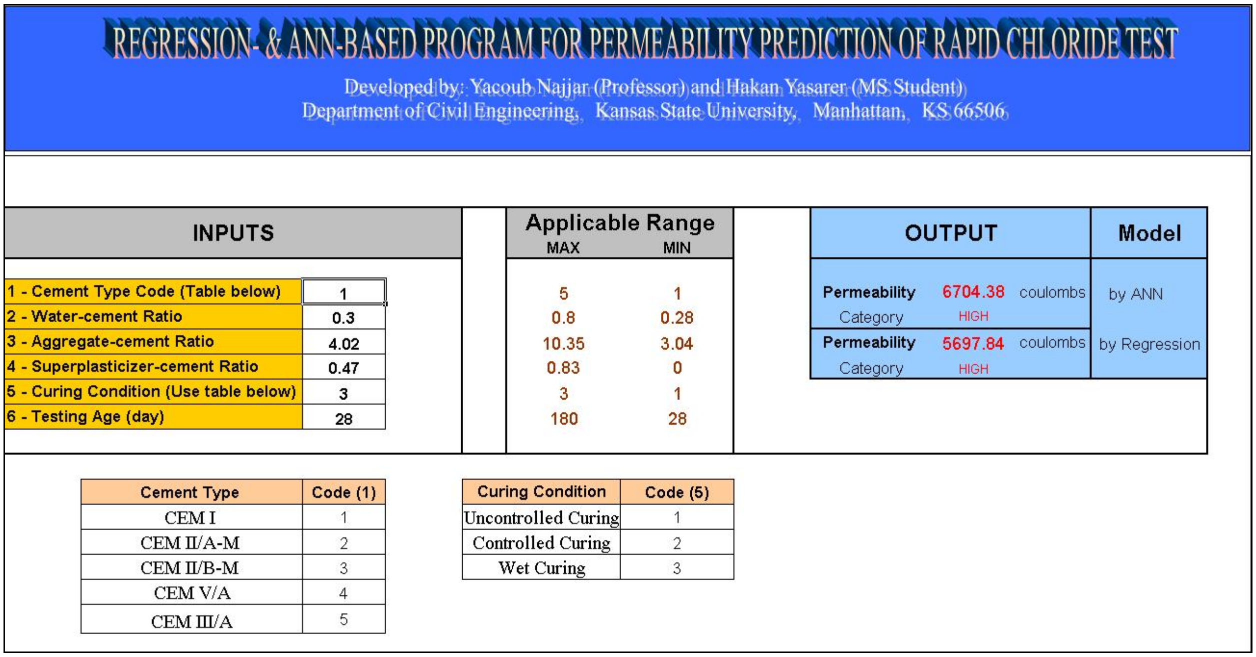

Figure 5.15 Excel Application Screen-shot

Table 5.1 Properties of cements used (redrawn from Guneysi, 2009)

Chemical Composition	CEM I	CEM II/A-M	CEM II/B-M	CEM V/A	CEM III/A
Silicone dioxide,	20.64	18.38	28.34	25.63	28.81
Aluminum oxide,	5.06	5.05	7.33	5.06	7.2
Ferric Oxide,	3.14	2.89	2.89	3.72	2.31
Calcium Oxide ,	63.98	61.78	52.55	48	49.94
Magnesium Oxide ,	1.2	1.36	2.09	-	4.44
Sulfur trioxide,	2.38	2.34	2.88	2.3	2.41
Sodium oxide,	0.31	0.28	0.21	-	0.15
Potassium oxide,	0.8	0.73	-	-	0.87
Chloride,	0.035	0.036	-	0.01	0.027
Insoluble residue,	0.46	0.48	7.8	-	0.64
Loss of ignition	1.72	6.44	1.16	-	0.83
Free lime	1.41	1.44	0.35	-	0.83
Results of physical tests					
Specific Gravity	3.15	3.12	3.01	3.05	2.94
Vicat (hour:minute)					
Start	02:28	02.28	02:40	02:32	02:40
Stop	03:02	03:08	03:30	03:22	03:30
Le Chatelier (mm)	2	2	1	1	1
Fineness(%)					
45μm	11.7	18.1	-	-	1.3
90μm	0.8	3	6.4	0.2	0.0
200μm	0.0	0.4	0.7	-	-
Specific Surface (m^2/kg)	336	334	406	430	464
$f_{cc}(2\,day)(MPa)$	27.5	23.7	23.1	20	13.3
$f_{cc}(7\,day)(MPa)$	41.3	39	35.9	31	24.6
$f_{cc}(28\,day)(MPa)$	51.4	46.2	51.2	45	-
Component fraction in cement (% by height)					
Clinker, K	95.5	78.7	70.5	57.5	46.7
Blast Furnace Slag, S	0	2.0	13.0	21.8	48.3
Limestone, L	0	11.9	0	3.0	0
Natural Pozzolans, P	0	3.2	13.0	12.6	0
Gypsum	4.5	4.2	3.5	5.1	5.0
Total	100	100	100	100	100

Table 5.2 Sieve analysis and physical properties of aggregates (redrawn from Guneysi, 2009)

Sieve Size	Fine Aggregate		Course Aggregate	
	Natural Sand	Crushed Sand	No I	No II
31.5	100	100	100	100
16.0	100	100	100	76.9
8.0	100	98.7	62.6	1.6
4.0	98.2	89.8	22.8	0.9
2.0	94.8	53.6	3.5	0.7
1.0	91.2	34.6	2.3	0.6
0.50	82.3	22.3	1.8	0.2
0.25	14.3	9.5	1.4	0.2
Fineness modulus	1.19	2.92	5.06	6.19
Specific Gravity	2.60	2.69	2.70	2.70
Absorbtion	0.50	1.00	0.50	0.40

Table 5.3 Properties of the superplasticizer (redrawn from Guneysi, 2009)

SG	State	Freezing Point	Color	Chloride Content	Nitrate Content	Main Component
1.22	Liquid	-4	Dark Brown	None	None	Sulphonated Naphthalene

Table 5.4 Statistical Accuracy Measures of the ANN-Models

Model		**Model 1**	Model 2	Model 3
Architecture		**12-(4-5-9-4500)-1**	12-(3-4-9-4900)-1	12-(6-6-9-600)-1
Training	MARE(%)	**8.46%**	14.48%	18.52%
	R2	**0.97239**	0.95978	0.85477
	ASE	**0.001242**	0.001812	0.009302
Testing	MARE(%)	**27.22%**	27.83%	27.48%
	R2	**0.78471**	0.83083	0.78019
	ASE	**0.010815**	0.007625	0.01043
Validation	MARE(%)	**32.05%**	33.33%	24.62%
	R2	**0.43369**	0.44789	0.56189
	ASE	**0.028268**	0.024029	0.018297
All Data	MARE(%)	**15.68%**	17.75%	20.68%
	R2	**0.93012**	0.92135	0.82852
	ASE	**0.002965**	0.00324	0.008192
Final Structure		**12 - 5 - 1**	12 - 4 - 1	12 - 6 - 1

Table 5.5 Comparisons of Statistical Accuracy Measures for ANN and Regression Models

Statistical Measures	ANN (12 - 5 - 1)	REGRESSION
MARE (%)	15.68%	32.68%
SDE (%)	21.71%	56.20%
R^2	0.930	0.676

Table 5.6 Classification Evaluation Results for ANN and Regression Models

Classification	ANN	REGRESSION
Success (%)	89.06%	75 %
Failure (%)	10.94%	25%
Max. Degree of miss-classification	1	4

CHAPTER 6 – BOIL TESTING: DEVELOPMENT OF KDOT-BASED PREDICTION MODEL

6.1 Introduction

Permeability of the concrete in a portland cement concrete pavement is a major factor for long-term durability. The permeability of concrete depends on its pore network, which comes primarily from the excess water used during mixing in the initial hardening process. The porosity of concrete consists of closed or logged pores in addition to a network of interconnected pores (Saraswathy, 2008). Pore size ranges from a few angstroms to about 100 A° for the so called 'gel pores', from 100 to 100000 A° in 'capillary pores', and a few millimeters in 'air or large pores'. Inter connected pores endow the concrete permeability. All the hydrated cement products are subjected to attack by sulphates, chlorides and acids, and water. This is because of a low equilibrium solubility of the hydrated components and low mass transfer of well cured concrete. It is a common practice to evaluate the water permeability characteristics when assessing the durability characteristics. Permeability can be measured by conducting standard test methods. In this chapter, % of water absorption, % of permeable voids and % of total voids have been determined as per ASTM C 642-97. This test was done as per procedure given in ASTM C 642-97 by oven-drying method. In this chapter, the measurements as part of ASTM C 642-97 such as Oven-dry mass (A), Saturated surface-dry weight (B) and Curing time (CT) were used to develop prediction models by ANN and Regression to predict Saturated surface-dry weight after boiling(C), and Weight in water after boiling (D). Therefore, two models are developed to predict C and D individually using the same database. Finally, absorption after immersion and boiling, bulk density, bulk density after immersion, bulk density after immersion and boiling, apparent density, and volume of permeable pore space (voids) can be calculated by the equations provided in the following sections. A, B, C, D and CT are the only values used for model development. However, volume of permeable pore space is the final value calculated out of A, C and D and was used for accuracy measure comparisons accordingly. In this chapter, ANN approach was used to model the absorption and volume of permeable voids of concrete. Regression approach was also used to ensure the developed ANN model has comparable accuracy measures. In the following sections, the test method procedure and model development procedure are described in details.

6.2 Problem Statement

In recent years, durability problems in concrete structures have been widespread. Due to the high number of incidents and repair costs, there have been many research investigations (Examples: Feldman *et al.*, 1994; Bassuoni *et al.,* 2005) conducted to better understand the test methods. For this reason, the Boil Test has been used as an alternative method for Rapid Chloride Permeability which the researchers and government agencies use. However, the five hour actual testing time needed have made contractors and inspectors hesitant to require the test. During the summer time, the construction industry is really active and because of that numerous amounts of concrete samples, either collected in the field or mixed in the lab by the government agencies, are placed in the curing room for 7, 28, and 56 days and will be processed for testing at later dates. However, due to inadequate amount of test equipments, concrete samples must be kept in curing room for more than 56 days. This is the reason that concrete samples in the database used have an age range from 7 to 96 days. A prediction model is proposed to overcome these issues. Thus, in this chapter, the question to be answered with this research is: Can the five hours boil testing time be replaced, with reasonable degree of accuracy, with a permeability response prediction model?

6.3 Data Description

The database for the development of the boil void prediction model was provided by KDOT. The samples included in the database were either prepared in the laboratory or collected in the field. In order to properly characterize the permeability of concrete, a total of 414 datasets were used to build the desired database; 211, 112 and 91 datasets are used, respectively, for training, testing and validation purposes. By using the database, the ANN- and Regression-Based models are developed to predict the boil permeability response in order to choose the best prediction model. Three ANN-based models are developed and the most accurate model has been selected based on the accuracy measure criteria such as Mean Absolute Relative Error (MARE), Average-Squared-Error (ASE) and Coefficient of Determination (R^2) values. The predicted permeability response is computed via Excel-based Program by entering the needed input variables such as oven dry weight (A), saturated surface dry weight (B), and curing time. Further details are given in the following sections.

6.3.1 Laboratory Procedure

For this test, three samples per mix design are prepared and tested separately. The samples shall consist of 2" thick by 4" diameter specimens taken from the top portion of cylinders or cores. It is specified in ASTM C 642-97 that the volume of the each portion shall not be less than 350 cm^3; and each portion shall be free from observable cracks, fissures, or shattered edges.

6.3.1.1 Oven Dry Mass (A)

After determining the mass of the portions, they are oven dried at 100 to 110^{o}C for not less than 24 hours. After removing each specimen from the oven, they are allowed to cool in a desiccator to a temperature of 20 to 25^{o}C, after which the mass is determined. If the specimen is comparatively dry when its mass is first determined, and the second mass closely agrees with the first, consider it dry. If the specimen is wet when its mass is first determined, it needs to be replaced in the oven for a second drying treatment of 24 hours and the mass determination is done again. If the third value checks with the second, it is considered as dry. In case of any doubt, the specimen can be redried for 24 hours until the check values of mass are obtained. If the difference between values obtained from two successive values of mass exceeds 0.5% of the lesser value, the specimen is returned to the oven for an additional 24 hours drying period, and the procedure is repeated until the difference between any two successive values is less than 0.5% of the lowest value obtained. This value is designated as A.

6.3.1.2 Saturated Mass after Immersion (B)

After final drying, cooling, and the determination of mass, the specimen is immersed in water at approximately 21^{o}C for not less than 48 hours until two successive values of mass of the surface-dried sample at intervals of 24 hours show an increase in mass of less than 0.5% of the larger value. The surface of the specimen is dried by removing surface moisture with a towel, after which the specimen mass is determined. The final surface-dry mass after immersion is designated as B.

6.3.1.3 Saturated Mass after Boiling (C)

The specimen processed as described in 6.3.1.2 is placed in a suitable receptacle, covered with tap water, and boiled for 5 hours. Then, it's allowed to cool by natural loss of heat for not less than 14 hours to a final temperature of 20 to 25^{o}C. The surface moisture is removed by a towel and the mass of the specimen is determined. The soaked, boiled, and surface-dried mass is designated as C.

6.3.1.4 Immersed Apparent Mass

The specimen is suspended in a container covered up with water by a wire and then its submerged weight is determined. This apparent mass is designated as D.

6.3.1.5 Calculation

By using the values determined in accordance with the procedure described, absorption after immersion and boiling, bulk density, bulk density after immersion, and bulk density after immersion and boiling, and apparent density, the volume of permeable pore space (voids) can be calculated using following equations:

$$\text{Absorption after immersion (\%)} = \left[\frac{\text{B - A}}{\text{A}}\right] \times 100 \qquad 6.1$$

$$\text{Absorption after immersion and boiling (\%)} = \left[\frac{C - A}{A}\right] \times 100 \qquad 6.2$$

$$Bulk\ density\,(dry) = g_1 = \left[\frac{A}{C - D}\right] \times \rho \qquad 6.3$$

$$Bulk\ density\ after\ immersion = \left[\frac{B}{C - D}\right] \times \rho \qquad 6.4$$

$$Bulk\ density\ after\ immersion\ and\ boiling = \left[\frac{C}{C - D}\right] \times \rho \qquad 6.5$$

$$Apparent\ density = g_2 = \left[\frac{A}{A - D}\right] \times \rho \qquad 6.6$$

$$\text{Volume of permeable pore space (voids(\%))} = \left[\frac{g_2 - g_1}{g_2}\right] \times 100 \ \ or\ \left[\frac{C - A}{C - D}\right] \times 100 \qquad 6.7$$

where:

A = Mass of oven-dried sample in air (grams)

B = Mass of surface-dry sample in air after immersion (grams)

C = Mass of surface-dry sample in air after immersion and boiling (grams)

D = Apparent mass of sample in water after immersion and boiling (grams)

g_1 = Bulk density (Mg/m^3)

g_2 = Apparent density (Mg/m^3)

ρ = Density of water ($1\ Mg/m^3 = 1\ g/cm^3$)

It is noted in ASTM C 642-97 that this test method does not involve a determination of absolute density. Hence, such pore space as may be present in the specimen that is not emptied during the specified drying or is not filled with water during the specified immersion and boiling or both is considered "impermeable" and is not differentiated from the solid portion of the specimen for the calculations, especially those for percent voids. Depending on the pore size distribution and the pore entry radii of the concrete and on the purposes for which the test results are desired, the procedures of this test method may be adequate, or they may be insufficiently accurate. In the event that it is desired to fill more of the pores than will be filled by immersion and boiling, various techniques involving the use of vacuum treatment or increased pressures may be used. If a rigorous measure of total pore space is desired, this can only be obtained by determining absolute density by first reducing the sample to discrete particles, each of which is sufficiently small so that no impermeable pore space can exist within any of the particles. If the absolute density were determined and designated g_3, then:

$$\text{Total void volume}\,(\%) = \left[\frac{g_3 - g_1}{g_3}\right] \times 100 \qquad 6.8$$

Since there is no reference standard available for comparison, bias for this test method can not be determined. So, in this study, it is not aimed to come up with a discussion of whether or not this test method is reliable. However, some of results are evaluated to better understand the test method for future studies.

6.4 ANN Model Development

The ANN model was developed in four sequential stages. In the first stage, the ANN architecture was determined based on problem characteristics and ANN knowledge, and input and output categories were chosen accordingly. This step also includes classifying the datasets as training, testing or validation sets. In the second stage, the network was trained and tested on the experimental data to obtain the optimum number of hidden nodes and iterations for the ANN architecture determined in stage one. In the third stage, the best performing network obtained from the second stage is validated on the validation database. If accuracy measures from training, testing and validation database are very comparable, then the model may not be trained on all data. In the fourth stage, the best performing network obtained in the second stage is retrained on all experimental data to increase the prediction accuracy and evaluate how well the ANN model characterized the desired behavior. Normally, retraining the network with all experimental data is expected to provide reliable predictions and accuracy measures if the dataset classification is done in an appropriate manner. However, it has been shown through several research studies by Najjar and Coworkers [Najjar & Ali (1998a, b), Najjar & Basheer (1996a), and Najjar et al. (1996b)] that stage four is recommended to arrive at a better performing network. In this chapter, four sequential stages have been conducted twice to arrive at two desired prediction models for C and D. In order to develop boil test permeability prediction model, two models for predicting C and D have been proposed and three best performing model for each one have been developed to obtain the most accurate response. The network developed for C and D has one hidden layer. Fully connected internal structure, i.e. any node in one layer connects to all the nodes in the next layer. ANN Model architectures for C and D are explained in details.

6.4.1 ANN Model Architecture for C

Based on the knowledge gained from experimental data analysis, ANN model architecture for C has been built by considering 3 inputs and 1 output, which respectively are:

Inputs:

1- (A) Mass of oven-dried sample in air (grams)
2- (B) Mass of surface-dry sample in air after immersion (grams)

3- (CT) Curing Time (days)

Output:

1- (C) Mass of surface-dry sample in air after immersion and boiling (grams)

In this study, 3 models giving appropriate accuracy statistical measures have been selected based on optimum hidden nodes, minimum values of Mean Absolute Relative Error (MARE) and Averaged-Squared-Error (ASE) and maximum values of Coefficient of Determination (R^2). Total 414 datasets are used to build the desired database; 211, 112 and 91 sub-database are used, respectively, for training, testing and validation purposes. Datasets that include minimum and maximum values of each variable are included in the training phase in order for the network to represent the characteristics of the response. The maximum and minimum ranges of each input/output variable for ANN model development are chosen on purpose to be wider than their actual ranges for better mathematical mapping.

Model Training and Testing for C

Based on statistical measures such as Averaged-Squared-Error (ASE), Coefficient of determination (R^2) and Mean Absolute Relative Error (MARE), the optimal network structure for the Model C1 was found at 3 hidden nodes and 20000 iterations. The corresponding accuracy measures for this network are ASE_{tr}=0.000103, R^2_{tr}=0.989, $MARE_{tr}$=0.34% (for training database) and ASE_{ts}=0.00009, R^2_{ts}=0.984, $MARE_{ts}$= 0.31% (for testing database). The optimal network for Model C2 was found at 3 hidden nodes and 19500 iterations. The corresponding accuracy measures for this network are ASE_{tr}=0.000027, R^2_{tr}=0.997, $MARE_{tr}$=0.16% (for training database) and ASE_{ts}=0.000023, R^2_{ts}=0.996, $MARE_{ts}$= 0.15% (for testing database). The optimal network for Model C3 was found at 4 hidden nodes and 19900 iterations. The corresponding accuracy measures for this network are ASE_{tr}=0.000035, R^2_{tr}=0.996, $MARE_{tr}$=0.18% (for training database) and ASE_{ts}=0.000033, R^2_{ts}=0.994, $MARE_{ts}$= 0.18 (for testing database). The training graphical comparison plots between predicted and actual response for Model C1, Model C2 and Model C3 are shown, respectively, in Figure 6.1, Figure 6.2 and Figure 6.3. The testing graphical comparison plots between predicted and actual response for Model C1, Model C2 and Model C3 are shown, respectively, in Figures 6.4, 6.5 and 6.6. Also, statistical accuracy measures for the training and testing are shown in Table 6.1 with the best performing is identified in bold.

Model Validation for C

After training and testing, respectively, on 211 and 112 datasets, validation is conducted by using the remaining 91 datasets. After classifying the datasets as training, testing, and validation as described in Section 6.4, the network was trained and tested on experimental data to obtain the optimum number of hidden nodes and iterations for the ANN architecture determined in the stage one. For model validation, the third stage is performed by utilizing the best performing network, identified in stage two, to predict the output of the validation datasets. The graphical comparison plots between predicted and actual response, for validation datasets, for Model C1, Model C2 and Model C3 are shown, respectively, in Figures 6.7, 6.8 and 6.9. Also, corresponding statistical accuracy measures are shown in Table 5.1 where the best performing network is identified in bold.

Model Selection for C

Statistical accuracy measures for training and testing databases at optimal ANN structure with 3 hidden nodes and 19,500 iterations showed better prediction accuracy compared with those for models C1 and C3. Even though Model C1 has same amount of hidden nodes as Model C2, Model C2 has better accuracy measures than Model C1. All of three models can be used as a prediction model since they all have considerably good statistical results. In this case, the best-performing model is considered in the final selection. For this reason, Model C2 has been chosen to be used as the best network structure. Thus, all of the 414 datasets from the Boil test were used to retrain the network at this optimal structure to obtain the generalized response throughout the entire database. Statistical measures of the selected model trained with all data are: ASE_{all}=0.000025, R^2_{all} =0.997 and $MARE_{all}$=0.164%. The graphical comparison plots between predicted and actual response for Model C1, Model C2 and Model C3 are shown, respectively, in Figures 6.10, 6.11 and 6.12. Statistical accuracy measures for all 3 models are shown in Table 6.1. The good agreement between predicted results and experimentally observed results is apparent. The network structure of the best performing model is depicted in Figure 6.13.

6.4.2 Regression Model for C

Regression analysis is another method to understand how the typical value of the dependent variable changes when the independent variables are varied. In other words, it is to understand which among the independent variables are related to the dependent variables. Regression model development has been accomplished using the Excel Data Analysis Toolkit. The 412 datasets used for ANN-Model development were used herein to obtain the prediction model. The input variables and the output as used in ANN-Model development are respectively:

Inputs:

1- (A) Mass of oven-dried sample in air (grams)
2- (B) Mass of surface-dry sample in air after immersion (grams)
3- (CT) Curing Time (days)

Output:

1- (C) Mass of surface-dry sample in air after immersion and boiling (grams)

Using linear regression approach, the following equation was developed;

$$C = 7.555 - 0.0727A + 1.065B - 0.010CT \qquad 6.9$$

Statistical measures of linear regression model obtained using Excel Data Analysis Toolkit are: MARE (%) = 0.171%, R^2_{all} = 0.996 and Standard Deviation of Error, SDE, (%) = 0.255%. The graphical comparison plot between predicted and actual response is shown in Figure 6.14. The comparison of ANN Model and Regression Model are depicted in Table 6.2. It is very clear from the comparison plots in Figure 6.11 and 6.14 that the ANN model is slightly out performing the regression-based model. This indicates that the modeled behavior is mostly linear. In this case, generally ANN-based models will not show significant improvements over linear regression type models.

6.4.3 ANN Model Architecture for D

Based on the knowledge gained from experimental data analysis, ANN model architecture for D has been built by considering 3 inputs and 1 output, which respectively are:

Inputs:

1- (A) Mass of oven-dried sample in air (grams)
2- (B) Mass of surface-dry sample in air after immersion (grams)
3- (CT) Curing Time (days)

Output

1- (D) Apparent mass of sample in water after immersion and boiling (grams)

In this section, 3 models giving appropriate accuracy statistical measures have been selected based on optimum hidden nodes, minimum values of Mean Absolute Relative Error (MARE) and Averaged-Squared-Error (ASE) and maximum values of Coefficient of Determination (R^2). Total 414 datasets are used to build the desired database; 211, 112 and 91 sub-database are used, respectively, for training, testing and validation purposes. Datasets that include minimum and maximum values of each variable are included in the training phase in order for the network to represent the characteristics of the response. The maximum and minimum ranges of each input/output variable for ANN model development are chosen on purpose to be wider than their actual ranges for better mathematical mapping.

Model Training and Testing for D

Based on statistical measures such as Averaged-Squared-Error (ASE), Coefficient of determination (R^2) and Mean Absolute Relative Error (MARE), the optimal network structure for the Model D1 was found at 2 hidden nodes and 20,000 iterations. The corresponding accuracy measures for this network are ASE_{tr}=0.000776, R^2_{tr}=0.926, $MARE_{tr}$=1.203% (for training database) and ASE_{ts}=0.0006, R^2_{ts}=0.943, $MARE_{ts}$= 1.132% (for testing database). The optimal network for Model D2 was found at 3 hidden nodes and 20,000 iterations. The corresponding accuracy measures for this network are ASE_{tr}=0.00073, R^2_{tr}=0.929, $MARE_{tr}$=1.144% (for training database) and ASE_{ts}=0.000536, R^2_{ts}=0.948, $MARE_{ts}$= 1.077% (for testing database). The optimal network for Model D3 was found at 4 hidden nodes and 20,000 iterations. The corresponding accuracy measures for this network are ASE_{tr}=0.000729, R^2_{tr}=0.929, $MARE_{tr}$=1.144% (for training database) and ASE_{ts}=0.000536, R^2_{ts}=0.948, $MARE_{ts}$= 1.076 (for testing database). The training graphical comparison plots between predicted and actual response for Model D1, Model D2 and Model D3 are shown, respectively, in Figure 6.15,

Figure 6.16 and Figure 6.17. The testing graphical comparison plots between predicted and actual response for Model D1, Model D2 and Model D3 are shown, respectively, in Figures 6.18, 6.19 and 6.20. Also, statistical accuracy measures for the training and testing are shown in Table 6.3 with the best performing is identified in bold.

Model Validation for D

After training and testing, respectively, on 211 and 112 datasets, validation is conducted by using the remaining 91 datasets. After classifying the datasets as training, testing, and validation as described in Section 6.4, the network was trained and tested on experimental data to obtain the optimum number of hidden nodes and iterations for the ANN architecture determined in the stage one. For model validation, the third stage is performed by utilizing the best performing network, identified in stage two, to predict the output of the validation datasets. The graphical comparison plots between predicted and actual response, for validation datasets, for Model D1, Model D2 and Model D3 are shown, respectively, in Figures 6.21, 6.22 and 6.23. Also, corresponding statistical accuracy measures are shown in Table 6.2 where the best performing network is identified in bold.

Model Selection for D

Statistical accuracy measures for training and testing databases, for Model D2, at optimal ANN structure with 3 hidden nodes and 20,000 iterations showed better prediction accuracy compared with those for Model D1 and D3. Moreover, all of the three models have performed considerably well. However, Model D2 has the least ASE, MARE, and the most R^2 among the other models. The best-performing model is considered in the final selection. For this reason, Model D2 has been chosen to be used as the best network structure. Thus, all of the 414 datasets from the Boil test were used to retrain the network at this optimal structure to obtain the generalized response throughout the entire database. Statistical measures of selected model trained with all data are: ASE_{all}=0.000643, R^2_{all} =0.934 and $MARE_{all}$=1.110%. The graphical comparison plots between predicted and actual response for Model D1, Model D2 and Model D3 are shown, respectively, in Figures 6.24, 6.25 and 6.26. Corresponding statistical accuracy measures for all 3 models are shown in Table 6.2. The good agreement between predicted results and experimentally acquired results is apparent. The network structure of the best performing model (Model D2) is depicted in Figure 6.27.

6.4.4 Regression Model for D

Regression analysis is as discussed before has been accomplished using Excel Data Analysis Toolkit. Total 414 datasets used for ANN-Model development were utilized herein to obtain the regression prediction model. The input variables and the output as used in ANN-Model development are respectively:

Inputs:

1- (A) Mass of oven-dried sample in air (grams)
2- (B) Mass of surface-dry sample in air after immersion (grams)
3- (CT) Curing Time (days)

Output:

1- (D) Apparent mass of sample in water after immersion and boiling (grams)

Using linear regression approach, the following equation was developed;

$$D = -129.1371 + 0.1679A + 0.5463B + 0.0175CT \qquad 5.10$$

Statistical measures of linear regression model obtained using Excel Data Analysis Toolkit are: MARE (%) = 1.30%, R^2_{all} = 0.909 and Standard Deviation of Error, SDE, (%) = 1.762%. The graphical comparison plot between predicted and actual response is shown in Figure 6.14. The statistical comparison of ANN Model and Regression Model are depicted in Table 6.2. It is very clear from the comparison plots in Figure 6.11 and 6.14 that the ANN model is slightly out performing the regression-based model. As in the case of Model C, this indicates that the modeled behavior is mostly linear. As stated earlier, in this case, ANN-based models will generally not show significant improvements over linear regression counterparts.

6.5 Excel Application for the Void Model

By using the connection weights, threshold values and coefficients which are described in Chapter 3, the excel-based application is developed. In this application, the two developed models by ANN and Regression to predict C and D are combined in one Excel sheet where the connection weights of Model C and Model D and linear regression equations are utilized. In other words, operations of one function for Model C and one function for Model D are merged in one user-friendly application. By entering the compatible input variables for A, B and Curing time in the Excel interface shown in Figure 6.29, ANN- and Regression-based models utilize all 3 input values (user-provided) to predict the C and D values. Percentage of volume permeable pore space (voids) is then calculated since C and D are known variables. The computed C and D values are placed in the output cells colored with blue and % volume of permeable pore space (voids) is placed in the cells colored with pink as depicted in Figure 6.29. The applicable ranges for the input variables are also shown in Figure 6.29. Any value of input variable that is outside the applicable range may cause the models to produce unreliable predictions.

6.6 Predicting % of Voids

By using the developed Excel sheet described in Section 6.5, % volume of permeable pore space (voids) are calculated for all 414 datasets. Actual and predicted values are then compared. The statistical accuracy measures of ANN Model are; MARE (%) = 3.431%, R^2_{all} = 0.894 and Standard Deviation of Error, SDE, (%) = 4.822%. The ANN graphical comparison plot between predicted and actual response is shown in Figure 6.30. The statistical accuracy measures for the linear regression model are; MARE (%) = 3.698%, R^2_{all} = 0.883 and Standard Deviation of Error, SDE, (%) = 4.928%. The Regression-based graphical comparison plots between predicted and actual response is shown in Figure 6.31. The statistical comparison of ANN Model and Regression Model are listed in Table 6.5. As can be seen from the comparison plots in Figure 6.30 and 6.31 and the comparison in Table 6.5, the ANN model is slightly out performing the regression-based model. Therefore, both ANN-Model and Regression-Model can be used efficiently to predict % voids typically obtained from the boil test. These models can also be used to verify experimentally-based boil test results regarding the %voids in concrete samples.

6.7 Concluding Remarks

In this chapter, a static artificial neural network with a backpropagation learning algorithm was developed to predict the Boil Test-based % voids in concrete mixes. As seen from the graphical results depicted in Figures 6.1 to 6.31 and the accuracy measures of the developed ANN models listed in Table 6.1, 6.3, Model C2 and Model D2 have been selected to aid in characterizing the % void response. The comparison of the predicted responses by ANN and Regression shown in Table 6.2, 6.4 and 6.5 indicates that ANN model attains better prediction accuracy than the Regression model even though the statistical difference between the ANN model and Regression model is not significant. It is apparent that the ANN model and Regression model have efficiently characterized the Boil test response. Therefore, ANN- and Regression-based model can reliably be used for % void prediction tasks to reduce the duration of the 5 hours testing period as long as the input variables fall within the applicable ranges. Moreover, developed ANN and Regression models can be used to verify measured responses for planned-to-be conducted Boil tests without the need for any additional experimental-based information. Even though the development of the ANN model requires good fundamental understanding of the Boil Test procedure and ANN knowledge, Excel-based application described in section 6.5, which is the utilization tool of the developed ANN model, is simple to use while not requiring the user to acquire specific knowledge about model development. ANN and Regression models overcome the drawback of the 5 hours testing time; making it a powerful, rapid, and low cost alternative to obtain the % void of concrete mixes with a reliable level of accuracy. Due to fact that the database for model development was provided by KDOT, the developed Boil Test % void prediction models in this study are applicable only for KDOT applications. A similar research procedure can be performed to develop reliable prediction models.

6.8 Tables and Figures

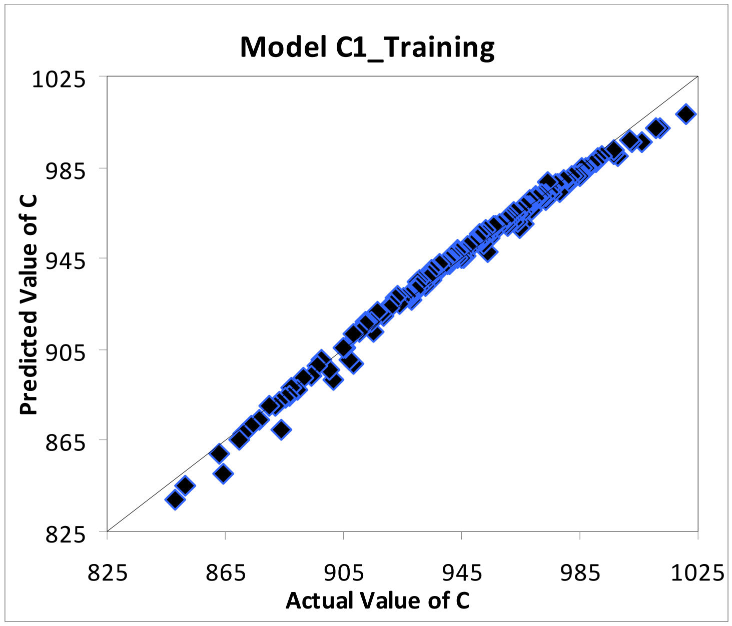

Figure 6.1 Training Graphical Prediction Accuracy for the Model C1

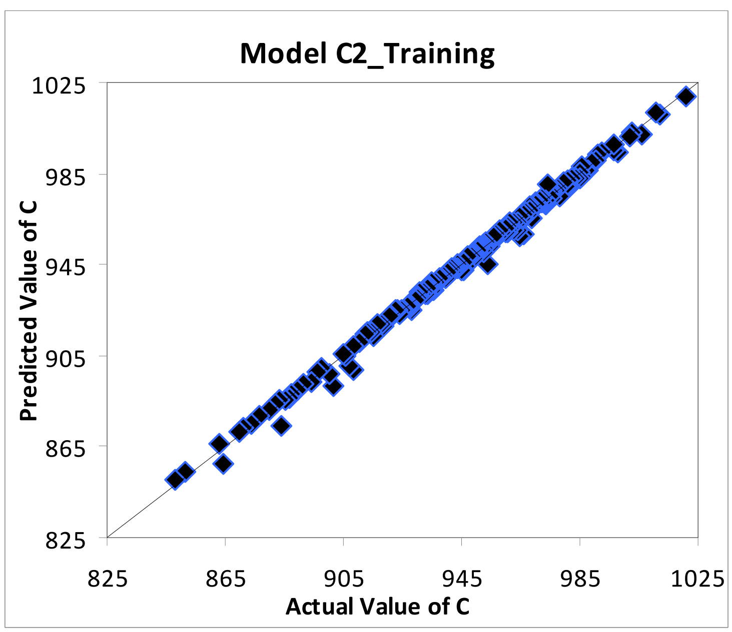

Figure 6.2 Training Graphical Prediction Accuracy for the Model C2

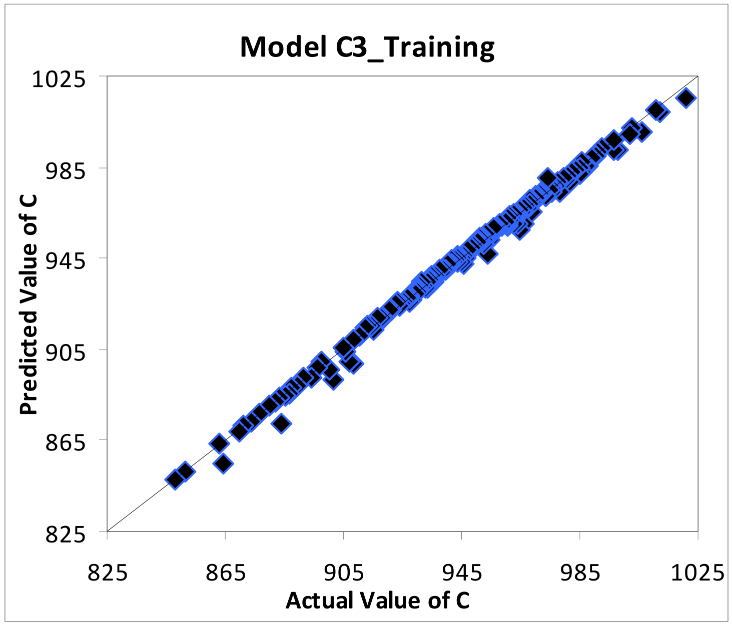

Figure 6.3 Training Graphical Prediction Accuracy for the Model C3

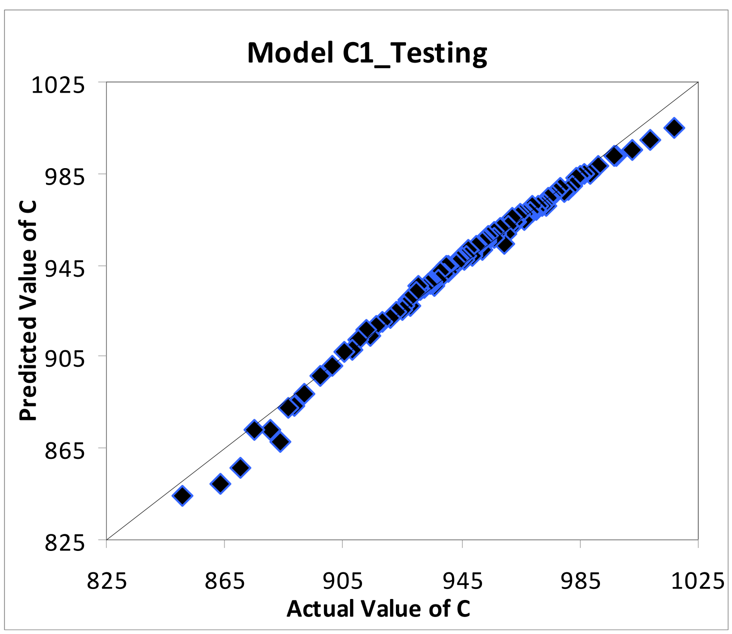

Figure 6.4 Testing Graphical Prediction Accuracy for the Model C1

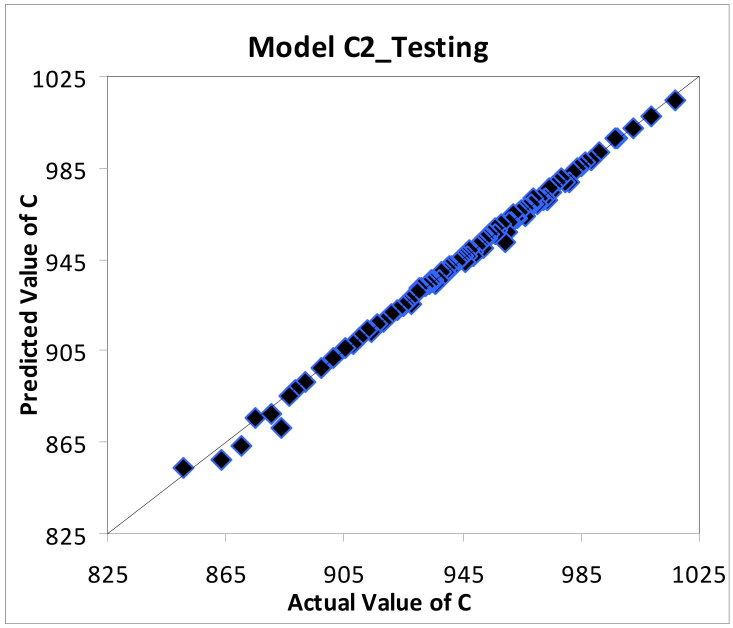

Figure 6. 5 Testing Graphical Prediction Accuracy for the Model C2

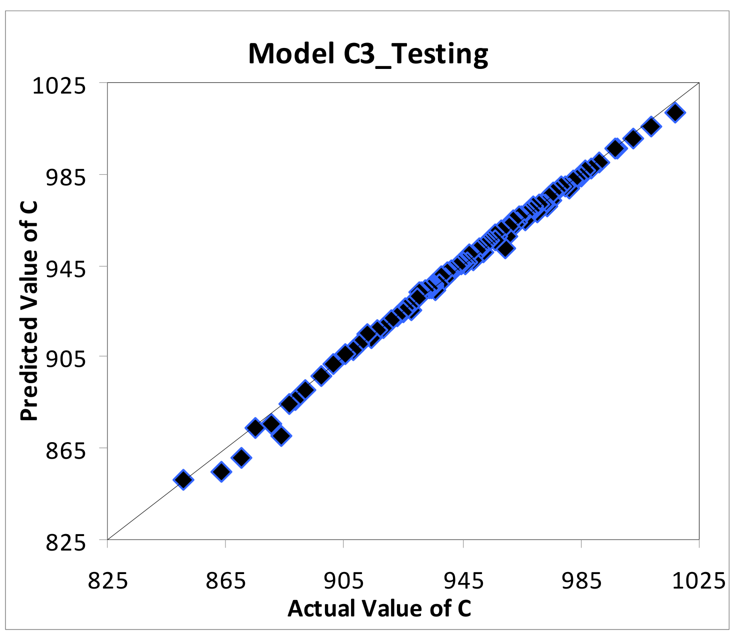

Figure 6.6 Testing Graphical Prediction Accuracy for the Model C3

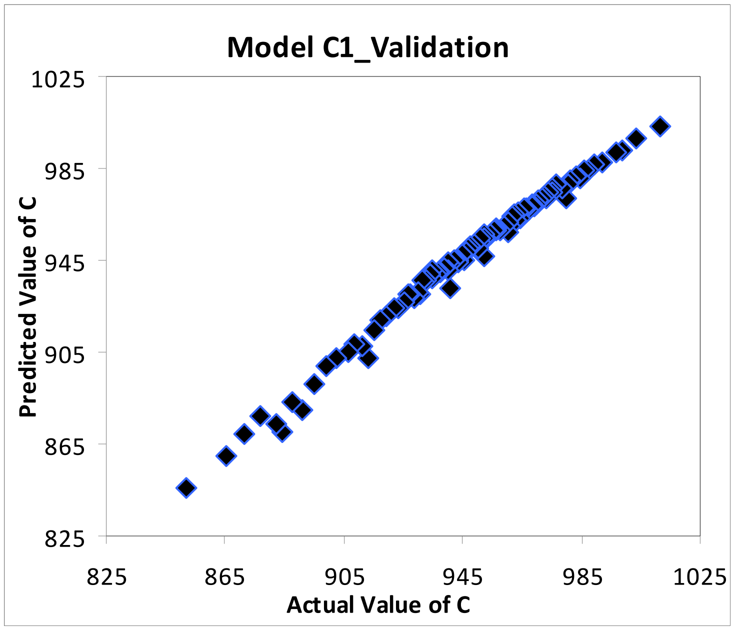

Figure 6.7 Validation Graphical Prediction Accuracy for the Model C1

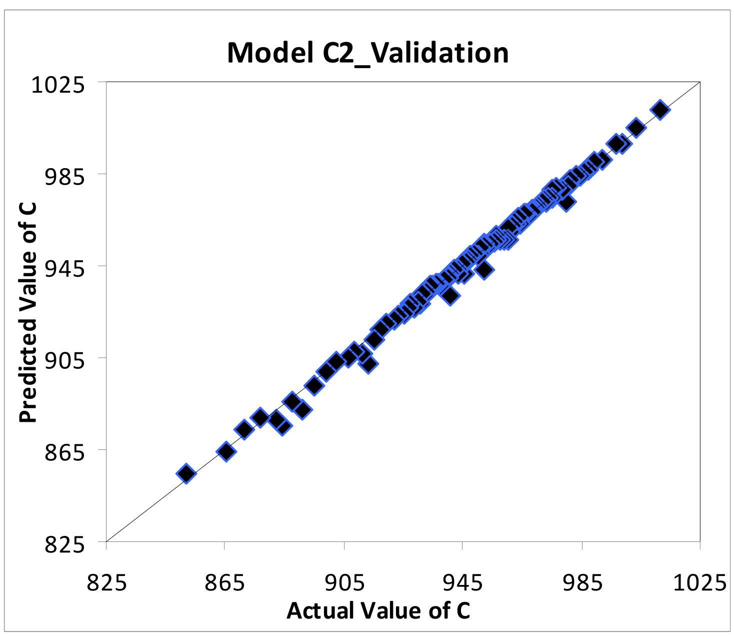

Figure 6.8 Validation Graphical Prediction Accuracy for the Model C2

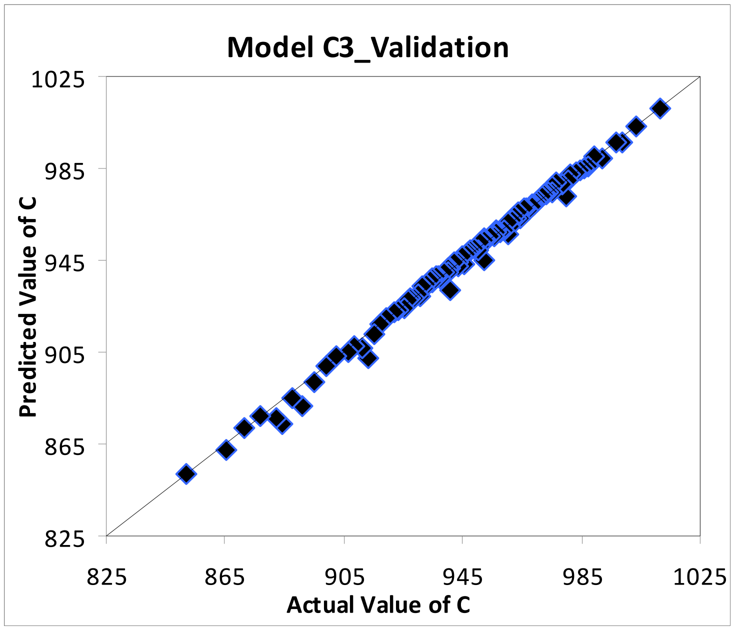

Figure 6.9 Validation Graphical Prediction Accuracy for the Model C3

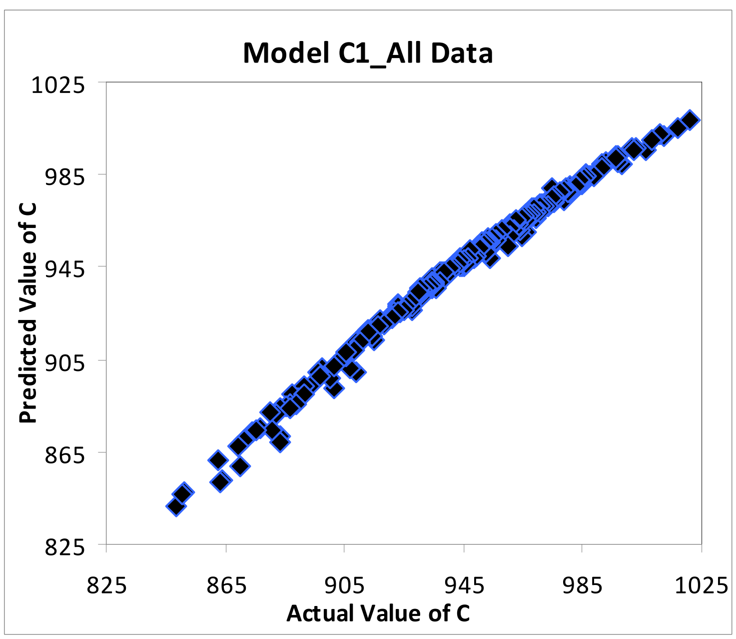

Figure 6.10 All Data Graphical Prediction Accuracy for the Model C1

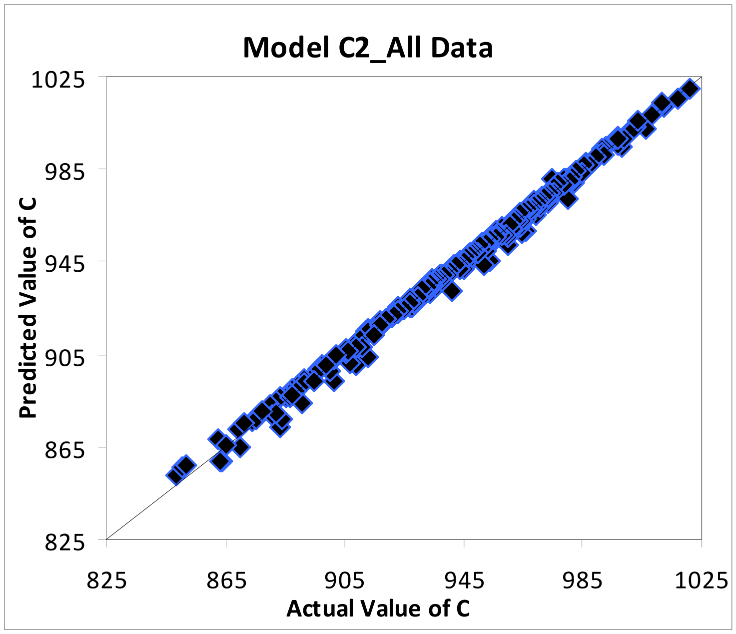

Figure 6.11 All Data Graphical Prediction Accuracy for the Model C2

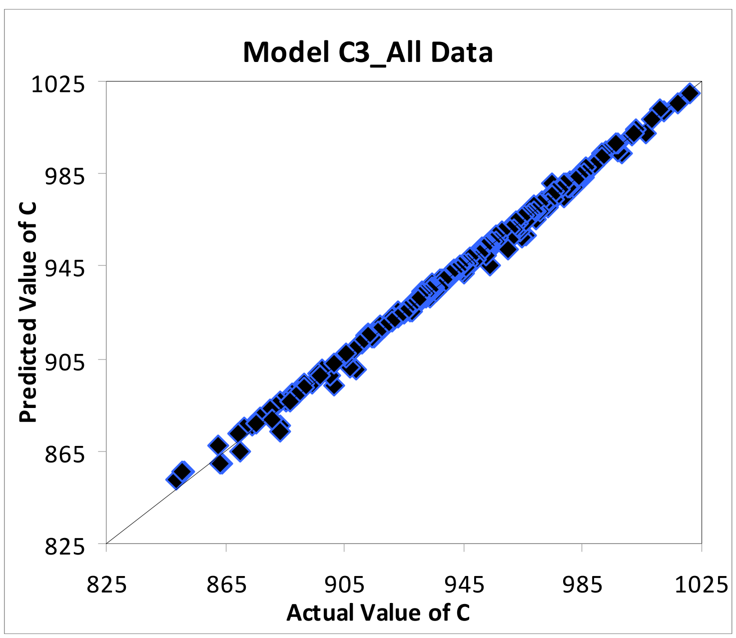

Figure 6.12 All Data Graphical Prediction Accuracy for the Model C3

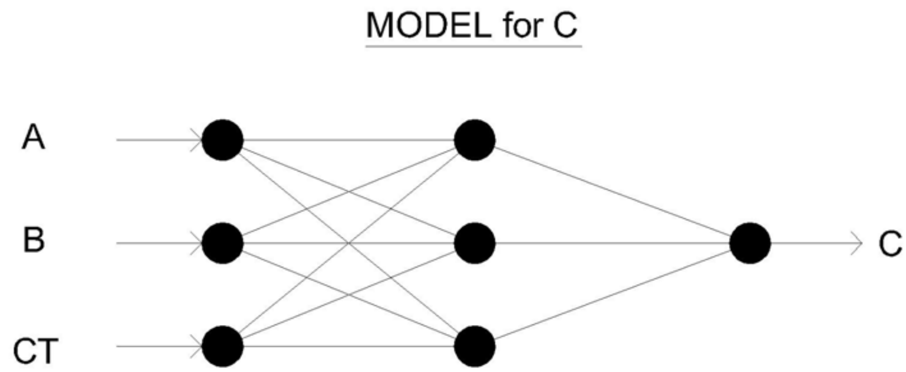

Figure 6.13 The Network Structure of the Best Performing Model of C

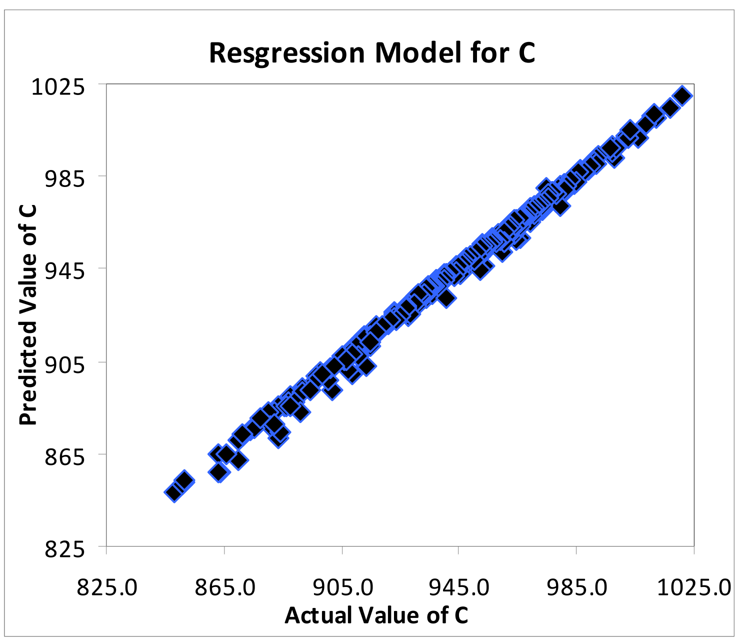

Figure 6.14 Graphical Prediction Accuracy for the Regression Model of C

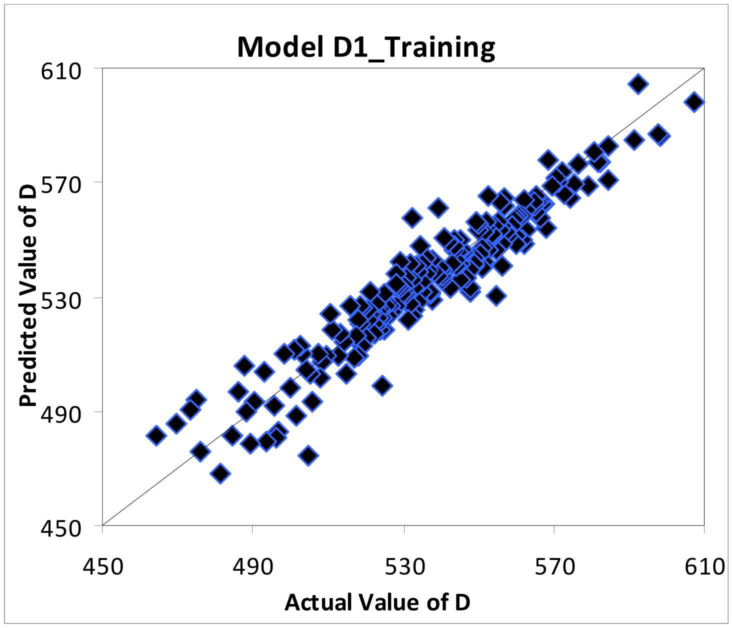

Figure 6.15 Training Graphical Prediction Accuracy for the Model D1

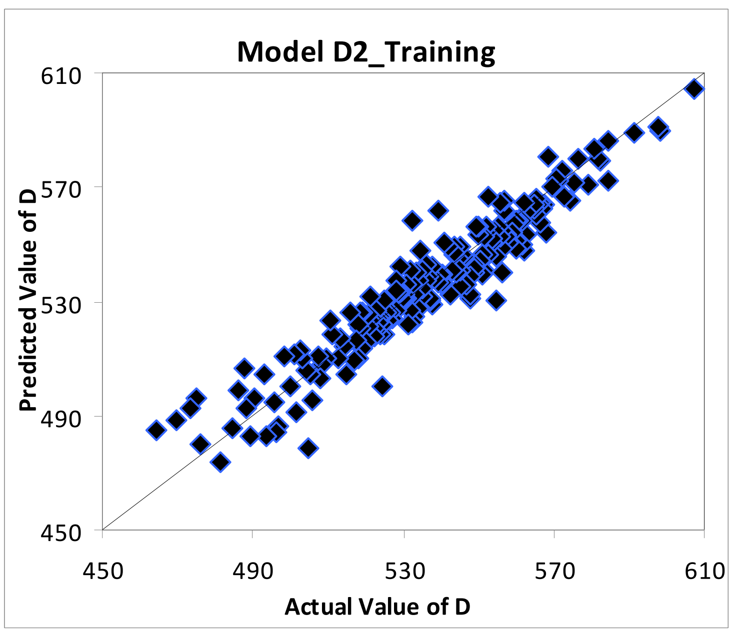

Figure 6.16 Training Graphical Prediction Accuracy for the Model D2

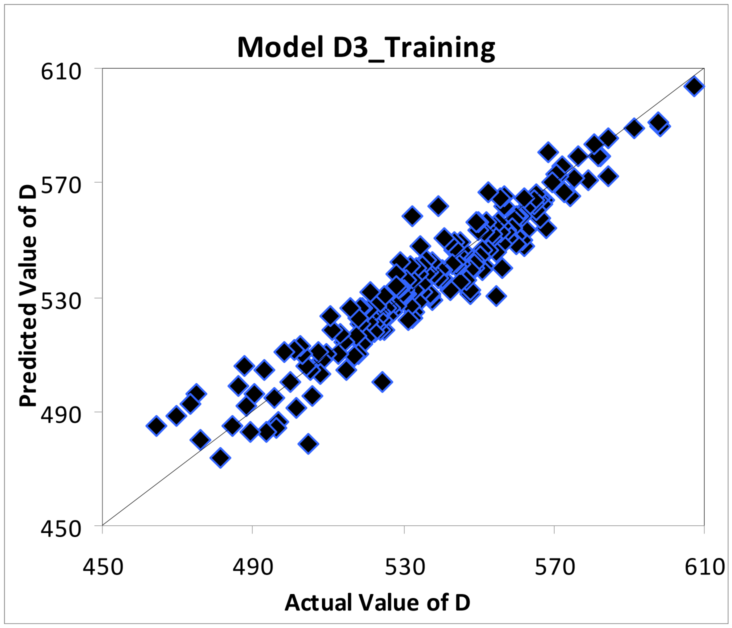

Figure 6.17 Training Graphical Prediction Accuracy for the Model D3

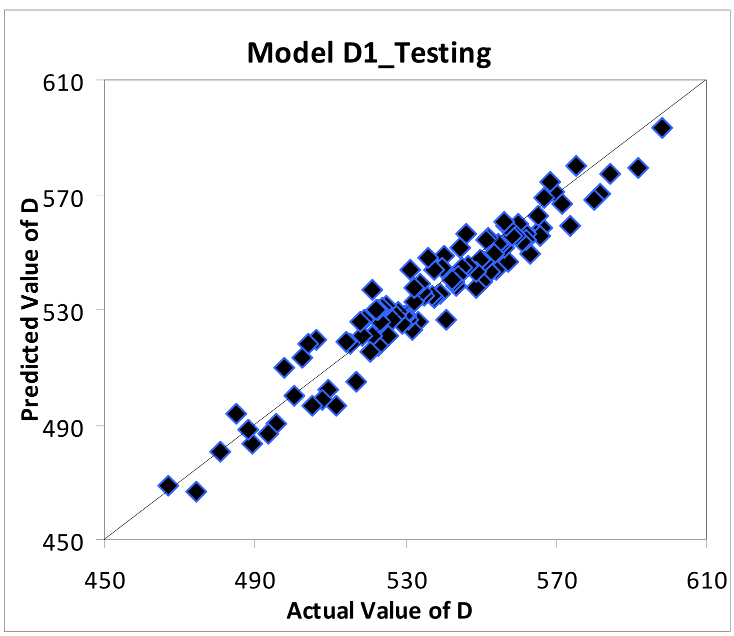

Figure 6.18 Testing Graphical Prediction Accuracy for the Model D1

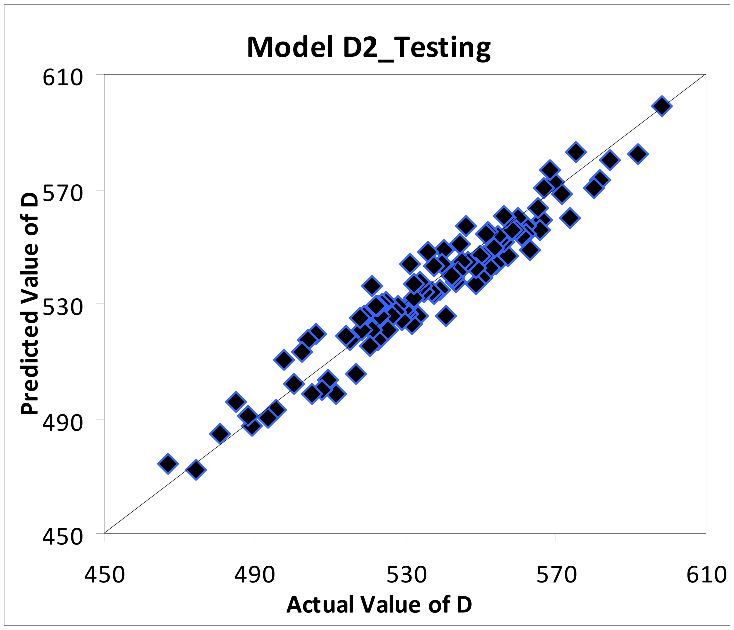

Figure 6.19 Testing Graphical Prediction Accuracy for the Model D2

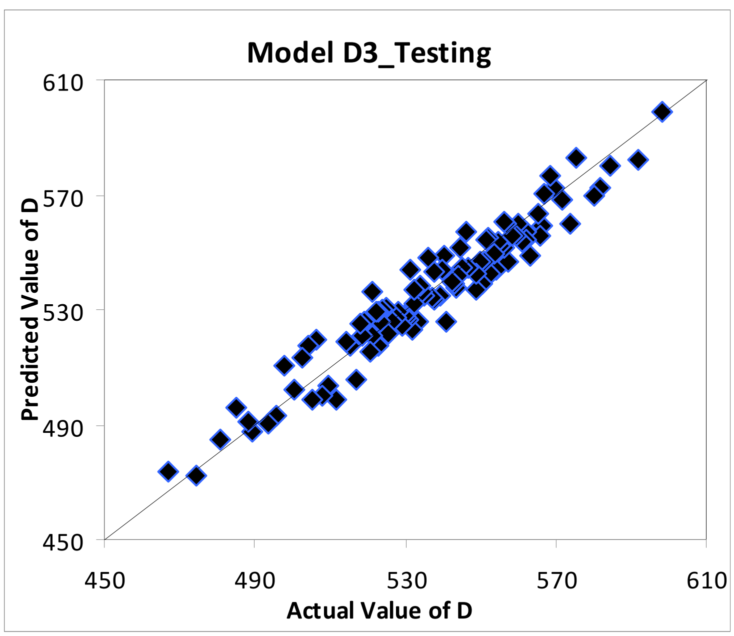

Figure 6.20 Testing Graphical Prediction Accuracy for the Model D3

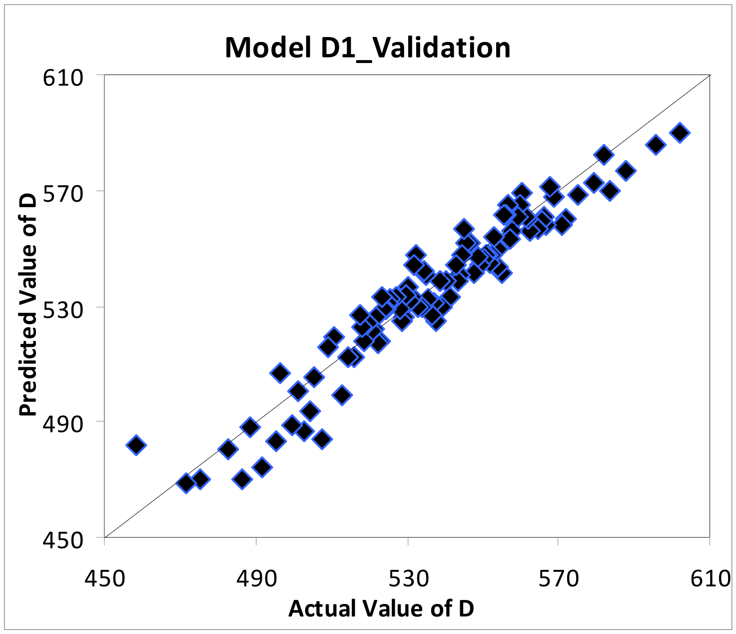

Figure 6.21 Validation Graphical Prediction Accuracy for the Model D1

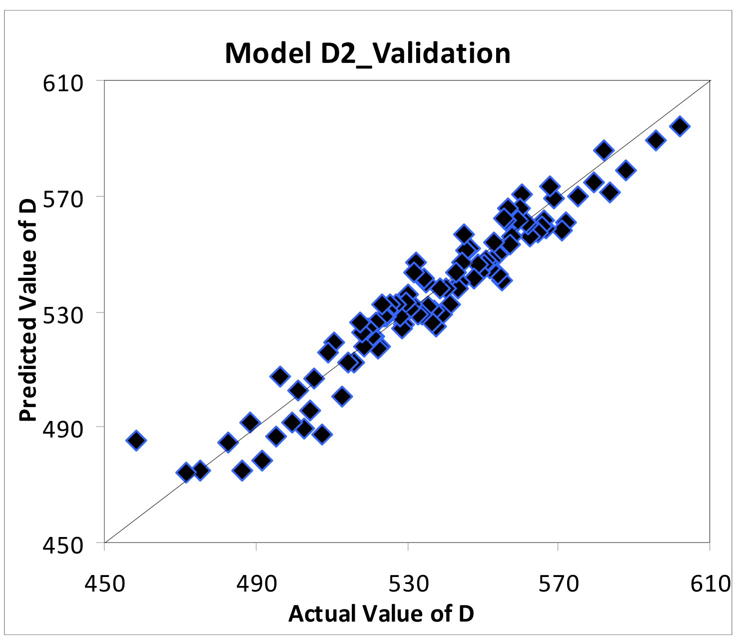

Figure 6.22 Validation Graphical Prediction Accuracy for the Model D2

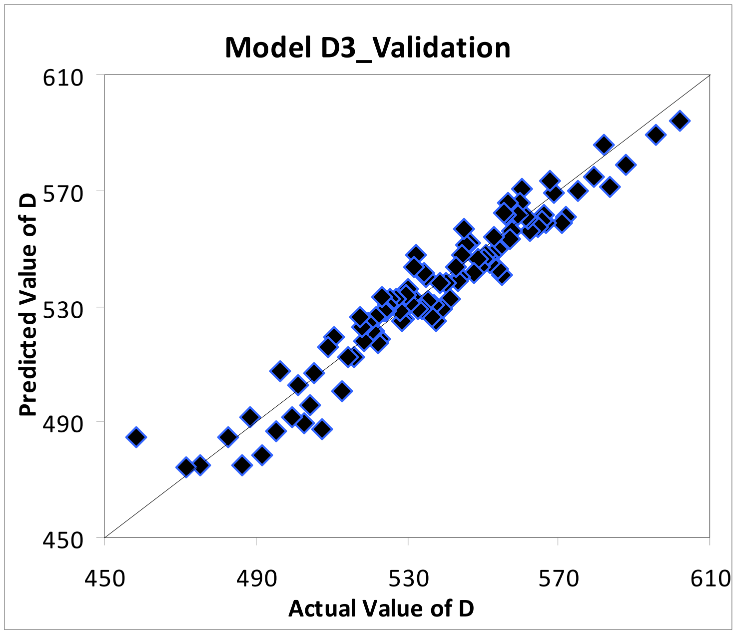

Figure 6.23 Validation Graphical Prediction Accuracy for the Model D3

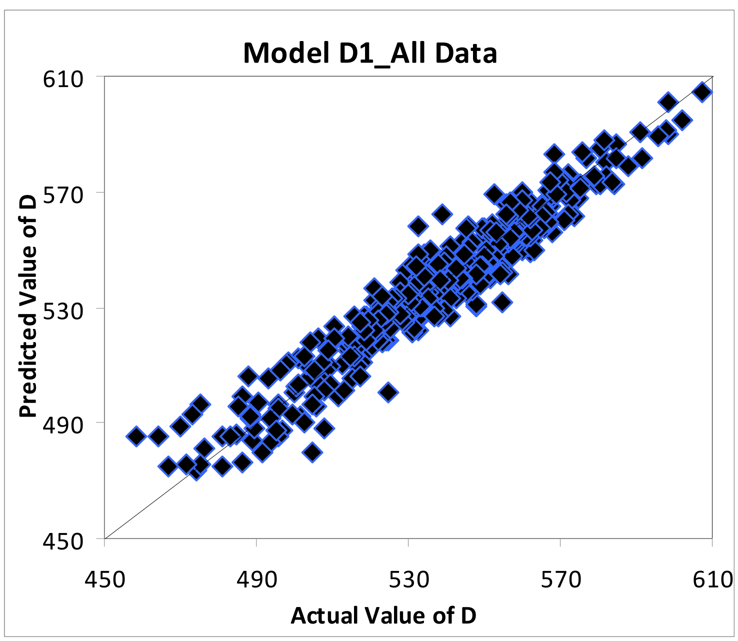

Figure 6.24 All Data Graphical Prediction Accuracy for the Model D1

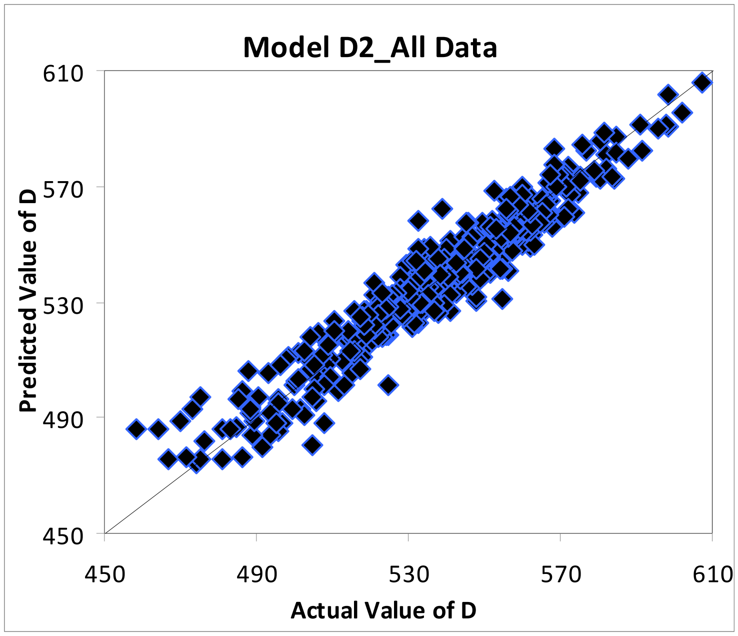

Figure 6.25 All Data Graphical Prediction Accuracy for the Model D2

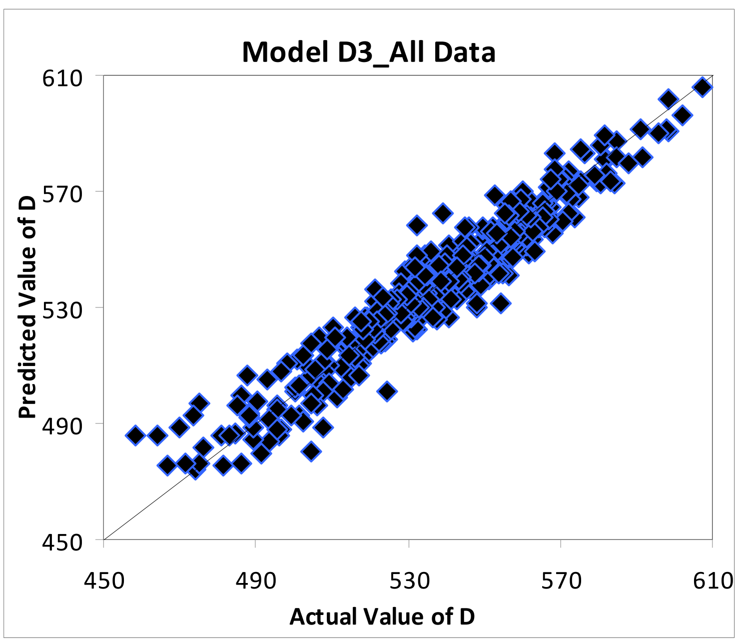

Figure 6.26 All Data Graphical Prediction Accuracy for the Model D3

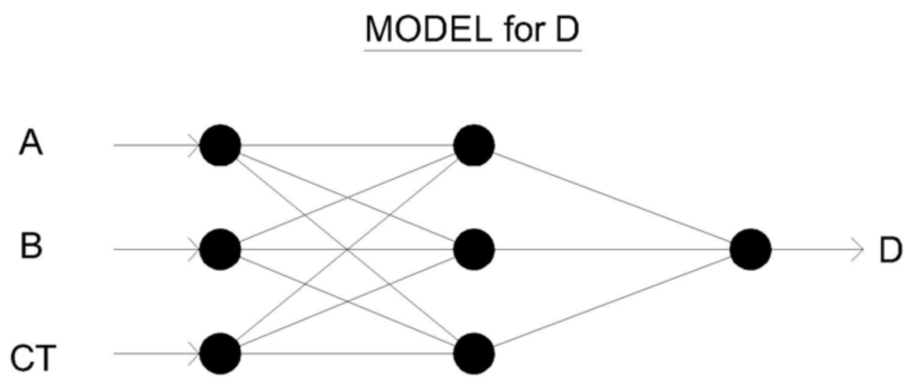

Figure 6.27 The Network Structure of the Best Performing Model of D

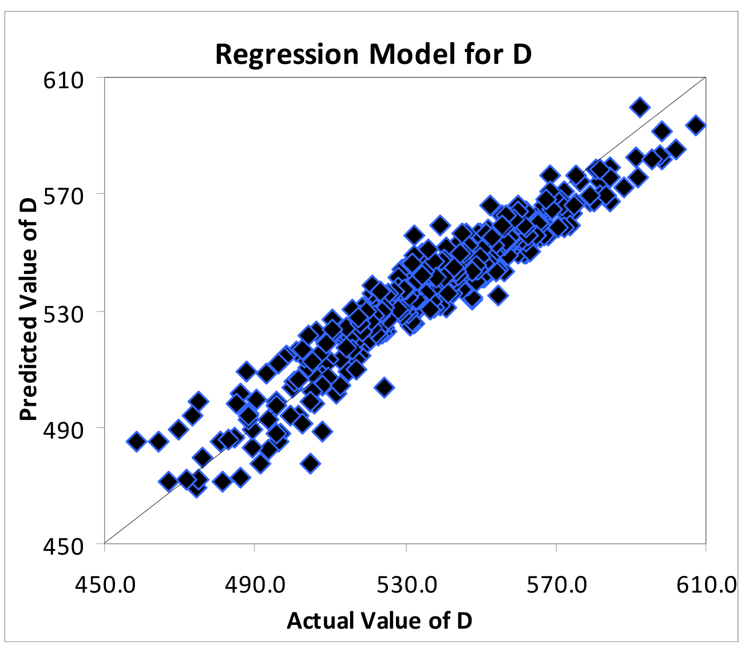

Figure 6.28 Graphical Prediction Accuracy for the Regression Model of D

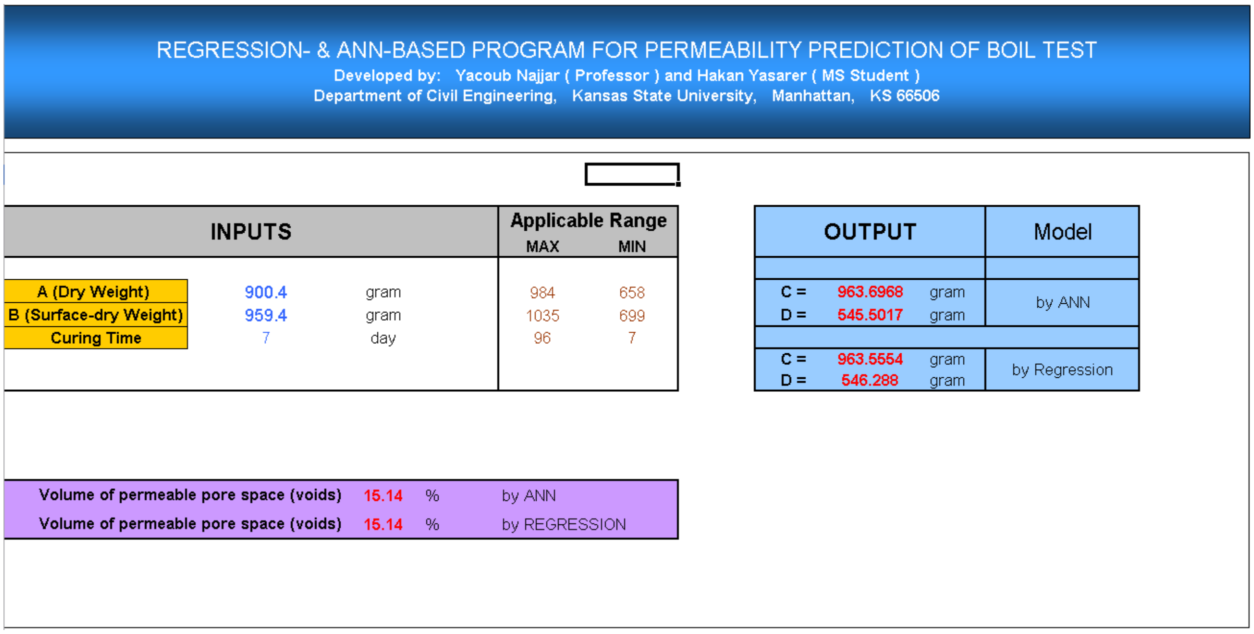

Figure 6.29 Excel Application Screen-shot for the Void Model

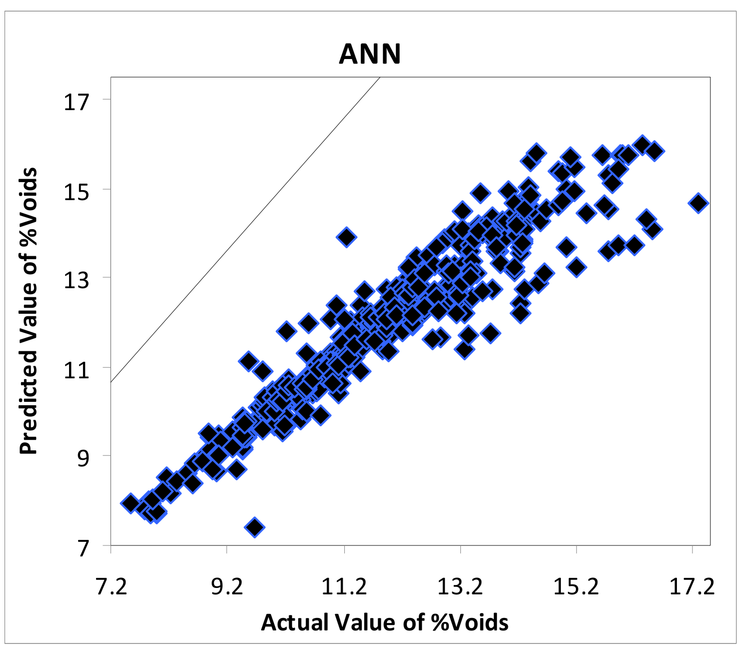

Figure 6.30 Calculated %Volume of Permeable Pore Space by ANN Model

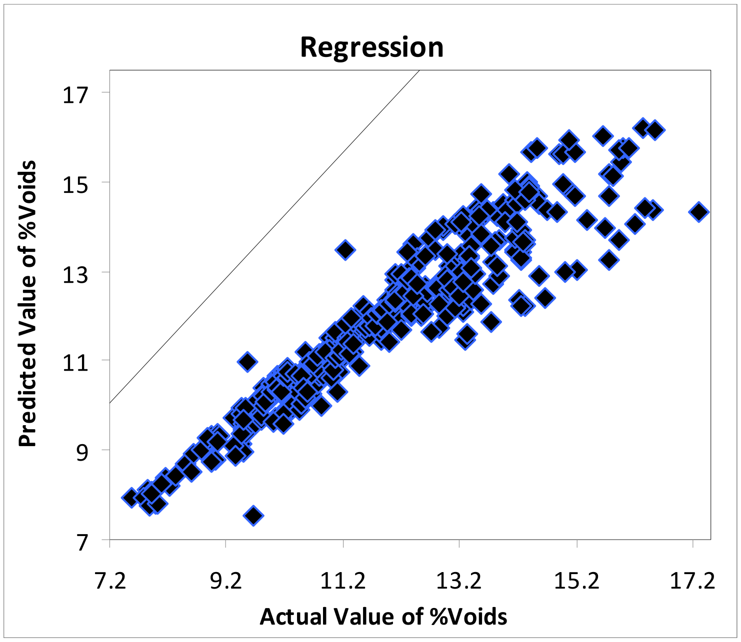

Figure 6.31 Calculated %Volume of Permeable Pore Space by Regression Model

Table 6.1 Statistical Accuracy Measures of the ANN-Models of C

Model		Model C1	**Model C2**	Model C3
Architecture		3-(1-3-18-20000)-1	**3-(2-3-18-19500)-1**	3-(3-4-18-19900)-1
Training	MARE(%)	0.336%	**0.164%**	0.184%
	R2	0.989	**0.997**	0.996
	ASE	0.000103	**0.000027**	0.000035
Testing	MARE(%)	0.310%	**0.149%**	0.177%
	R2	0.984	**0.996**	0.994
	ASE	0.00009	**0.000023**	0.000033
Validation	MARE(%)	0.319%	**0.174%**	0.189%
	R2	0.989	**0.996**	0.996
	ASE	0.000087	**0.000033**	0.000037
All Data	MARE(%)	0.33%	**0.164%**	0.16%
	R2	0.989	**0.997**	0.997
	ASE	0.000092	**0.000025**	0.000025
Final Structure		3 - 3 - 1	**3 - 3 - 1**	3 - 4 - 1

Table 6.2 Comparisons of Statistical Accuracy Measures for ANN and Regression Models of C

Statistical Measures	ANN (3 – 3 – 1)	REGRESSION
MARE (%)	0.164%	0.171%
SDE(%)	0.245%	0.255%
R^2	0.997	0.996

Table 6.3 Statistical Accuracy Measures of the ANN-Models of D

Model		Model D1	**Model D2**	Model D3
Architecture		3-(1-2-12-20000)-1	**3-(1-3-12-20000)-1**	3-(2-4-12-20000)-1
Training	MARE(%)	1.203%	**1.144%**	1.144%
	R2	0.926	**0.929**	0.929
	ASE	0.000776	**0.00073**	0.000729
Testing	MARE(%)	1.132%	**1.077%**	1.076%
	R2	0.943	**0.948**	0.948
	ASE	0.0006	**0.000536**	0.000536
Validation	MARE(%)	1.21%	**1.14%**	1.15%
	R2	0.918	**0.926**	0.925
	ASE	0.00072	**0.000631**	0.000633
All Data	MARE(%)	1.112%	**1.110%**	1.111%
	R2	0.933	**0.934**	0.933
	ASE	0.000644	**0.000643**	0.000644
Final Structure		3 - 2 - 1	**3 - 3 - 1**	3 - 4 - 1

Table 6.4 Comparisons of Statistical Accuracy Measures for ANN and Regression Models of D

Statistical Measures	ANN (3 – 3 – 1)	REGRESSION
MARE (%)	1.110%	1.300%
SDE(%)	1.449%	1.762%
R^2	0.934	0.909

Table 6.5 Comparisons of Statistical Accuracy Measures for Calculated %Voids by ANN and Regression Models

Statistical Measures	ANN	REGRESSION
MARE (%)	3.431%	3.698%
SDE(%)	4.822%	4.928%
R^2	0.894	0.883

CHAPTER 7- SUMMARY, CONCLUSIONS AND RECOMMENDATIONS

7.1 Summary

For long term durability of concrete, permeability is a highly important parameter which needs to be evaluated to reduce the potential risk of chloride-induced corrosion damage. Recognizing this fact, an enormous amount of efforts were devoted to better understand this phenomenon and to evaluate the potential hazards and consequences of chloride-induced corrosion. Therefore, permeability is used as one of the main assessment criteria which has been established based on empirical, conventional and correlation techniques. For this reason, the two test methods to determine the permeability of concrete were established. The most common and reliable method to determine the permeability of concrete is the rapid chloride permeability test which measures the electrical conductance of concrete to provide a rapid indication of its resistance to the penetration of chloride ions. Additionally, another test as of an alternative method for rapid chloride permeability test is the Boil Test which is conducted to measure the volume of permeable pore space. In applications such as quality control and acceptance testing, the experimental methods are always preferred to evaluate the permeability of concrete response. However, their cost, inadequate test equipment and qualified technicians needed to conduct the sample preparation and test procedure, and actual testing time are a concern for owners and inspectors.

During the last 20 years, artificial neural networks (ANN) have come out as a new powerful numerical technique able to learn by example. The learning by example technique allows ANN to successfully mimic the information process as occurs in the human brain. Among the several neuronets that have been developed, the three-layered feed-forward error-backpropagation network with supervised learning was chosen for material characterization.

The first main objective of this study was to investigate the ability of backpropagation ANN to contain the complex correlations and gain the main logic for a better characterization. To achieve this objective, rapid chloride permeability and Boil Test databases were used to train, test and validate the ANN models. Moreover, the developed models were simplified to produce accurate permeability response equation that can be easily used for prediction.

Rapid chloride permeability and Boil Test databases were developed from previously collected experimental tests by KDOT. Also, another Rapid Chloride database in which different input variables (mix-design) involved was developed with the information collected from literature. Several training cases were developed using various combinations of available input variables. The three best performing ANN-based models for each database were investigated in more depth. Prediction accuracy of the developed models was illustrated and verified. Then, the results obtained by ANN-based model and Regression-based model were compared graphically and numerically. As a result, the knowledge gained in the trained ANN-based models was utilized to produce relevant numerical applications capable of characterizing the permeability response behavior of concrete.

7.2 Conclusions

Based on results obtained from the first part of this study, the following sets of conclusions are drawn:

1. A static artificial neural network with backpropagation algorithm was developed using KDOT Rapid Chloride Permeability test database to model the permeability response of concrete. Comparison between experimental data and ANN model predictions indicated that the developed ANN model has efficiently characterized the Rapid Chloride Test response. Therefore, the developed ANN model can be used by KDOT to verify measured responses for planned-to-be conducted experimental studies, quality control and acceptance testing without the need for any additional experimental-based information. The developed Excel-based application is simple and doesn't require the user to have specific knowledge.
2. A static ANN with a backpropagation algorithm was developed using mix-design based Rapid Chloride Permeability test database collected from literature to model the permeability response of concrete. It can be inferred that the developed ANN model has successfully captured the Rapid Chloride Permeability response. In addition, the ANN

model has a high prediction capability of the chloride permeability of concrete in terms of quantitative and categorical variables. In this study, a significant compromise between the literature data and ANN model has been shown. The mix-design based ANN model can be used for early prediction, quality control and acceptance testing without the need for any additional experimental-based information.

3. Another static ANN with backpropagation algorithm was developed using KDOT Boil test database to model the determination of permeable voids of concrete. Comparison between experimental data and ANN model predictions has proven that the developed ANN model has efficiently characterized the determination of permeable voids. Therefore, the developed ANN model can be used by KDOT to verify measured responses for planned-to-be conducted experimental studies, quality control and acceptance testing without the need for any additional experimental-based information. The developed user-friendly Excel-based application is simple and doesn't require the user to have specific knowledge.

The results indicated that the methodology described using Backpropagation Artificial Network is a useful, powerful tool not only for accurately predicting permeability, but also to identifying correlations between output and inputs. However it is necessary to mention that the accuracy of the neural network highly depends on the accuracy of the database. A significant amount of inaccurate data may lead to inappropriate and unreliable results. The small database may not be enough to capture the features of the proposed network structure which otherwise will generate inaccurate or unreliable predictions but in this study, ANN models overcame the drawback of testing time; making it a powerful, rapid, low cost alternative to determine the permeability of concrete mixes with a considerably reliable level of accuracy. All of the results obtained with this approach and the verifications carried out demonstrated the applicability of artificial neural networks in the concrete materials industry. This study has also proven that ANN approach is an up-to-date application which can also be used for modelling of some concrete properties.

7.3 Recommendations

Even though the results obtained in this study are reasonably acceptable, the developed ANN models in this study have few drawbacks. First, it is not recommended to use KDOT permeability prediction models by other agencies since some of the measurements are not specified in ASTM standards. The number of datasets used in Mix-design based Rapid Chloride test model development may not be enough to generalize the permeability response of concrete mixes. For this reason, more experimental results are recommended to be included in ANN model development for future studies.

It is specified in ASSHTO T-277 that factors which are known to affect chloride ion penetration include: water-cement ratio, the presence of polymeric admixtures, sample age, air-void system, aggregate type, degree of consolidation, and type of curing. Thus, ongoing research for KDOT rapid chloride permeability test will look into expanding the models to include mix-design parameters. Moreover, the period from sample preparation to taking the measurements will be considered in the following phases of the ongoing research. In the second phase of the study, the difficulties due to lack of mix-design parameters and supplementary materials' information will be clarified and the ongoing research will be conducted to investigate correlation between mix-design parameters and the measurements (A, B and C) taken before the test. In the third phase of the study, correlations between the measurements and the charge (coulomb) passed through the sample will be investigated. Consequently, two combined prediction models will be developed and the permeability response of the concrete will be estimated accordingly by using mix-design information. In addition, ongoing research for the KDOT Boil Test will look into expanding the ANN models to contain mix-design parameters. In this case, the part of the research related to Boil test will be about modeling with mix-design parameters to predict the variables (A and B) used in this study. Then, second phase will inspect the correlation between predicted variables (A and B) and C and D.

References

AASHTO T 277-86 (1990). "Electrical Indication of Concrete's Ability to Resist Chloride". American association of states highway and transportation officials, standard specifications -part II, Washington, DC, 12 pp.

Agrawal, S. K. and Daiutolo, H. (1992). "Reflex-percussive grooves for runways: Alternative to saw-cutting", *Transportation Research Board*, No. 836, pp. 55-60.

Alhozaimy A., Sorushian P., and Mirza F. (1996). "Effects of curing conditions and age on chloride permeability of fly ash mortar", *ACI Mater Journal* 93(1), pp. 87-95.

Ali, H. E. (2000), "Neuronet-based liquefaction potential assessment and stress-strain behavior simulation of sandy soils", PhD dissertation, Kansas State University, Manhattan, KS, 263 pp.

Alexander, M.G. and Magee, B.J. (1999). "Durability performance of concrete containing condensed silica fume", *Cement Concrete Research*, 29 (6), pp. 917-922.

Alonso C., Andrade C., Castellote M., and Castro P. (2000). "Chloride threshold values to depassivate reinforcing bars embedded in a standardized OPC mortar". *Cement Concrete Research* 30(7), pp.1047-55.

ASTM C 642 (1997). "Standard Test Method for Density, Absorption, and Voids in Hardened Concrete," ASTM International, West Conshohocken, PA, pp. 3.

ASTM C 1202 (2000). "Electrical Indication of Concrete's Ability to Resist Chloride Ion Penetration," ASTM International, West Conshohocken, PA, 4 (02), pp. 6.

Basheer I. A. (1998), "Neuromechanistic-based modeling and simulation of constitutive behavior of fine-grained soils", *PhD dissertation*, Kansas State University, Manhattan, KS, 410 pp.

Basheer, I. A. and Najjar, Y.M. (1994) Predicting the permeability of compacted clay using an artificial neural network. *Proceedings of the Artificial Neural Networks in Engineering Conference*, Nov 13-16. Volume 4, pp. 1161-1166.

Bassuoni, M.T., Greenough, T.R., and Nehdi, M.L., (2005). "Rapid chloride penetrability test: A new look", *33rd CSCE Annual Conference - Canadian Society for Civil Engineering*, v 2005, p GC-186-1-GC-186-10.

Bentz, D. P. (2000). "Influence of Silica Fume on Diffusivity in Cement-based Materials. II. Multi-Scale Modeling of Concrete Diffusivity", *Cement and Concrete Research* 30 (7), pp 1121-1129.

Bentz, D. P. (2007). "A virtual Rapid Chloride Permeability Test", *Cement & Concrete Composites* 29 (10), pp 723-731.

Berke, N. S. (1989). "Resistance of micro-silica concrete to steel corrosion, erosion, and chemical attack", *Proceedings of the international conference on fly ash, silica fume, slag, and natural pozzolans in concrete*. Farmington Hills, Michigan: American Concrete Institute, pp. 861-86.

Boddy, A., Hooton, R. D., and Gruber, K. A. (2001). "Long-term testing of the chloride-penetration resistance of concrete containing high-reactivity metakaolin", *Cement Concrete Research,* 31(5), pp. 759-65.

Claisse, P. A., Elsayad, H. I., and Ganjian, E. (2010). "Modelling the rapid chloride permeability test", *Cement and concrete research* 40 (3), pp 405-409.

Cybenko, G. (1989). "Approximation by superposition of a sigmoid function. Mathematics of Control", *Signals and Systems*, 2(4), pp. 303-314.

Fausett, L. (1994). "Fundamentals of Neural Networks: Architectures, Algorithms, and Applications", Prentice Hall, Inc., Upper Saddle River, NJ, 461 pp.

Feldman, R. F., Chan, G. W., Brousseau, R. J., and Tumidajski, P. J. (1994). "Investigation of the rapid chloride permeability test", *ACI Materials Journal* 91 (3), pp 246-255.

Feldman, R., Prudencio, L. R., and Chan, G. (1999). "Rapid chloride permeability test on the blended cement and other concretes: correlations between charge, initial current and conductivity", *Construction Build Material* 13(3), pp. 54-149.

Felker, V., Hossain, M., Najjar, Y. M., and Barezinsky, R. (2003) "Modeling the Roughness of Kansas PCC Pavements: A Dynamic ANN Approach," *CD-ROM of the Transportation Research Board 82nd Annual Meeting*, Washington DC, January 12-16, 2003, paper # 03-2569.

Feng, N., Feng, X., Hao, T., and Xing, F. (2002). "Effect of ultrafine mineral powder on the charge passed of the concrete", *Cement Concrete Research* 32(4), pp. 623-7.

Funahashi, K. I. (1989). "On the approximate realization of continuous mapping by neural networks", *Neural Networks* 2(3), pp. 183-192.

Ghaboussi, J., Garett, J. H. and Wu, X. (1991), "Knowledge-based modeling of material behavior with neural networks", *Journal of Engineering Mechanics*, 117 (1), pp. 132-153.

Gonzalez-Fonteboa, B. and Martinez-Abella, F. (2008). "Concretes with aggregates from demolition waste and silica fume", *Materials and mechanical properties*, Building and Environment 43 (4), pp 429-437.

Guneyisi, E. (1999). "Effect of binding material composition on strength and chloride permeability of high strength concrete", *MS Thesis*, Department of Civil Engineering, Bogazici University, Turkey, 85 pp.

Guneyisi E, Ozturan T, and Gesoglu M. (2002). “Laboratory investigation of chloride permeability for high performance concrete containing fly ash and silica fume”, *Proceedings of the international conference on challenges of concrete construction,* Dundee, Scotland, pp.295-305.

Guneyisi E., Geseoglu M., Ozturan T., and Ozbay E. (2009). “Estimation of chloride permeability of concretes by empirical modeling: Considering effects of cement type, curing condition and age”, *Construction and building Materials*, 23 (1), pp. 469- 481.

Gu, P., Beaudoin, J. J., Zhang, M. H., and Malhotra, V. M. (1999). “Performance of steel reinforcement in portland cement and high-volume fly ash concretes exposed to chloride solution”, *ACI Material Journal* 96 (5), pp. 551-8.

Hartman, E. J., Keeler, J. D., and Kowalski, J. M. (1990). “Layered neural networks with Gaussian hidden units as universal approximations”, *Neural Computation*, 2(2), pp. 210-215.

Haykin, S. (1999). Neural networks: *A Comprehensive Foundation*, Second Edition, Prentice Hall, Upper Saddle River, New Jersey 07458.

Herz J., Krogh A., and Palmer R. (1991). *Introduction to the Theory of Neural Computation*, Volume 1, Addison-Wesley Publishing Company, Redwood City, California, 350 pp.

Hooton, R.D., Pun, P., Kojundic, T., and Fidjestol, P. (1997). “Influence of silica fume on chloride resistance of concrete”, *Proc. of the PCI/FHWA International Symposium on High Performance Concrete.* pp. 245-261.

Hopfield, J.J. (1982). “Neural networks and physical systems with emergent collective computational abilities,” *Proc. National Academy of Science*, USA, Vol. 79, pp. 2554-2558.

Hornik, K., Stinchcombe, M., and White, H. (1989) “Multilayer feedforward networks are universal approximators,” *Neural Networks* 2 (5), pp. 359-366.

Hussain, S.E. and Rasheeduzzafar (1994). “Corrosion resistance of fly ash blended cement concrete”, *ACI Mater Journal* 91(3), pp. 264-72.

Joshi, P. and Chan, C. (2002), “Rapid Chloride Permeability Testing”, *Concrete Construction-World of Concrete* 47 (12), pp. 37-43.

Krose, B. and Smagt, P. V. D. (1996). “*An Introduction to Neural Networks*”. Eight Edition. The University of Amsterdam, Amsterdam, Netherlands. pp. 33-44.

Lamound, J. F. and Pielert, J. H. (2006). “Significance of Tests and Properties of Concrete and Concrete-Making Materials”. Volume 169 D-STP. *ASTM International*, West Conshohocken, PA. 303 pp.

Liu, Z. and Beaudoin, J. I. (2000). “The permeability of Cement Systems to Chloride Ingress and Related Test Methods. Cement”, *Concrete, and Aggregates* 22 (1), pp 16-23.

Lomboy, G. and Kejin, W. (2009). “Effects of strength, permeability, and air void parameters on freezing-thawing resistance of concrete with and without air entrainment”, *Journal of ASTM International* 6 (10), Report number JA1102454, West Conshohocken, PA, 14 pp.

Luping, T. and Nilsson, L. (1992). “Rapid determination of the chloride diffusivity in concrete by applying an electrical field”. *ACI Materials Journal* 89 (1), pp 40-53.

Mackechnie, J.R. and Alexander, M.G. (2004). “Rapid assessment of chloride resistance of concrete using the chloride conductivity test”, *The Indian concrete journal* 78 (3), pp 164-169.

Mackechnie, J. R. and Alexander, M. G. (2000). “Rapid Chloride test comparisons”, *Concrete International* 22 (5), pp. 5-40.

Malhotra, V. M. (1998). "*Role of Supplementary cementing materials in reducing greenhouse gas emissions*". CANMET Report MTL 98-03, Ottawa, Canada, pp. 27-42.

Mandavilli, S. and Najjar, Y. M. (2004). "Study of Crash Rates and Development of Investment Index For Kansas Rural Road Network," *CD-ROM of the Transportation Research Board 83rd Annual Meeting*, Washington DC, January 11-15, 2004, paper # 04-2815.

Manmohan, D. and Mehta, P. K. (1981). "Influence of pozzolanic slag and chemical admixtures on pore-size distribution and permeability of hardened cement pastes". *Cement Concrete Aggregate* 3 (1), pp. 63-67.

Nagataki, S and Ujike, I. I. (1986). "Air permeability of concretes mixed with fly ash and condensed silica fume". *Proceedings second international conference on the use of fly ash, blast furnace slag, and silica fume in concrete*, Spain, Madrid, pp. 1049-68.

Naik, R. N., Sing, S., and Ramme, B. (1998). "Mechanical properties and durability of concrete made with blended fly ash", *ACI Materials Journal* 95 (4), pp. 62-454.

Najjar, Y. M. and Ali H. E. (1998a). "On the use of BPNN in liquefaction potential assessment tasks," *Proceedings, International Workshop on Artificial Intelligence and Mathematical Methods in Pavement and Geomechanical Systems*, Attoh-Okine N.O. (ed.), pp. 55-63.

Najjar, Y. M. and Ali, H. E. (1998b). "SPT-based liquefaction potential assessment: An artificial neural network approach," *Proceedings (CD-ROM), 12th ASCE Specialty Conference on Engineering Mechanics*, Murakami, H. and Luco, J. E. (eds.), pp. 960-963.

Najjar, Y. M. and Basheer, I. A. (1996a). "Utilizing computational neural networks for evaluating the permeability of compacted clay liners," *Geotechnical and Geological Engineering*, 14 (3), pp. 193-212.

Najjar, Y. M., Basheer, I. A., and Ali, H. A. (1996b). "Modelling stress-strain response of clay using neural nets," *Proceedings of the 11th ASCE Speality Conference on Engineering Mechanics*, Lin, Y. K. and Su, T.C. (eds.), ASCE, New York, NY, pp. 697-700.

Najjar, Y. M., Basheer, I. A., and McReynolds, R. L. (1997). "*Modeling the Durability of Aggregate Used in Concrete Pavement Construction: A Neuro-Reliability-Based Approach*", Final Report no.: KS-97-3, Kansas Department of Transportation.

Najjar, Y. M. and Huang, C. (2007) "Simulating the Stress-Strain Behavior of Georgia Kaolin via Recurrent Neuronet Approach," *Computers and Geotechnics*, Vol. 34, pp. 364-361.

Najjar, Y. M. and McRyenold, R. (2003) "Modeling the Joint Deterioration Behavior of PCC Kansas Pavements via Dynamic ANN Approach," ASCE Geotechnical Special Publication # 123, pp. 209-222.

Najjar, Y. M. and Mryyan, S. (2009). "ANN-Based Profiling: Data Importance," *Intelligent Engineering Systems through Artificial Neural Networks*, Vol. 19, pp. 155-162.

Najjar, Y. M. and Zhang, X. (2000). "Characterizing the 3D Stress-Strain Behavior of Sandy Soils: A neuro-Mechanistic Approach", *ASCE Geotechnical Special Publications*, No. 96, pp. 43-57.

Oh, B. H., Cha, S. W., Jang, B. S., and Jang, S. P. (2002). "Development of high performance concrete having high resistance to chloride penetration". *Nuclear Engineering Design,* 212 (1-3), pp. 221-231.

Ozyildirim, C. and Halstead, W. J. (1994). "Improved concrete quality with combinations of fly ash and silica fume", *ACI Mater Journal* 91 (6), pp. 587-94.

Ozyildirim, C. (1994). "Laboratory investigation of low-permeability concretes containing slag and silica fume", *ACI Material Journal*, 91 (2), pp. 197-202.

Padmini, A. K., Ramamurthy, K., and Mathews, M. S. (2002). "Relative moisture movement through recycled aggregate concrete", Magazine of Concrete Research 54 (5), pp 377-384.

Pham, D. T. (1994), " Neural Networks in Engineering" in Applications of Artificial intelligence in engineering IX", AIENG/94, *Proc. 9th Int. Conf., Rzevski et al. (eds.)*, Computational Mechanics Publications, Southempton, Boston, pp 3-36.

Plante, P. and Bilodeau, A. (1989). "Rapid Chloride Ion Permeability Test Data on Concrete Incorporating Supplementary Cementing Materials, Fly Ash, Silica Fume, Slag, and Natural Pozzolans in Concrete", SP-114, *Proceedings Third International Conference*, Trondheim, Norway, American Concrete Institute, P.O. Box 19150, Detroit, Ml 48219.

Ramezanianpour, A. A. and Malhotra, V. M. (1995). "Effect of curing on the compressive strength, resistance to chloride ion penetration and porosity of concretes incorporating slag, fly ash, or silica fume", *Cement Concrete Comp.*, 17 (2), pp 125-133.

Riding, K. A., Poole, J. L., Schindler, A. K., Juenger, M. C. G., and Folliard, K. J. (2008). "Simplified Concrete Resistivity and Rapid Chloride Permeability test method", *ACI Materials Journal* 105 (4), pp 390-394.

Rumelhart, D. E., Hinton, G. E., and Williams, R. J. (1986). "Learning representation by back-propagating errors". *Nature*, pp. 323, 533-536.

Rumelhart, D. E. and McClelland, J. L. (1986), "Parallel distributed processing: explorations in the microstructure of cognition", Vol. 1, MIT Press, Cambridge, MA, 567 pp.

Sahraman, M. and Li, V. C. (2009). "Influence of microcracking on water absorption and sorptivity of ECC", *Materials and Structures/Materiaux et Constructions* 42 (5), pp 593-603.

Saraswathy, V. and Song, Ha-Won (2008) "Evaluation of Cementitious Repair Mortars for Corrosion Resistance", *Portugaliae Electrochimica Acta* 26(5), pp. 417-432.

Shi, C. (2004). "Effect of mixing proportions of concrete on its electrical conductivity and the rapid chloride permeability test (ASTM C1202 or ASSHTO T277) results", 34 (3), pp 537-545.

Srinivasan, P., Firdows, M. Z. M., Prabakar, J., and Chellappan, A. (2007). "A Simple Accelerated Test Method for Rapid Assessment of Chloride Penetration of Concrete with and without Surface Coating", *Indian Concrete Journal* 81 (1), pp 43-47.

Stanish, K. D., Hooton, R. D., and Thomas, M. D. A., (2000). "*Testing the Chloride Penetration Resistance of Concrete: A Literature Review,*" FHWA Contract DTFH61-97-R-00022, University of Toronto, Toronto, ON, Canada, June 2000, 6 pp.

Swamy, R.N. (1991). "*Blended Cements in Construction*", Elsevier Science Publishing Co., New York, NY, 508 pp.

Thomas, M. (1996). "Chloride thresholds in marine concrete", *Cement Concrete Research* 26(4), pp. 513-519.

Tosun, K., Felekoglu, B., and Baradan, B. (2008). "Effectiveness of alkyl alkoxy silane treatment in mitigating alkali-silica reaction", *ACI Materials Journal* 105 (1), pp 20-27.

Whiting, D. (1981) "*Rapid Determination of the Chloride Permeability of Concrete*," Final Report No. FHWA/RD-81/119, Federal Highway Administration, NTIS No. PB 82140724.

Wu, X. and Ghaboussi, J. (1995), "*Neural network based material modeling*", Report No. SRS-599, Department of Civil Engineering, University of Illinois Urbana-Champaign, IL.

Yang, C. C. and Chiang, C. T. (2005). “On the relationship between pore structure and charge passed from RCPT in mineral-free cement-based materials”, *Material Chem. Phys.,* 93 (1), pp. 202-207.

Zhao, T. J., Zhou, Z. H., Zhu, J. Q., and Feng, N. Q. (1998). “An Alternating Test Method for Concrete Permeability”, *Cement and Concrete Research* 28 (1), pp 7-12.

Zupan, J. and Gasteiger, J. (1993). “*Neural Networks for Chemists: An Introduction*”, VCH publishers, New York, NY.